



Weierstrass Fractal Drums -I – A Glimpse of Complex Dimensions

Claire David, Michel Lapidus

► To cite this version:

Claire David, Michel Lapidus. Weierstrass Fractal Drums -I – A Glimpse of Complex Dimensions. 2022. hal-03642326v1

HAL Id: hal-03642326

<https://hal.sorbonne-universite.fr/hal-03642326v1>

Preprint submitted on 15 Apr 2022 (v1), last revised 12 Jun 2023 (v2)

HAL is a multi-disciplinary open access archive for the deposit and dissemination of scientific research documents, whether they are published or not. The documents may come from teaching and research institutions in France or abroad, or from public or private research centers.

L'archive ouverte pluridisciplinaire **HAL**, est destinée au dépôt et à la diffusion de documents scientifiques de niveau recherche, publiés ou non, émanant des établissements d'enseignement et de recherche français ou étrangers, des laboratoires publics ou privés.

Weierstrass Fractal Drums - I

—

A Glimpse of Complex Dimensions

Claire David¹ and Michel L. Lapidus^{2 *}

March 31, 2022

¹ Sorbonne Université

CNRS, UMR 7598, Laboratoire Jacques-Louis Lions, 4, place Jussieu 75005, Paris, France

² University of California, Riverside – Department of Mathematics, Riverside, CA 92521–0135, USA

Abstract

We establish a *fractal tube formula* for the Weierstrass Curve, which gives, for small values of a strictly positive parameter ε , an explicit expression for the volume of the ε -neighborhood of the Curve. For this purpose, we prove new geometric properties of the Curve and of the associated function, in relation with its local Hölder and reverse Hölder continuity, with explicit estimates that had not been obtained before. We also show that the Codimension $2 - D_{\mathcal{W}}$ is the optimal Hölder exponent for the Weierstrass function \mathcal{W} , from which it follows that, as is well known, \mathcal{W} is nowhere differentiable. Then, the formula, that yields the expression of the ε -neighborhood, consists of a fractal power series, with underlying exponents the Complex Codimensions. This enables us to obtain the associated *tube and distance fractal zeta functions*, whose poles yield the set of Complex Dimensions. We prove that the nonzero Complex Dimensions are periodically distributed along countably many vertical lines, with the same oscillatory period. By considering the lower Minkowski content of the Curve, which we prove to be strictly positive, we then show that the Weierstrass Curve is Minkowski nondegenerate, as well as not Minkowski measurable, but admits a nontrivial average Minkowski content – and that, as expected, the Minkowski dimension (or box dimension) $D_{\mathcal{W}}$ is the Complex Dimension with maximal real part, and zero imaginary part.

MSC Classification: 11M41, 28A12, 28A75, 28A80.

Keywords: Weierstrass Curve, best Hölder exponent, Complex Dimensions of a relative fractal drum, box-counting (or Minkowski) dimension, fractal tube formula, tube zeta function, distance zeta function, (upper, lower and average) Minkowski content, Minkowski non-measurability, Minkowski nondegeneracy, nowhere differentiability.

*The research of M. L. L. was supported by the Burton Jones Endowed Chair in Pure Mathematics, as well as by grants from the U. S. National Science Foundation.

Contents

1	Introduction	2
2	Geometric Framework	6
3	Tubular Neighborhood	33
4	Fractal Tube Formulas, Complex Dimensions and Average Minkowski Content	52
4.1	Preliminaries	52
4.2	Fractal Tube Formulas and Fractal Zeta Functions	55
4.3	Complex Dimensions	62
4.3.1	Main Results	62
4.3.2	Exceptional Cases	63
4.3.3	Possible Interpretation	65
4.3.4	Compatibility with the General Theory of Complex Dimensions	66
4.4	Minkowski Dimension, Minkowski Nondegeneracy, and Average Minkowski Content . .	67
4.5	The Non-Integer Case	71
5	Concluding Comments	72

1 Introduction

Among the so-called “pathological objects” that appeared in the XIXth century, the Weierstrass Curve (\mathscr{W} -Curve) stands as one of the most fascinating and intriguing ones. At first, it was simply designed and thought of in order to be continuous everywhere, while being nowhere differentiable. Given $\lambda \in]0, 1[$, and b such that $\lambda b > 1 + \frac{3\pi}{2}$, the associated function is defined as the sum of the uniformly convergent trigonometric series

$$x \in \mathbb{R} \mapsto \sum_{n=0}^{\infty} \lambda^n \cos(\pi b^n x) .$$

The original proof, by K. Weierstrass [Wei75], in the case where b is an odd positive integer, can also be found in [Tit39] (pages 351-353). It has been completed by the one, now classical, given by G. H. Hardy [Har16], in the more general case, where b is any real number such that $\lambda b > 1$.

As is discussed in [Dav21], the introduction of this function challenged all the existing theories that went back to André-Marie Ampère, and has led to the emergence of many new functions possessing the same type of properties.

History then left it aside for a while, before new discovered properties brought it back once again to the forefront. It happened, in particular, that, in addition to its nowhere differentiability, the function – and the associated Curve – have self-similarity properties. After the works of A. S. Besicovitch and H. D. Ursell [BU37], Benoît Mandelbrot [Man77], [Man83], particularly highlighted the fractal properties of the Weierstrass Curve. He also conjectured that the Hausdorff dimension of the graph is given by $D_{\mathscr{W}} = 2 + \frac{\ln \lambda}{\ln b} = 2 - \ln_b \frac{1}{\lambda}$.

Interesting discussions and results in relation to this question may be found in the book of K. Falconer [Fal86]. As for the box dimension, a first series of results have been obtained by J.-L. Kaplan, J. Mallet-Paret and J. A. Yorke [KMPY84], where the authors show that it is equal to the Lyapunov dimension of the equivalent attracting torus. Then, the problem was tackled by F. Przytycki and M. Urbański [PU89], as well as by T.-Y. Hu and K.-S. Lau [HL93].

As for the Hausdorff dimension, the first key result was obtained by F. Ledrappier [Led92], where the Curve is considered as “the repeller for some expanding self-mapping on $[0, 1] \times \mathbb{R}$ ”, in the case where b is an integer, an assumption that is of importance, in so far as a Markov partition for the mapping $x \mapsto bx \bmod 1$ is involved. The resulting dynamics thus obeys the Markov property, a fact that has naturally led the author of [Led92] to using such notions as topological – metric entropies, explored in his earlier joint work with L. S. Young [LY85]. An interesting and useful connection was therefore established between Lyapunov exponents and dimensions, in this context. Another result was then obtained by B. Hunt [Hun98] in 1998 in the case where arbitrary phases are included in each cosinoidal term of the summation. Later, in 2014, K. Barański, B. Bárány and J. Romanowska [BBR14] showed that, for any value of the real number b , there is a threshold value λ_b belonging to the interval $\left] \frac{1}{b}, 1 \right[$ such that the Hausdorff dimension is equal to $D_{\mathcal{W}}$, for every b in $\left] \lambda_b, 1 \right[$. The results obtained by W. Shen in [She18] went further than the main result of [BBR14] and, in fact, showed that the Hausdorff dimension of the Weierstrass Curve is equal to $D_{\mathcal{W}}$, for any (allowed) values of the parameters. Furthermore, in [Kel17], G. Keller proposed a very original and much simpler proof of the main results of [BBR14].

In [Dav18], the first author proved – in the case when $b = N_b$ is an integer, and in contrast to the then existing work – that the Minkowski dimension (or box-counting dimension) of the Weierstrass Curve could be obtained in a simple way, without requiring any theoretical background in dynamical systems theory. The proof relies on the use of prefractal approximations; that is, here, a suitable sequence of finite graphs which converges towards the Weierstrass Curve. They are obtained by means of a suitable nonlinear iterated function system (IFS) [Dav19], where, as in the case of the horseshoe attractor introduced by Stephen Smale, the nonlinear maps involved are not contractions, but possess what can be viewed as an equivalent property, since, at each step of the iterative process, they reduce the values of the two-dimensional Lebesgue measures of a given sequence of rectangles covering the Curve. As expected, the Weierstrass Curve is invariant with respect to the family of those maps, which provides us in this context with a result equivalent to the one that can be found in [BD85].

Interestingly, the intrinsic properties of the intriguing maps which constitute the nonlinear IFS can be directly linked to the computation of the box dimension of the Weierstrass Curve, and to a new proof of the nowhere differentiability of the Weierstrass function, as shown in [Dav21].

Yet, thus far, no connection has been established with the theory of Complex Dimensions. Therefore, the following questions arise naturally in this setting: Can one prove that the Minkowski (or box) dimension of the Weierstrass Curve is, also, a Complex Dimension? Can we also determine all of the (possible) Complex Dimensions of this Curve, as well as obtain an associated fractal tube formula, in the form of a fractal power series involving the underlying Complex Dimensions? (See [LRŽ17b], Problem 6.2.24, page 560.)

The foundations of the theory of **Complex Dimensions** were laid by M. L. Lapidus and his collaborators in [Lap91], [Lap92], [Lap93], [LP93], [LM95], [LvF00], [LP06], [Lap08], [LPW11], [ELMR15], [LvF13], [LRŽ17a], [LRŽ18], [Lap19], [HL21] and [Lap22], in particular. The theory provides a very natural and intuitive way to characterize *fractal strings* or *drums*, in relation with their intrinsic vibrational properties. Geometrically, in the latter case, this means studying the oscillations of a small neighborhood of the boundary, i.e., of a tubular neighborhood, where points are located within an epsilon distance from any edge. As is explained in [Lap19], a fractal may be viewed “as a musical instrument tuned to play certain notes with frequencies (respectively, amplitudes) essentially equal to the real parts (respectively, the imaginary parts) of the underlying complex dimensions”. One can also imagine a “*geometric wave* propagating through the fractal” [Lap19].

The one-dimensional theory of Complex Dimensions (i.e., that of fractal strings) was developed,

in particular, in the books by the second author and M. van Frankenhuysen [LvF00], [LvF13], where general explicit formulas and fractal tube formulas were obtained for fractal strings (see [LvF13], Chapters 5 and 8). Later, in the book [LRŽ17b] – as well as in a series of accompanying papers, including [LRŽ17a] and [LRŽ18] – the higher-dimensional theory of Complex Dimensions was developed by the second author, G. Radunovic and D. Žubrinić, in the general case of bounded subsets of Euclidean space \mathbb{R}^N and of relative fractal drums of \mathbb{R}^N , with $N \geq 1$ being an arbitrary integer. General fractal tube formulas were also obtained in this context and applicable to a large variety of examples; see [LRŽ17b], Chapter 5, and [LRŽ18]. In short, Complex Dimensions are defined as the poles of the meromorphic continuation of suitable geometric or fractal zeta functions, associated with the fractal under study. A geometric object is then said to be *fractal* if it admits at least one *nonreal Complex Dimension*, thereby giving rise to geometric oscillations via the corresponding fractal tube formula. For example, in agreement with one’s intuition, the Devil’s Staircase (i.e., the graph of the Cantor–Lebesgue function) is shown to be fractal, in this sense, whereas it is not fractal according to Benoît B. Mandelbrot’s definition in [Man83], because its topological and Hausdorff dimensions coincide.

Under a mild assumption, the (upper) Minkowski dimension of the geometric object under study is equal to the abscissa of convergence of the geometric, distance or tube, fractal zeta functions, and is the only Complex Dimension located on the real axis and with maximal real part, therefore giving rise, via the corresponding fractal tube formula, to geometric, spectral, or dynamical oscillations with the largest amplitudes. We note that fractal tube formulas express the volume of (small) ε -neighborhoods of the fractal as a fractal power series, with exponents the underlying Complex Codimensions.

Building on the work on multifractal zeta functions and Complex Dimensions of multifractals strings developed in [LR09], [LLVR09], [ELMR15], along with the work on Complex Dimensions and fractal tube formulas in [LvF00], [LvF13]. L. O. R. Olsen [Ols13a], [Ols13b], also obtained a suitable multifractal analog of fractal tube formulas in this context.

A clear summary of the theory of Complex Dimensions for fractal strings can be found in [Ols01], while a long survey of the theory of Complex Dimensions, both for fractal strings and in higher dimensions, is given in [Lap19].

A question which naturally arises in this context is that of differential operators on such structures. In the case of fractal strings, as an echo to noncommutative geometry, where *spectral triples* are involved, a *geometric zeta function* provides the set of complex modes, while the dimensions stand as its nonreal poles. The occurrence of the zeta function can be understood very intuitively, in so far as it simply represents the trace of the differential operator at a complex order s . Thus, the poles are nothing but the maximal orders of differentiation. Hence, dimensions.

The notion of a *fractal drum* extends that of a *fractal string*: at stake is an open subset with a fractal boundary. In the Euclidean plane, this boundary is a curve. The word “drum” calls for vibrations: intuitively, one understands that they occur in a small neighborhood of the boundary, a tubular neighborhood, the Lebesgue measure of which is associated to a *tube zeta function* which, similarly, enables one to obtain the Complex Dimensions, which stand as characteristic numbers that account for specific geometric properties of the fractal boundary, here, the underlying curve.

For the Koch Snowflake Curve, a *fractal tube formula* was obtained by M. L. Lapidus and E. P. J. Pearse in [LP06]. As was pointed out in [LRŽ17b] (see Problem 6.2.24, page 560), the case of **the Weierstrass Curve** remained a *difficult open problem*, which we propose to completely solve in this paper. It is directly associated to our previous work [Dav18], in so far as precise estimates are required for the elementary heights of the sequence of natural prefractal approximations tending towards the Curve. As is often the case in such a situation, we significantly improve these estimates, which also

enable us to obtain the exact values of the local extrema, and to obtain the optimal Hölder exponent of \mathscr{W} . Those extrema – which form a dense subset of the Weierstrass Curve – directly depend on the choice of an initial set of points, which happen to be here the fixed points of the nonlinear iterated function system involved in the construction of the Curve; see [Dav19] for further details. Moreover, we introduce *the concept of **self-shape similarity***, a more general one than the standard notion of *self-similarity*.

One of the novelties of our approach is that our tubular neighborhood is located on both sides of the Curve, which seems natural, because vibrations may occur on either side of the underlying fractal drum. The method we use is similar to the one of [LP06] and [LPW11] (see also [LvF00], §10.3, and [LvF13], §12.4), without resorting *a priori* to the distance or the tube zeta function. Once the fractal tube formula has been obtained, however, we deduce from it the explicit form of the fractal (tube and distance) zeta functions, along with the Complex Dimensions of the Weierstrass Curve.

The main results obtained in this paper, where we consider the case $b = N_b$ being an integer, can be found in the following places:

- i. In Corollary 2.12, and Theorem 2.13, along with Corollary 2.14, where we prove the sharp local Hölder continuity, and a sharp discrete version of reverse Hölder continuity, with optimal Hölder exponent, for the Weierstrass function \mathscr{W} , equal to the (Minkowski) Codimension $2 - D_{\mathscr{W}} = \ln_{N_b} \frac{1}{\lambda}$. It follows, in particular, that \mathscr{W} is nowhere differentiable – as is well known, although our method of proof is completely different from the usual ones.
- ii. In Theorems 4.7 and 4.11, which yield, for small values of the positive parameter ε , the expression of the area of the ε -neighborhood of the Curve – a Weierstrass Fractal Tube Formula, which (apart from two terms associated with the Complex Dimensions 0 and -2) consists of an expansion of the form

$$\sum_{\alpha \text{ real part of a Complex Dimension}} \varepsilon^{2-\alpha} G_{\alpha} \left(\ln_{N_b} \left(\frac{1}{\varepsilon} \right) \right), \quad (\star)$$

where, for any real part α of a Complex Dimension, G_{α} denotes a continuous and one-periodic function. Furthermore, for $\alpha = \alpha_{max} = D_{\mathscr{W}}$, the Minkowski dimension of the Curve – i.e., for α being equal to the maximal real part of the Complex Dimensions of the Weierstrass Curve – the periodic function $G_{\alpha_{max}}$ is nonconstant, as well as bounded away from zero and infinity. As is the case in the general theory of fractal tube formulas (see [LvF13], [LRŽ17b], Chapter 8 and Chapter 5, respectively), the resulting fractal power series has for exponents the Complex Codimensions of the Weierstrass Curve. Observe that each nonconstant periodic function in (\star) gives rise to multiplicatively periodic (or log-periodic) oscillations in the scaling variable ε .

- iii. In Theorem 4.10, where we exhibit the possible Complex Dimensions of the Curve, as the poles of the associated Tube Zeta Function, itself obtained in Theorem 4.8. Equivalently, in the light of [LRŽ17a], [LRŽ17b], since $D_{\mathscr{W}} < 2$, the Complex Dimensions are also the poles of the distance zeta function of the Weierstrass Curve. In particular, we show that the Complex Dimensions (other than 0 and -2) are all simple and periodically distributed (with the same period $p = \frac{2\pi}{\ln N_b}$, the natural oscillatory period of the Weierstrass Curve) along countably many vertical lines, with abscissae $D_{\mathscr{W}} - k(2 - D_{\mathscr{W}})$ and $1 - 2k$, where k in \mathbb{N} is arbitrary. In addition, -2 and 0 are also Complex Dimensions, and they are simple.

- iv. In Theorem 4.12 and Corollary 4.13, where we prove the nondegeneracy of the Curve, in the Minkowski sense (see [LRŽ17b]), coming from the fact that the upper and lower Minkowski contents of the Curve are respectively positive and finite. As a result, the Minkowski dimension (or box-counting dimension) $D_{\mathscr{W}}$ of the Weierstrass Curve exists, i.e., the lower and upper Minkowski dimensions of the Curve coincide. Also, since the periodic function $G_{D_{\mathscr{W}}}$ is not constant, it follows that the Weierstrass Curve is not Minkowski measurable. Moreover, we show that the average Minkowski content of the Weierstrass Curve exists, is positive and finite, as well as coincides with the average value of the periodic function $G_{D_{\mathscr{W}}}$.
- v. As a corollary of Theorem 4.12, the fact that the number $D_{\mathscr{W}}$ is both the Minkowski Dimension and a Complex Dimension of the Weierstrass Curve; see Corollary 4.13.
- vi. The *fractality* of the Weierstrass Curve, in the sense of [LvF13], [LRŽ17b], [Lap19]; i.e., the existence of *nonreal* Complex Dimensions (with real part $D_{\mathscr{W}}$) giving rise to geometric oscillations, in the Fractal Tube Formula obtained in this paper (Theorems 4.7 and 4.11), as described in *ii.* above. In fact, in the terminology of [LvF13] and [LRŽ17b], the Weierstrass Curve is fractal in countably many dimensions d_k , with $d_k \rightarrow -\infty$, as $k \rightarrow \infty$.

As could have been expected, the Minkowski dimension (or box dimension) $D_{\mathscr{W}}$ coincides with the maximum value of the real parts of the Complex Dimensions of the Curve. By considering the lower Minkowski content, which we prove to be strictly positive, we show that $D_{\mathscr{W}}$ is, as expected, a Complex Dimension.

We also briefly evoke, in Subsection 4.5, the noninteger case, i.e., when b is any positive real number satisfying $\lambda b > 1$. This case will be studied in detail in a future work.

Now, the determination of those dimensions, as important as it may be, is not an end in itself. In fact, the Complex Dimensions directly echo the fractal cohomological properties of the Curve, which will be the subject of a second paper, [DL22b]. The results of this paper and of [DL22b] are announced in the survey article [DL22a], where their main results are presented in a summarized form.

2 Geometric Framework

Henceforth, we place ourselves in the Euclidean plane of dimension 2, equipped with a direct orthonormal frame. The usual Cartesian coordinates are denoted by (x, y) . The horizontal and vertical axes will be respectively referred to as $(x'x)$ and $(y'y)$.

Notation 1 (Set of all Natural Numbers and Intervals).

As in Bourbaki [Bou04] (Appendix E. 143), we denote by $\mathbb{N} = \{0, 1, 2, \dots\}$ the set of all natural numbers, and set $\mathbb{N}^{\star} = \mathbb{N} \setminus \{0\}$.

Given a, b with $-\infty \leq a \leq b \leq \infty$, $]a, b[= (a, b)$ denotes an open interval, while, for example, $]a, b] = (a, b]$ denotes a half-open, half-closed interval.

Notation 2 (Wave Inequality Symbol).

Given two positive numbers a and b , we will use the notation $a \lesssim b$, when there exists a strictly positive constant C such that $a \leq C b$.

Notation 3. In the sequel, λ and N_b are two real numbers such that

$$0 < \lambda < 1 \quad , \quad N_b \in \mathbb{N}^* \quad \text{and} \quad \lambda N_b > 1 \quad . \quad (\clubsuit)$$

As explained in [Dav19], we deliberately made the choice to introduce the notation N_b which replaces the initial b , in so far as, in Hardy's paper [Har16] (in contrast to Weierstrass's original article [Wei75]), b is any positive real number satisfying $\lambda b > 1$, whereas we deal here with the specific case of a natural integer, which accounts for the natural notation N_b ; see, however, Section 4.5.

Definition 2.1 (Weierstrass Function, Weierstrass Curve).

We consider the *Weierstrass function* \mathscr{W} , defined, for any real number x , by

$$\mathscr{W}(x) = \sum_{n=0}^{\infty} \lambda^n \cos(2\pi N_b^n x) \quad .$$

We call the associated graph the *Weierstrass Curve*.

Due to the one-periodicity of the \mathscr{W} -function, from now on, and without loss of generality, we restrict our study to the interval $[0, 1[= [0, 1)$.

Notation 4 (Logarithm).

Given $y > 0$, $\ln y$ denotes the natural logarithm of y , while, given $a > 0$, $a \neq 1$, $\ln_a y = \frac{\ln y}{\ln a}$ denotes the logarithm of y in base a ; so that, in particular, $\ln = \ln_e$.

Notation 5. For the parameters λ and N_b satisfying condition (\clubsuit) (see Notation 3), we denote by

$$D_{\mathscr{W}} = 2 + \frac{\ln \lambda}{\ln N_b} = 2 - \ln_{N_b} \frac{1}{\lambda} \in]1, 2[$$

the box-counting dimension (or Minkowski dimension) of the Weierstrass Curve $\Gamma_{\mathscr{W}}$, which happens to be equal to its Hausdorff dimension [KMPY84], [BBR14], [She18], [Kel17]. As was mentioned earlier, our results in this paper will also provide a direct geometric proof of the fact that $D_{\mathscr{W}}$, the Minkowski dimension (or box-counting dimension) of $\Gamma_{\mathscr{W}}$, exists and takes the above value.

Remark 2.1. As can be found, for instance, in [Fal86], we recall that the *box-counting dimension* (or *box dimension*, in short), of $\Gamma_{\mathscr{W}}$,

$$D_{\mathscr{W}} = - \lim_{\delta \rightarrow 0^+} \frac{\ln N_{\delta}(\Gamma_{\mathscr{W}})}{\ln \delta} \quad , \quad (\diamond)$$

where $N_\delta(\Gamma_{\mathcal{W}})$ stands for any of the following quantities:

- i. the smallest number of sets of diameter at most δ that cover $\Gamma_{\mathcal{W}}$ on $[0, 1[$;
- ii. the smallest number of closed balls of radius δ that cover $\Gamma_{\mathcal{W}}$ on $[0, 1[$;
- iii. the smallest number of cubes of side δ that cover $\Gamma_{\mathcal{W}}$ on $[0, 1[$;
- iv. the number of δ -mesh cubes that intersect $\Gamma_{\mathcal{W}}$ on $[0, 1[$;
- v. the largest number of disjoint balls of radius δ with centers in $\Gamma_{\mathcal{W}}$ on $[0, 1[$.

Furthermore, for the Weierstrass Curve $\Gamma_{\mathcal{W}}$, as, more generally, for any bounded subset of Euclidean space – the box-counting dimension coincides with the Minkowski dimension (the definition of which is recalled in Definition 4.5 below).

We stress that our results will imply that the Minkowski (or box-counting) dimension of the Weierstrass Curve exists; more specifically, the above limit exists and is equal to $D_{\mathcal{W}} = 2 + \frac{\ln \lambda}{\ln N_b}$.

Convention (The Weierstrass Curve as a Cyclic Curve).

In the sequel, we identify the points $(0, \mathcal{W}(0))$ and $(1, \mathcal{W}(1)) = (1, \mathcal{W}(0))$.

Remark 2.2. The above convention makes sense, because the points $(0, \mathcal{W}(0))$ and $(1, \mathcal{W}(1))$ have the same vertical coordinate, in addition to the periodic properties of the \mathcal{W} -function.

Property 2.1. *(Symmetry with Respect to the Vertical Line $x = \frac{1}{2}$)*

Since, for any $x \in [0, 1]$,

$$\mathcal{W}(1 - x) = \sum_{n=0}^{\infty} \lambda^n \cos(2\pi N_b^n - 2\pi N_b^n x) = \mathcal{W}(x),$$

the Weierstrass Curve is symmetric with respect to the vertical straight line $x = \frac{1}{2}$.

Proposition 2.2 (Nonlinear and Noncontractive Iterated Function System (IFS)).

Following our previous work [Dav18], we approximate the restriction $\Gamma_{\mathcal{W}}$ to $[0, 1[\times \mathbb{R}$, of the Weierstrass Curve, by a sequence of graphs, built through an iterative process. For this purpose, we use the nonlinear iterated function system (IFS) of the family of C^∞ maps from \mathbb{R}^2 to \mathbb{R}^2 denoted by

$$\mathcal{T}_{\mathcal{W}} = \{T_0, \dots, T_{N_b-1}\},$$

where, for any integer i belonging to $\{0, \dots, N_b - 1\}$ and any point (x, y) of \mathbb{R}^2 ,

$$T_i(x, y) = \left(\frac{x+i}{N_b}, \lambda y + \cos\left(2\pi \left(\frac{x+i}{N_b}\right)\right) \right).$$

Remark 2.3. As is explained in [Dav19], it happens that the maps T_i , with $i = 0, \dots, N_b - 1$, comprising the IFS $\mathcal{T}_{\mathcal{W}}$ in the statement of Proposition 2.2 just above – are not contractions, *in the classical sense*. As a result, the nonlinearity of the IFS, $\mathcal{T}_{\mathcal{W}} = \{T_i\}_{i=0}^{N_b-1}$, does not enable one to resort to the probabilistic approach of M. F. Barnsley and S. Demko [BD85], or to the earlier work of J. E. Hutchinson [Hut81], which is applicable in the case of standard fractals such as the Sierpiński Gasket and the Koch Curve. Interestingly, even if they are not contractions, our maps possess what can be viewed as satisfying an equivalent property, since, at each step of the iterative process, they reduce the two-dimensional Lebesgue measures of a given sequence of rectangles covering the Curve. This is due to the fact that they correspond, in a sense, to the composition of a contraction of ratio r_x in the horizontal direction, and a dilatation of factor r_y in the vertical direction, with $r_x r_y < 1$. Such maps are considered, for example, in the book of Robert L. Devaney [Dev03], where they play a part in the first step of the horseshoe map process introduced by Stephen Smale.

Property 2.3 (Attractor of the IFS).

The Weierstrass Curve is the attractor of the IFS $\mathcal{T}_{\mathcal{W}}$: $\Gamma_{\mathcal{W}} = \bigcup_{i=0}^{N_b-1} T_i(\Gamma_{\mathcal{W}})$.

Proof. We refer to our works [Dav18], [Dav19]. □

Notation 6 (Fixed Points).

For any integer i belonging to $\{0, \dots, N_b - 1\}$, we denote by

$$P_i = (x_i, y_i) = \left(\frac{i}{N_b - 1}, \frac{1}{1 - \lambda} \cos\left(\frac{2\pi i}{N_b - 1}\right) \right)$$

the unique fixed point of the map T_i (see [Dav19]).

Definition 2.2 (Sets of Vertices, Prefractals).

We denote by V_0 the ordered set (according to increasing abscissa), of the points

$$\{P_0, \dots, P_{N_b-1}\}.$$

The set of points V_0 – where, for any i of $\{0, \dots, N_b - 2\}$, the point P_i is linked to the point P_{i+1} – constitutes an oriented finite graph, ordered according to increasing abscissa, which we will denote by $\Gamma_{\mathcal{W}_0}$. Then, V_0 is called *the set of vertices* of the graph $\Gamma_{\mathcal{W}_0}$.

For any natural integer m , i.e., $m \in \mathbb{N}$, we set $V_m = \bigcup_{i=0}^{N_b-1} T_i(V_{m-1})$.

The set of points V_m , where two consecutive points are linked, is an oriented finite graph, ordered according to increasing abscissa, which we will call the **m^{th} -order \mathcal{W} -prefractal**. Then, V_m is called *the set of vertices* of the prefractal $\Gamma_{\mathcal{W}_m}$; see Figures 1, 2, 3.

Definition 2.3 (Adjacent Vertices, Edge Relation).

For any natural integer m , the prefractal graph $\Gamma_{\mathcal{W}_m}$ is equipped with an edge relation \sim_m , as follows: two vertices X and Y of $\Gamma_{\mathcal{W}_m}$, i.e. two points belonging to V_m , will be said to be *adjacent* (i.e., neighboring or junction points) if and only if the line segment $[x, y]$ is an edge of $\Gamma_{\mathcal{W}_m}$; we then write $x \sim_m y$. Note that this edge relation depends on m , which means that points adjacent in V_m might not remain adjacent in V_{m+1} .

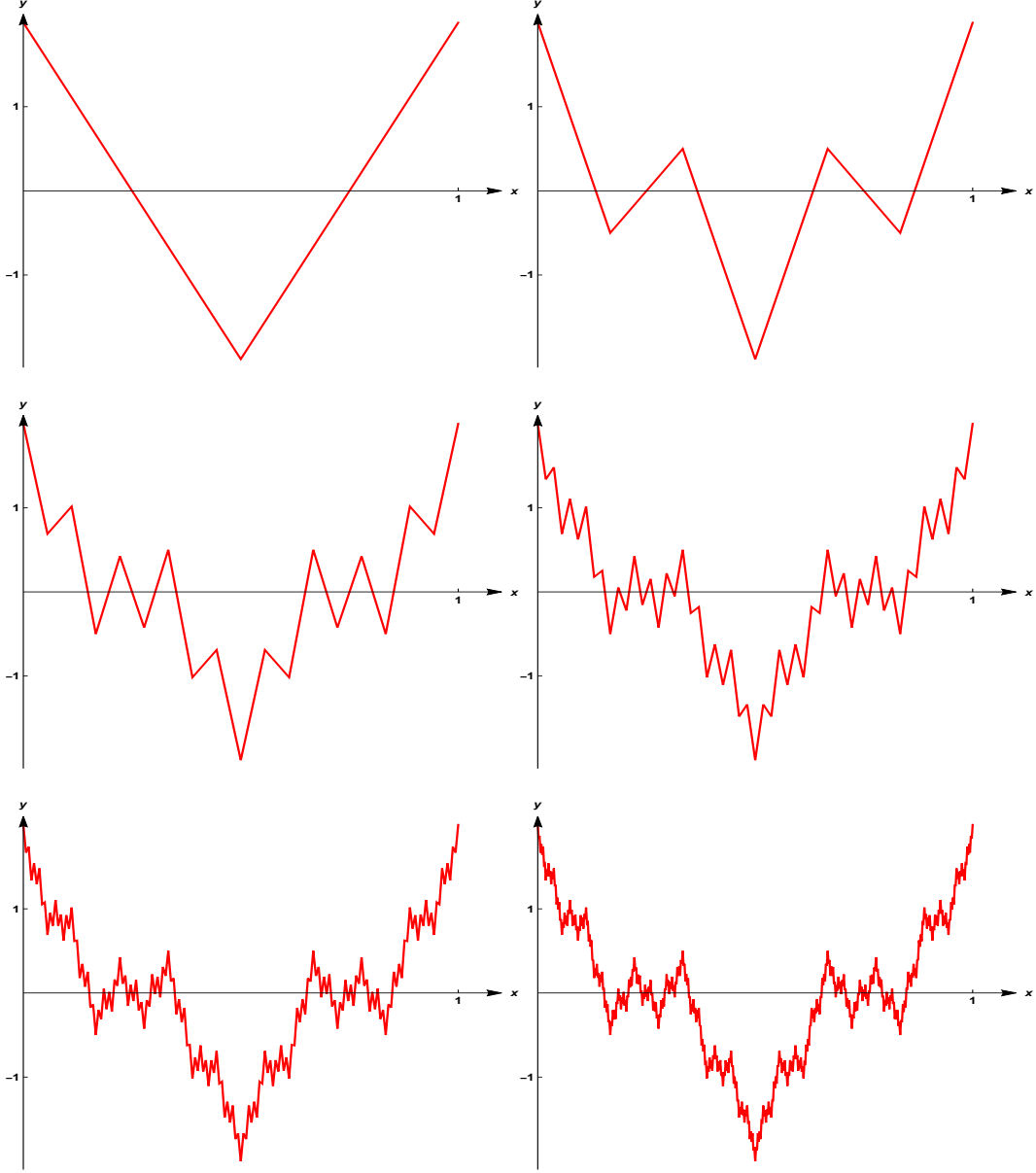


Figure 1: The prefractal graphs $\Gamma_{\mathcal{W}_0}, \Gamma_{\mathcal{W}_1}, \Gamma_{\mathcal{W}_2}, \Gamma_{\mathcal{W}_3}, \Gamma_{\mathcal{W}_4}, \Gamma_{\mathcal{W}_5}$, in the case where $\lambda = \frac{1}{2}$ and $N_b = 3$.

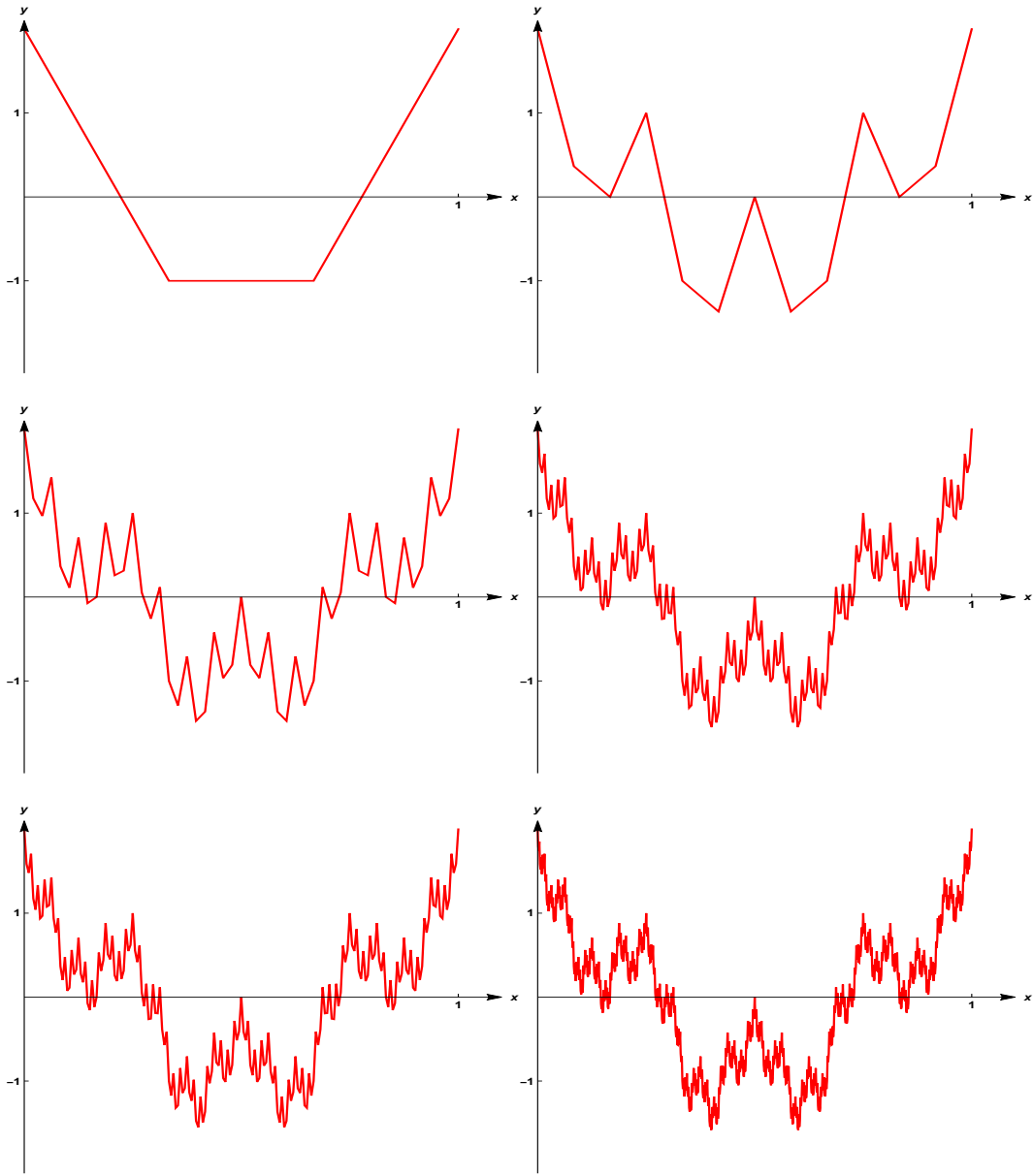


Figure 2: The prefractional graphs $\Gamma_{W_0}, \Gamma_{W_1}, \Gamma_{W_2}, \Gamma_{W_3}, \Gamma_{W_4}, \Gamma_{W_5}$, in the case where $\lambda = \frac{1}{2}$ and $N_b = 4$.

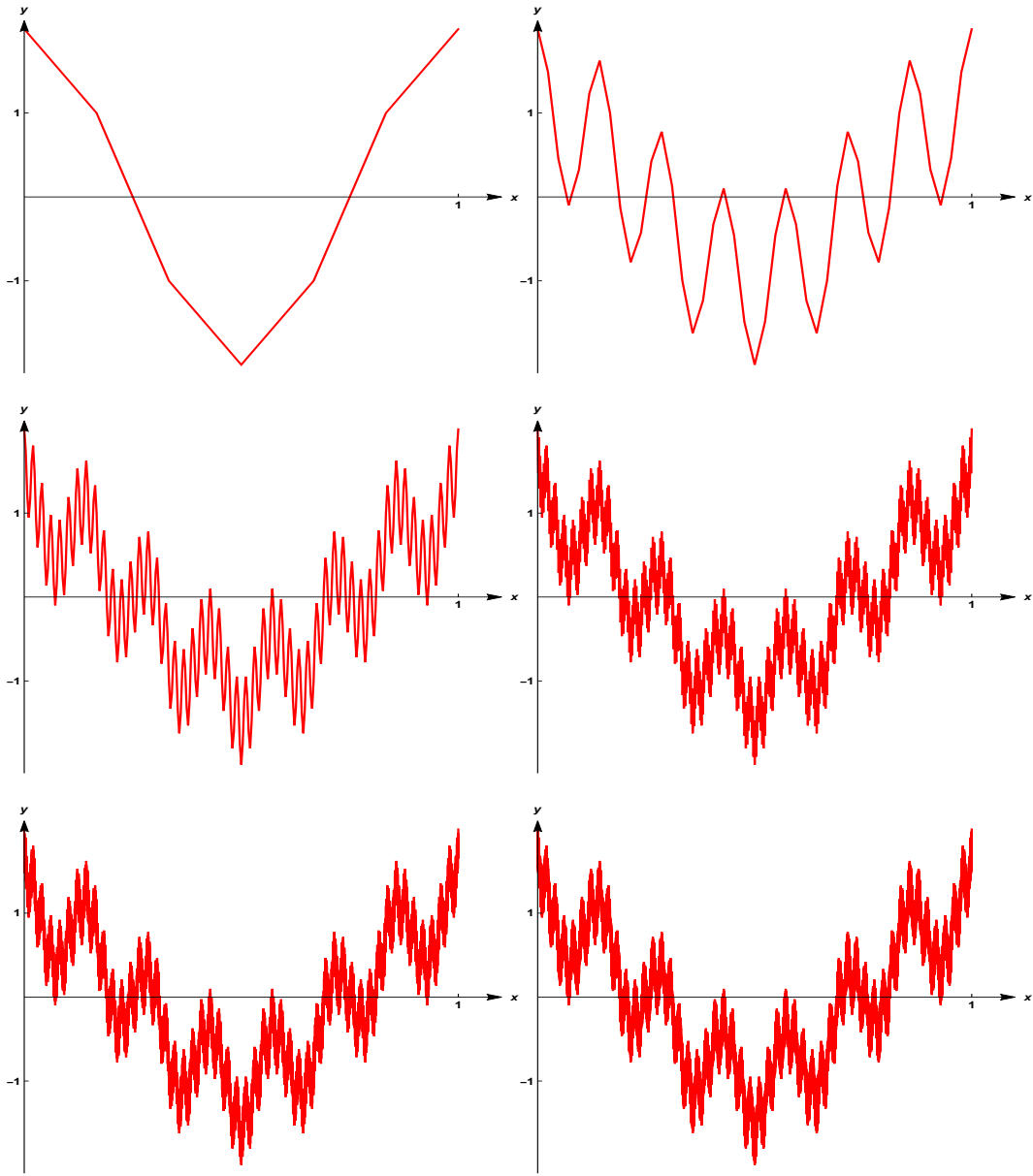


Figure 3: The prefactal graphs $\Gamma_{\mathcal{W}_0}, \Gamma_{\mathcal{W}_1}, \Gamma_{\mathcal{W}_2}, \Gamma_{\mathcal{W}_3}, \Gamma_{\mathcal{W}_4}, \Gamma_{\mathcal{W}_5}$, in the case where $\lambda = \frac{1}{2}$ and $N_b = 7$.

Property 2.4. [Dav18] *For any natural integer m :*

- i. $V_m \subset V_{m+1}$.
- ii. $\#V_m = (N_b - 1) N_b^m + 1$, where $\#V_m$ denotes the number of elements in the finite set V_m .
- iii. The prefractal graph $\Gamma_{\mathcal{W}_m}$ has exactly $(N_b - 1) N_b^m$ edges.
- iv. The consecutive vertices of the prefractal graph $\Gamma_{\mathcal{W}_m}$ are the vertices of N_b^m simple nonregular polygons $\mathcal{P}_{m,k}$ with N_b sides. For any strictly positive integer m , the junction point between two consecutive polygons is the point

$$\left(\frac{(N_b - 1)k}{(N_b - 1)N_b^m}, \mathcal{W} \left(\frac{(N_b - 1)k}{(N_b - 1)N_b^m} \right) \right), \quad 1 \leq k \leq N_b^m - 1.$$

Hence, the total number of junction points is $N_b^m - 1$. For instance, in the case $N_b = 3$, the polygons are all triangles; see Figure 4.

In the sequel, we will denote by \mathcal{P}_0 **the initial polygon**, whose vertices are the fixed points of the maps T_i , $0 \leq i \leq N_b - 1$, introduced in Definition 2.2, i.e., $\{P_0, \dots, P_{N_b-1}\}$.

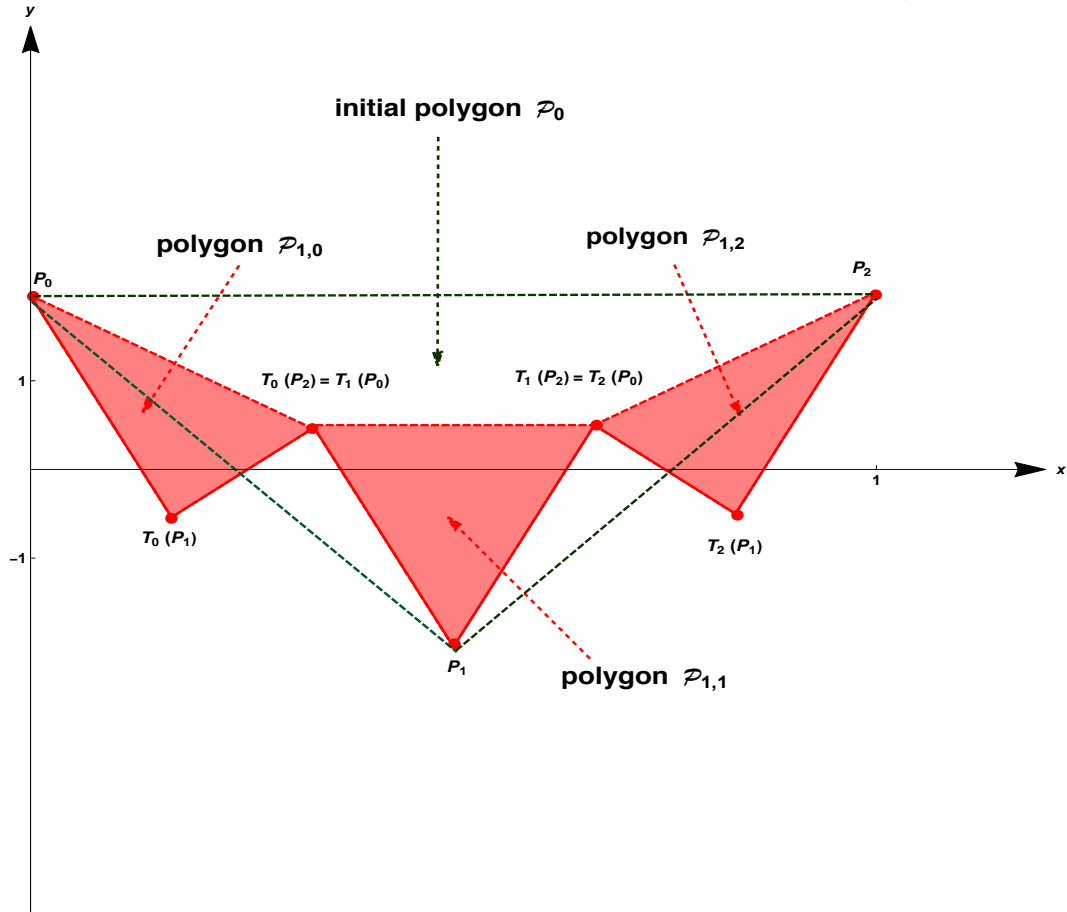


Figure 4: The initial polygon \mathcal{P}_0 , and the polygons $\mathcal{P}_{0,1}$, $\mathcal{P}_{1,1}$, $\mathcal{P}_{1,2}$, in the case where $\lambda = \frac{1}{2}$ and $N_b = 3$.

Definition 2.4 (Vertices of the Prefractals, Elementary Lengths, Heights and Angles).

Given a strictly positive integer m , we denote by $(M_{j,m})_{0 \leq j \leq (N_b-1)N_b^m-1}$ **the set of vertices** of the prefractal graph $\Gamma_{\mathcal{W}_m}$. One thus has, for any integer j in $\{0, \dots, (N_b-1)N_b^m-1\}$,

$$M_{j,m} = \left(\frac{j}{(N_b-1)N_b^m}, \mathcal{W} \left(\frac{j}{(N_b-1)N_b^m} \right) \right).$$

We also introduce, for any integer j in $\{0, \dots, (N_b-1)N_b^m-2\}$, the following quantities:

i. the elementary horizontal lengths:

$$L_m = \frac{j}{(N_b-1)N_b^m};$$

ii. the elementary lengths:

$$\ell_{j,j+1,m} = d(M_{j,m}, M_{j+1,m}) = \sqrt{L_m^2 + h_{j,j+1,m}^2};$$

iii. the elementary heights:

$$h_{j-1,j,m} = \left| \mathcal{W} \left(\frac{j}{(N_b-1)N_b^m} \right) - \mathcal{W} \left(\frac{j-1}{(N_b-1)N_b^m} \right) \right|, \quad h_{j,j+1,m} = \left| \mathcal{W} \left(\frac{j+1}{(N_b-1)N_b^m} \right) - \mathcal{W} \left(\frac{j}{(N_b-1)N_b^m} \right) \right|;$$

iv. the geometric angles:

$$\theta_{j-1,j,m} = ((y'y), (\widehat{M_{j-1,m}M_{j,m}})) \quad , \quad \theta_{j,j+1,m} = ((y'y), (\widehat{M_{j,m}M_{j+1,m}})),$$

which yield **the value of the geometric angle between consecutive edges** $[M_{j-1,m} M_{j,m}, M_{j,m} M_{j+1,m}]$:

$$\theta_{j-1,j,m} + \theta_{j,j+1,m} = \arctan \frac{L_m}{|h_{j-1,j,m}|} + \arctan \frac{L_m}{|h_{j,j+1,m}|}.$$

Property 2.5. *For the geometric angle $\theta_{j-1,j,m}$, with $0 \leq j \leq (N_b-1)N_b^m-1$ and $m \in \mathbb{N}$, we have the following relation:*

$$\tan \theta_{j-1,j,m} = \frac{h_{j-1,j,m}}{L_m}.$$

One now requires, at a given step $m \in \mathbb{N}^*$, the exact coordinates of the vertices of the prefractal graph $\Gamma_{\mathcal{W}_m}$, i.e. of the following set of points:

$$\left(\frac{j}{(N_b-1)N_b^m}, \mathcal{W} \left(\frac{j}{(N_b-1)N_b^m} \right) \right) \quad , \quad 0 \leq j \leq \#V_m.$$

Thus far, they could not be found in the existing literature on the subject.

For this purpose, it is interesting to use the scaling properties of the Weierstrass function.

Property 2.6 (Scaling Properties of the Weierstrass Function, and Consequences).

Since, for any real number x , $\mathcal{W}(x) = \sum_{n=0}^{\infty} \lambda^n \cos(2\pi N_b^n x)$, one also has

$$\mathcal{W}(N_b x) = \sum_{n=0}^{\infty} \lambda^n \cos(2\pi N_b^{n+1} x) = \frac{1}{\lambda} \sum_{n=1}^{\infty} \lambda^n \cos(2\pi N_b^n x) = \frac{1}{\lambda} (\mathcal{W}(x) - \cos(2\pi x)),$$

which yields, for any strictly positive integer m and any j in $\{0, \dots, \#V_m\}$,

$$\mathcal{W}\left(\frac{j}{(N_b - 1) N_b^m}\right) = \lambda \mathcal{W}\left(\frac{j}{(N_b - 1) N_b^{m-1}}\right) + \cos\left(\frac{2\pi j}{(N_b - 1) N_b^{m-1}}\right).$$

By induction, one then obtains that

$$\mathcal{W}\left(\frac{j}{(N_b - 1) N_b^m}\right) = \lambda^m \mathcal{W}\left(\frac{j}{(N_b - 1)}\right) + \sum_{k=0}^{m-1} \lambda^k \cos\left(\frac{2\pi N_b^k j}{(N_b - 1) N_b^m}\right).$$

Property 2.7. (A Consequence of the Symmetry with Respect to the Vertical Line $x = \frac{1}{2}$)

For any strictly positive integer m and any j in $\{0, \dots, \#V_m\}$, we have that

$$\mathcal{W}\left(\frac{j}{(N_b - 1) N_b^m}\right) = \mathcal{W}\left(\frac{(N_b - 1) N_b^m - j}{(N_b - 1) N_b^m}\right),$$

which means that the points

$$\left(\frac{(N_b - 1) N_b^m - j}{(N_b - 1) N_b^m}, \mathcal{W}\left(\frac{(N_b - 1) N_b^m - j}{(N_b - 1) N_b^m}\right)\right) \quad \text{and} \quad \left(\frac{j}{(N_b - 1) N_b^m}, \mathcal{W}\left(\frac{j}{(N_b - 1) N_b^m}\right)\right)$$

are symmetric with respect to the vertical line $x = \frac{1}{2}$.

Definition 2.5 (Left-Side and Right-Side Vertices).

Given natural integers m, k such that $0 \leq k \leq N_b^m - 1$, and a polygon $\mathcal{P}_{m,k}$, we define:

- i. The set of its *left-side vertices* as the set of the first $\left\lfloor \frac{N_b - 1}{2} \right\rfloor$ vertices, where $[y]$ denotes the integer part of the real number y .
- ii. The set of its *right-side vertices* as the set of the last $\left\lfloor \frac{N_b - 1}{2} \right\rfloor$ vertices.

When the integer N_b is odd, we define the bottom vertex as the $\left(\frac{N_b - 1}{2}\right)^{th}$ one; see Figure 6.

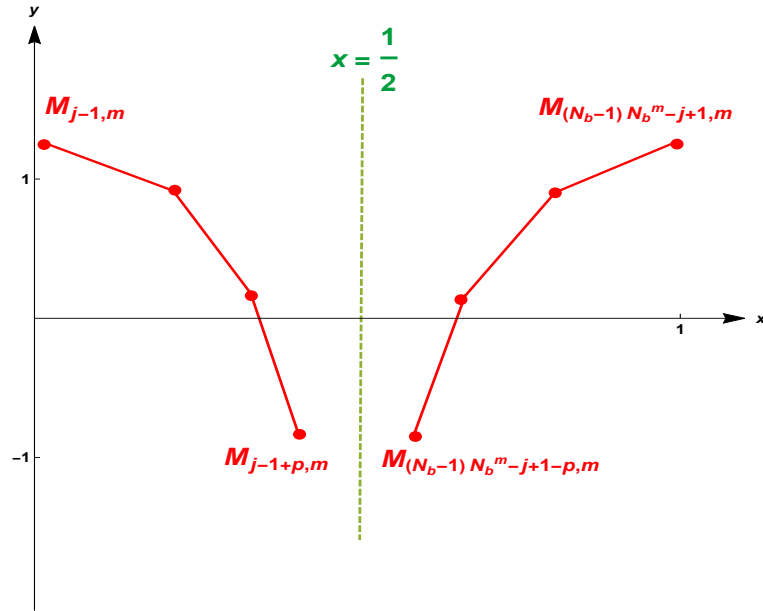


Figure 5: Symmetric points with respect to the vertical line $x = \frac{1}{2}$.

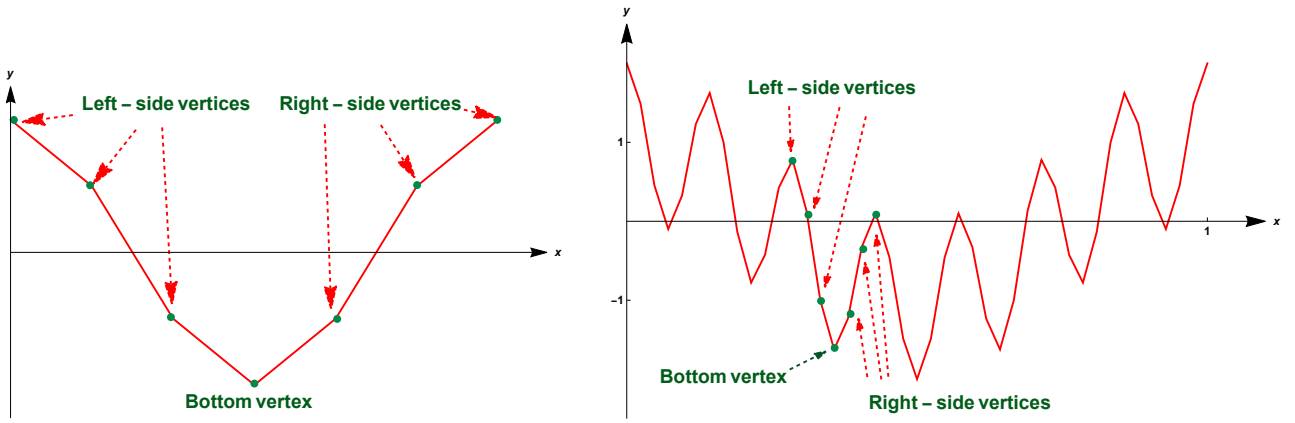


Figure 6: The left-side and right-side vertices.

Property 2.8. Since, for any natural integer n ,

$$N_b^n = (1 + N_b - 1)^n = \sum_{k=0}^n \binom{n}{k} (N_b - 1)^k \equiv 1 \pmod{N_b - 1},$$

one obtains, for any integer j in $\{0, \dots, N_b - 1\}$:

$$\mathcal{W}\left(\frac{j}{N_b - 1}\right) = \sum_{n=0}^{\infty} \lambda^n \cos\left(2\pi N_b^n \frac{j}{N_b - 1}\right) = \sum_{n=0}^{\infty} \lambda^n \cos\left(\frac{2\pi j}{N_b - 1}\right) = \frac{1}{1 - \lambda} \cos\left(\frac{2\pi j}{N_b - 1}\right).$$

We observe that the point

$$\left(\frac{j}{N_b - 1}, \mathcal{W}\left(\frac{j}{N_b - 1}\right)\right) = \left(\frac{j}{N_b - 1}, \frac{1}{1 - \lambda} \cos\left(\frac{2\pi j}{N_b - 1}\right)\right)$$

is also **the fixed point** of the map T_j introduced in Property 2.2.

Property 2.9.

For $0 \leq j \leq \frac{(N_b - 1)}{2}$ (resp., for $\frac{(N_b - 1)}{2} \leq j \leq N_b - 1$), we have that

$$\mathcal{W}\left(\frac{j+1}{N_b - 1}\right) - \mathcal{W}\left(\frac{j}{N_b - 1}\right) \leq 0 \quad \left(\text{resp., } \mathcal{W}\left(\frac{j+1}{N_b - 1}\right) - \mathcal{W}\left(\frac{j}{N_b - 1}\right) \geq 0\right).$$

Proof. For any integer j in $\{0, \dots, N_b - 1\}$,

$$\mathcal{W}\left(\frac{j+1}{N_b - 1}\right) - \mathcal{W}\left(\frac{j}{N_b - 1}\right) = \frac{1}{1 - \lambda} \left(\cos\left(\frac{2\pi(j+1)}{N_b - 1}\right) - \cos\left(\frac{2\pi j}{N_b - 1}\right) \right).$$

i. For $0 \leq j \leq \frac{N_b - 1}{2}$:

$$0 \leq \frac{2\pi j}{N_b - 1} \leq \pi \quad , \quad 0 \leq \frac{2\pi(j+1)}{N_b - 1} \leq \pi \left(1 + \frac{2}{N_b - 1}\right).$$

The limit case

$$\frac{2\pi(j+1)}{N_b - 1} = \pi \left(1 + \frac{2}{N_b - 1}\right)$$

only occurs when the integer N_b is odd, for the value $j = \frac{N_b - 1}{2}$, and corresponds to the bottom vertex of the initial polygon \mathcal{P}_0 . In this case, one has

$$\mathcal{W}\left(\frac{N_b - 1}{2}\right) = -\frac{1}{1 - \lambda}.$$

This case can thus be left aside.

One may therefore only consider the cases when $0 \leq \frac{2\pi j}{N_b - 1} \leq \frac{2\pi(j+1)}{N_b - 1} \leq \pi$.

The cosine function being nonincreasing on $[0, \pi]$, one obtains the expected result:

$$\mathscr{W}\left(\frac{j+1}{N_b-1}\right) - \mathscr{W}\left(\frac{j}{N_b-1}\right) \leq 0.$$

ii. For $\frac{(N_b-1)}{2} \leq j \leq N_b-1$:

$$\pi \leq \frac{2\pi j}{N_b-1} \leq 2\pi \quad , \quad \pi \left(1 + \frac{2}{N_b-1}\right) \leq \frac{2\pi(j+1)}{N_b-1} \leq \frac{2\pi N_b}{N_b-1}.$$

As previously, the limit case

$$\frac{2\pi(j+1)}{N_b-1} = \pi \left(1 + \frac{2}{N_b-1}\right)$$

can be left aside. The increasing property of the cosine function on $[\pi, 2\pi]$ then yields the expected result:

$$\mathscr{W}\left(\frac{j+1}{N_b-1}\right) - \mathscr{W}\left(\frac{j}{N_b-1}\right) \geq 0.$$

□

Notation 7 (Signum Function).

The *signum function* of a real number x is defined by

$$\text{sgn}(x) = \begin{cases} -1, & \text{if } x < 0, \\ 0, & \text{if } x = 0, \\ +1, & \text{if } x > 0. \end{cases}$$

Property 2.10. *Given any strictly positive integer m , we have the following properties:*

i. For any j in $\{0, \dots, \#V_m\}$, the point

$$\left(\frac{j}{(N_b-1)N_b^m}, \mathscr{W}\left(\frac{j}{(N_b-1)N_b^m}\right)\right)$$

is the image of the point

$$\left(\frac{j}{(N_b-1)N_b^{m-1}} - i, \mathscr{W}\left(\frac{j}{(N_b-1)N_b^{m-1}} - i\right)\right) = \left(\frac{j - i(N_b-1)N_b^{m-1}}{(N_b-1)N_b^{m-1}}, \mathscr{W}\left(\frac{j - i(N_b-1)N_b^{m-1}}{(N_b-1)N_b^{m-1}}\right)\right)$$

under the map T_i , $0 \leq i \leq N_b-1$.

Consequently, for $0 \leq j \leq N_b - 1$, the j^{th} vertex of the polygon $\mathcal{P}_{m,k}$, $0 \leq k \leq N_b^m - 1$, i.e., the point

$$\left(\frac{(N_b - 1)k + j}{(N_b - 1)N_b^m}, \mathscr{W} \left(\frac{(N_b - 1)k + j}{(N_b - 1)N_b^m} \right) \right)$$

is the image of the point

$$\left(\frac{(N_b - 1)(k - i(N_b - 1)N_b^{m-1}) + j}{(N_b - 1)N_b^{m-1}}, \mathscr{W} \left(\frac{(N_b - 1)(k - i(N_b - 1)N_b^{m-1}) + j}{(N_b - 1)N_b^{m-1}} \right) \right);$$

it is also the j^{th} vertex of the polygon $\mathcal{P}_{m-1,k-i(N_b-1)N_b^{m-1}}$. Therefore, there is an exact correspondance between vertices of the polygons at consecutive steps $m - 1$, m .

ii. Given j in $\{0, \dots, N_b - 2\}$ and k in $\{0, \dots, N_b^m - 1\}$, we have that

$$\text{sgn} \left(\mathscr{W} \left(\frac{k(N_b - 1) + j + 1}{(N_b - 1)N_b^m} \right) - \mathscr{W} \left(\frac{k(N_b - 1) + j}{(N_b - 1)N_b^m} \right) \right) = \text{sgn} \left(\mathscr{W} \left(\frac{j + 1}{N_b - 1} \right) - \mathscr{W} \left(\frac{j}{N_b - 1} \right) \right).$$

Proof.

i. One simply applies Proposition 2.3, in conjunction with Property 2.8.

For i in $\{0, \dots, N_b - 1\}$, we have that

$$\begin{aligned} & T_i \left(\frac{j - i(N_b - 1)N_b^{m-1}}{(N_b - 1)N_b^{m-1}}, \mathscr{W} \left(\frac{j - i(N_b - 1)N_b^{m-1}}{(N_b - 1)N_b^{m-1}} \right) \right) \\ & \quad || \\ & \left(\frac{j - i(N_b - 1)N_b^{m-1}}{(N_b - 1)N_b^m} + \frac{i}{N_b}, \lambda \mathscr{W} \left(\frac{j - i(N_b - 1)N_b^{m-1}}{(N_b - 1)N_b^{m-1}} \right) + \cos \left(2\pi \left(\frac{j - i(N_b - 1)N_b^{m-1}}{(N_b - 1)N_b^m} + \frac{i}{N_b} \right) \right) \right) \\ & = \left(\frac{j}{(N_b - 1)N_b^m}, \mathscr{W} \left(\frac{j}{(N_b - 1)N_b^{m-1}} - i \right) + \cos \left(2\pi \frac{j}{(N_b - 1)N_b^m} \right) \right) \\ & = \left(\frac{j}{(N_b - 1)N_b^m}, \mathscr{W} \left(\frac{j}{(N_b - 1)N_b^{m-1}} - i \right) + \cos \left(2\pi \frac{j - i}{(N_b - 1)N_b^m} + \frac{i}{N_b} \right) \right) \\ & = \left(\frac{j}{(N_b - 1)N_b^m}, \lambda \mathscr{W} \left(\frac{j}{(N_b - 1)N_b^{m-1}} \right) + \cos \left(2\pi \frac{j - i}{(N_b - 1)N_b^m} \right) \right) \\ & = \left(\frac{j}{(N_b - 1)N_b^m}, \mathscr{W} \left(\frac{j}{(N_b - 1)N_b^m} \right) \right). \end{aligned}$$

ii. We prove the result by induction on m . Accordingly, let us consider j in $\{0, \dots, N_b - 2\}$.

The result at *the initial step* $m = 1$ is satisfied, in so far as, for any integer k in $\{0, \dots, N_b - 1\}$:

$$\begin{aligned}
\mathcal{W}\left(\frac{k(N_b - 1) + j + 1}{(N_b - 1)N_b}\right) - \mathcal{W}\left(\frac{k(N_b - 1) + j}{(N_b - 1)N_b}\right) &= \lambda \left(\mathcal{W}\left(\frac{k(N_b - 1) + j + 1}{N_b - 1}\right) - \mathcal{W}\left(\frac{k(N_b - 1) + j}{N_b - 1}\right) \right) \\
&\quad + \cos\left(\frac{2\pi(k(N_b - 1) + j + 1)}{N_b - 1}\right) - \cos\left(\frac{2\pi(k(N_b - 1) + j)}{N_b - 1}\right) \\
&= \lambda \left(\mathcal{W}\left(k + \frac{j + 1}{N_b - 1}\right) - \mathcal{W}\left(k + \frac{j}{N_b - 1}\right) \right) \\
&\quad + \cos\left(\frac{2\pi(j + 1)}{N_b - 1}\right) - \cos\left(\frac{2\pi j}{N_b - 1}\right) \\
&= \lambda \left(\mathcal{W}\left(\frac{j + 1}{N_b - 1}\right) - \mathcal{W}\left(\frac{j}{N_b - 1}\right) \right) \\
&\quad + \mathcal{W}\left(\frac{j + 1}{N_b - 1}\right) - \mathcal{W}\left(\frac{j}{N_b - 1}\right) \\
&= (1 + \lambda) \left(\mathcal{W}\left(\frac{j + 1}{N_b - 1}\right) - \mathcal{W}\left(\frac{j}{N_b - 1}\right) \right).
\end{aligned}$$

Let us now assume that, for any integer k in $\{0, \dots, N_b^{m-1} - 1\}$,

$$\operatorname{sgn} \left(\mathcal{W}\left(\frac{k(N_b - 1) + j + 1}{(N_b - 1)N_b^m}\right) - \mathcal{W}\left(\frac{k(N_b - 1) + j}{(N_b - 1)N_b^m}\right) \right) = \operatorname{sgn} \left(\mathcal{W}\left(\frac{j + 1}{N_b - 1}\right) - \mathcal{W}\left(\frac{j}{N_b - 1}\right) \right).$$

Henceforth, we want to prove that, for any integer k in $\{0, \dots, N_b^{m-1} - 1\}$,

$$\operatorname{sgn} \left(\mathcal{W}\left(\frac{k(N_b - 1) + j + 1}{(N_b - 1)N_b^m}\right) - \mathcal{W}\left(\frac{k(N_b - 1) + j}{(N_b - 1)N_b^m}\right) \right) = \operatorname{sgn} \left(\mathcal{W}\left(\frac{j + 1}{N_b - 1}\right) - \mathcal{W}\left(\frac{j}{N_b - 1}\right) \right).$$

The induction hypothesis will be used in so far as any k in $\{0, \dots, N_b^{m-1} - 1\}$ can also be expressed in the following form:

$$k = \tilde{k} + i N_b^{m-1}, \quad 0 \leq \tilde{k} \leq N_b^{m-1} - 1, \quad 0 \leq i \leq N_b - 1.$$

This will be useful because of *the one-periodicity of the \mathcal{W} -function*, since, for any real number x and any integer i , we have that

$$\mathcal{W}(x + i) = \mathcal{W}(x).$$

Due to the symmetry with respect to the vertical line $x = \frac{1}{2}$ (see Property 2.1), given a natural integer m , one can, in addition, restrict oneself to the cases when

$$0 \leq (N_b - 1)k + j < (N_b - 1)k + j + 1 \leq \left\lceil \frac{(N_b - 1)N_b^m + 1}{2} \right\rceil = \frac{(N_b - 1)N_b^m}{2},$$

which yields

$$0 \leq \frac{(2(N_b - 1)k + 2j - 1)\pi}{2(N_b - 1)N_b^m} < \frac{(2(N_b - 1)k + 2j + 1)\pi}{(N_b - 1)N_b^m} \leq \pi.$$

Thus, we only have to consider the cases when

$$\sin\left(\frac{(2(N_b - 1)k + 2j - 1)\pi}{(N_b - 1)N_b^m}\right) \geq 0 \quad \text{and} \quad \sin\left(\frac{(2(N_b - 1)k + 2j + 1)\pi}{(N_b - 1)N_b^m}\right) \geq 0.$$

The remaining ones, namely, the cases when

$$\sin\left(\frac{(2(N_b - 1)k + 2j - 1)\pi}{(N_b - 1)N_b^m}\right) \leq 0 \quad \text{and} \quad \sin\left(\frac{(2(N_b - 1)k + 2j + 1)\pi}{(N_b - 1)N_b^m}\right) \leq 0,$$

are then obtained by symmetry.

Hence,

$$\begin{aligned} & \mathscr{W}\left(\frac{k(N_b - 1) + j + 1}{(N_b - 1)N_b^m}\right) - \mathscr{W}\left(\frac{j}{(N_b - 1)N_b^m}\right) \\ & \quad || \\ &= \lambda \left(\mathscr{W}\left(\frac{k(N_b - 1) + j + 1}{(N_b - 1)N_b^{m-1}}\right) - \mathscr{W}\left(\frac{k(N_b - 1) + j}{(N_b - 1)N_b^{m-1}}\right) \right) \\ & \quad + \cos\left(\frac{2\pi(k(N_b - 1) + j + 1)}{(N_b - 1)N_b^{m-1}}\right) - \cos\left(\frac{2\pi(k(N_b - 1) + j)}{(N_b - 1)N_b^{m-1}}\right) \\ &= \lambda \left(\mathscr{W}\left(\frac{k(N_b - 1) + j + 1}{(N_b - 1)N_b^{m-1}}\right) - \mathscr{W}\left(\frac{k(N_b - 1) + j}{(N_b - 1)N_b^{m-1}}\right) \right) \\ & \quad - 2 \sin\left(\frac{\pi}{(N_b - 1)N_b^{m-1}}\right) \sin\left(\frac{(2(N_b - 1)k + 2j + 1)\pi}{(N_b - 1)N_b^{m-1}}\right) \\ &= \lambda \left(\mathscr{W}\left(\frac{\tilde{k}(N_b - 1) + i(N_b - 1)N_b^{m-1} + j + 1}{(N_b - 1)N_b^{m-1}}\right) - \mathscr{W}\left(\frac{\tilde{k}(N_b - 1) + i(N_b - 1)N_b^{m-1} + j}{(N_b - 1)N_b^{m-1}}\right) \right) \\ & \quad - 2 \sin\left(\frac{\pi}{(N_b - 1)N_b^{m-1}}\right) \sin\left(\frac{(2(N_b - 1)k + 2j + 1)\pi}{(N_b - 1)N_b^{m-1}}\right) \\ &= \lambda \left(\mathscr{W}\left(i + \frac{\tilde{k}(N_b - 1) + j + 1}{(N_b - 1)N_b^{m-1}}\right) - \mathscr{W}\left(i + \frac{\tilde{k}(N_b - 1) + j}{(N_b - 1)N_b^{m-1}}\right) \right) \\ & \quad - 2 \sin\left(\frac{\pi}{(N_b - 1)N_b^{m-1}}\right) \sin\left(\frac{(2(N_b - 1)k + 2j + 1)\pi}{(N_b - 1)N_b^{m-1}}\right) \\ &= \lambda \left(\mathscr{W}\left(\frac{\tilde{k}(N_b - 1) + j + 1}{(N_b - 1)N_b^{m-1}}\right) - \mathscr{W}\left(\frac{\tilde{k}(N_b - 1) + j}{(N_b - 1)N_b^{m-1}}\right) \right) \\ & \quad - 2 \sin\left(\frac{\pi}{(N_b - 1)N_b^{m-1}}\right) \sin\left(\frac{(2(N_b - 1)k + 2j + 1)\pi}{(N_b - 1)N_b^{m-1}}\right). \end{aligned}$$

In the case when

$$0 \leq (N_b - 1)k + j + 1 \leq \left\lceil \frac{(N_b - 1)N_b^m + 1}{2} \right\rceil = \frac{(N_b - 1)N_b^m}{2},$$

one thus has

$$-2 \sin\left(\frac{\pi}{(N_b - 1) N_b^{m-1}}\right) \sin\left(\frac{(2(N_b - 1)k + 2j - 1)\pi}{(N_b - 1) N_b^{m-1}}\right) \leq 0.$$

The configuration of the initial polygon ensures, for $0 \leq j \leq \frac{N_b - 1}{2}$, that

$$\mathscr{W}\left(\frac{j+1}{N_b - 1}\right) - \mathscr{W}\left(\frac{j}{N_b - 1}\right) \leq 0$$

and therefore, thanks to the induction hypothesis,

$$\mathscr{W}\left(\frac{\tilde{k}(N_b - 1) + j + 1}{(N_b - 1) N_b^{m-1}}\right) - \mathscr{W}\left(\frac{\tilde{k}(N_b - 1) + j}{(N_b - 1) N_b^{m-1}}\right) \leq 0.$$

By induction, one thus obtains, for any natural integer m , any k in $\{0, \dots, N_b^m - 1\}$, and any j in $\{0, \dots, \frac{N_b - 3}{2}\}$, that

$$\mathscr{W}\left(\frac{(N_b - 1)k + j + 1}{(N_b - 1) N_b^m}\right) - \mathscr{W}\left(\frac{(N_b - 1)k + j}{(N_b - 1) N_b^m}\right) \leq 0,$$

as required. \square

Corollary 2.11 (Lower Bound for the Elementary Heights (Coming from Property 2.10)).

For any strictly positive integer m , and any j in $\{0, \dots, (N_b - 1) N_b^m\}$, we have that

$$\left| \mathscr{W}\left(\frac{j+1}{(N_b - 1) N_b^m}\right) - \mathscr{W}\left(\frac{j}{(N_b - 1) N_b^m}\right) \right| \geq \lambda \left| \mathscr{W}\left(\frac{j+1}{(N_b - 1) N_b^{m-1}}\right) - \mathscr{W}\left(\frac{j}{(N_b - 1) N_b^{m-1}}\right) \right|,$$

which yields, by induction,

$$\left| \mathscr{W}\left(\frac{j+1}{(N_b - 1) N_b^m}\right) - \mathscr{W}\left(\frac{j}{(N_b - 1) N_b^m}\right) \right| \geq \underbrace{\lambda^m}_{N_b^{m(D_{\mathscr{W}} - 2)}} \left| \mathscr{W}\left(\frac{j+1}{N_b - 1}\right) - \mathscr{W}\left(\frac{j}{N_b - 1}\right) \right|.$$

This improves our previous result in [Dav18].

Corollary 2.12 (Upper Bound for the Elementary Heights (Coming from Property 2.10)).

For any strictly positive integer m , and any j in $\{0, \dots, (N_b - 1) N_b^m\}$, we have that

$$\begin{aligned} \left| \mathscr{W}\left(\frac{j+1}{(N_b - 1) N_b^m}\right) - \mathscr{W}\left(\frac{j}{(N_b - 1) N_b^m}\right) \right| &\leq \lambda^m \left(\left| \mathscr{W}\left(\frac{j+1}{N_b - 1}\right) - \mathscr{W}\left(\frac{j}{N_b - 1}\right) \right| + \frac{2\pi N_b}{(N_b - 1) N_b^m (N_b - \lambda)} \right) \\ &\leq \underbrace{\lambda^m}_{N_b^{m(D_{\mathscr{W}} - 2)}} \left(\left| \mathscr{W}\left(\frac{j+1}{N_b - 1}\right) - \mathscr{W}\left(\frac{j}{N_b - 1}\right) \right| + \frac{2\pi N_b}{(N_b - 1) (N_b - \lambda)} \right), \end{aligned}$$

which also improves our previous result in [Dav18].

Proof. For any strictly positive integer m and any j in $\{0, \dots, (N_b - 1) N_b^m\}$, we have the following estimates:

$$\begin{aligned}
\left| \mathcal{W} \left(\frac{j+1}{(N_b-1) N_b^m} \right) - \mathcal{W} \left(\frac{j}{(N_b-1) N_b^m} \right) \right| &\leq \lambda \left| \mathcal{W} \left(\frac{j+1}{(N_b-1) N_b^{m-1}} \right) - \mathcal{W} \left(\frac{j}{(N_b-1) N_b^{m-1}} \right) \right| \\
&\quad + \left| \cos \left(\frac{2\pi(j+1)}{(N_b-1) N_b^{m-1}} \right) - \cos \left(\frac{2\pi j}{(N_b-1) N_b^{m-1}} \right) \right| \\
&\leq \lambda \left| \mathcal{W} \left(\frac{j+1}{(N_b-1) N_b^{m-1}} \right) - \mathcal{W} \left(\frac{j}{(N_b-1) N_b^{m-1}} \right) \right| \\
&\quad + \frac{2\pi}{(N_b-1) N_b^{m-1}},
\end{aligned}$$

which yields, by induction,

$$\begin{aligned}
\left| \mathcal{W} \left(\frac{j+1}{(N_b-1) N_b^m} \right) - \mathcal{W} \left(\frac{j}{(N_b-1) N_b^m} \right) \right| &\leq \lambda^m \left| \mathcal{W} \left(\frac{j+1}{N_b-1} \right) - \mathcal{W} \left(\frac{j}{N_b-1} \right) \right| + \sum_{k=0}^{m-1} \lambda^k \frac{2\pi}{(N_b-1) N_b^k} \\
&= \lambda^m \left| \mathcal{W} \left(\frac{j+1}{N_b-1} \right) - \mathcal{W} \left(\frac{j}{N_b-1} \right) \right| + \frac{2\pi \lambda^m}{(N_b-1) N_b^m \left(1 - \frac{\lambda}{N_b} \right)} \\
&= \lambda^m \left(\left| \mathcal{W} \left(\frac{j+1}{N_b-1} \right) - \mathcal{W} \left(\frac{j}{N_b-1} \right) \right| + \frac{2\pi N_b}{(N_b-1) N_b^m (N_b - \lambda)} \right),
\end{aligned}$$

as desired. \square

Remark 2.4. Corollaries 2.11 and 2.12 are important, because they enable one to obtain exact and more accurate values of the bounding constants C_{inf} and C_{sup} involved in the following inequality:

$$C_{inf} L_m^{2-D_{\mathcal{W}}} \leq |\mathcal{W}((j+1) L_m) - \mathcal{W}(j L_m)| \leq C_{sup} L_m^{2-D_{\mathcal{W}}} \quad , \quad m \in \mathbb{N}, 0 \leq j \leq (N_b - 1) N_b^m, \quad (\spadesuit)$$

where

$$C_{inf} = (N_b - 1)^{2-D_{\mathcal{W}}} \left| \mathcal{W} \left(\frac{j+1}{N_b-1} \right) - \mathcal{W} \left(\frac{j}{N_b-1} \right) \right|$$

and

$$C_{sup} = (N_b - 1)^{2-D_{\mathcal{W}}} \left(\left| \mathcal{W} \left(\frac{j+1}{N_b-1} \right) - \mathcal{W} \left(\frac{j}{N_b-1} \right) \right| + \frac{2\pi N_b}{(N_b-1) (N_b - \lambda)} \right) = C_{inf} + \frac{2\pi N_b (N_b - 1)^{1-D_{\mathcal{W}}}}{(N_b - \lambda)}.$$

One should note, in addition, that *these constants depend on the initial polygon \mathcal{P}_0 .*

Theorem 2.13 (Sharp Local Discrete Reverse Hölder Properties of the Weierstrass Function (Corollary of 2.11)).

For any natural integer m , let us consider a pair of real numbers (x, x') such that

$$x = \frac{(N_b - 1)k + j}{(N_b - 1)N_b^m} = ((N_b - 1)k + j) L_m \quad , \quad x' = \frac{(N_b - 1)k + j + \ell}{(N_b - 1)N_b^m} = ((N_b - 1)k + j + \ell) L_m ,$$

where $0 \leq k \leq N_b - 1^m - 1$, and

i. if the integer N_b is odd,

$$0 \leq j < \frac{N_b - 1}{2} \quad \text{and} \quad 0 < j + \ell \leq \frac{N_b - 1}{2}$$

or

$$\frac{N_b - 1}{2} \leq j < N_b - 1 \quad \text{and} \quad \frac{N_b - 1}{2} < j + \ell \leq N_b - 1 ;$$

ii. if the integer N_b is even,

$$0 \leq j < \frac{N_b}{2} \quad \text{and} \quad 0 < j + \ell \leq \frac{N_b}{2}$$

or

$$\frac{N_b}{2} + 1 \leq j < N_b - 1 \quad \text{and} \quad \frac{N_b}{2} + 1 < j + \ell \leq N_b - 1 ,$$

This means that the points $(x, \mathcal{W}(x))$ and $(x', \mathcal{W}(x'))$ are vertices of the polygon $\mathcal{P}_{m,k}$ (see Property 2.4 above), both located on the left-side of the polygon, or on the right-side; see Figure 6.

Then, one has the following (discrete, local) reverse-Hölder inequality, with sharp Hölder exponent $-\frac{\ln \lambda}{\ln N_b} = 2 - D_{\mathcal{W}}$,

$$C_{inf} |x' - x|^{2-D_{\mathcal{W}}} \leq |\mathcal{W}(x') - \mathcal{W}(x)| .$$

Proof. In the light of Property 2.9, one can restrict oneself to the case when

$$0 \leq j < \frac{N_b - 1}{2} \quad \text{and} \quad 0 < j + \ell \leq \frac{N_b - 1}{2} .$$

The expected result in the remaining case can easily be proved in a similar way. Since

$$\mathcal{W}(((N_b - 1)k + j + \ell) L_m) \leq \dots \leq \mathcal{W}(((N_b - 1)k + j + 1) L_m) \leq \mathcal{W}(((N_b - 1)k + j) L_m)$$

then, by applying the results of Remark 2.4, we have the following ℓ inequalities:

$$C_{inf} L_m^{2-D_{\mathcal{W}}} \leq -\mathcal{W}(((N_b - 1)k + j + 1) L_m) + \mathcal{W}(((N_b - 1)k + j) L_m)$$

$$C_{inf} L_m^{2-D_{\mathcal{W}}} \leq -\mathcal{W}(((N_b - 1)k + j + 2) L_m) + \mathcal{W}(((N_b - 1)k + j + 1) L_m)$$

.....

$$C_{inf} L_m^{2-D_{\mathcal{W}}} \leq -\mathcal{W}(((N_b - 1)k + j + \ell) L_m) + \mathcal{W}(((N_b - 1)k + \ell - 1) L_m) .$$

Thus, upon summation, we obtain that

$$\ell C_{inf} L_m^{2-D_{\mathcal{W}}} \leq -\mathcal{W}(((N_b - 1)k + j + \ell) L_m) + \mathcal{W}(((N_b - 1)k + j) L_m) .$$

Since $\ell \geq \ell^{2-D_{\mathcal{W}}}$ and $|x' - x| = \ell L_m$, one deduces the desired result. □

Remark 2.5. Thus far, no such *reverse Hölder estimates* had been obtained for the Weierstrass function. The fact that they are discrete ones is natural, since the Weierstrass Curve is approximated by a sequence of polygonal prefractal finite graphs. Recall that the countable set of vertices of all of these graphs is dense in the whole Weierstrass Curve.

Corollary 2.14 (Optimal Hölder Exponent for the Weierstrass Function).

The local reverse Hölder property of Theorem 2.13 – in conjunction with the Hölder condition satisfied by the Weierstrass function (see also [Zyg02], Chapter II, Theorem 4.9, page 47) – shows that the Codimension $2 - D_{\mathcal{W}} = -\frac{\ln \lambda}{\ln N_b} \in]0, 1[$ is the best (i.e., optimal) Hölder exponent for the Weierstrass function (as was originally shown, by a completely different method, by G. H. Hardy in [Har16]).

Note that, as a consequence, since the Hölder exponent is strictly smaller than one, the Weierstrass function \mathcal{W} is nowhere differentiable.

Remark 2.6. Indeed, if \mathcal{W} were differentiable at some point $x_0 \in [0, 1]$, then it would have to be locally Lipschitz at x_0 , and hence, its Hölder exponent at x_0 would be equal to 1, which is impossible.

Corollary 2.15 (Coming from Property 2.10).

Thanks to Remark 2.4, one may now write, for any strictly positive integer m and any integer j in $\{0, \dots, (N_b - 1) N_b^m - 1\}$:

i. for the elementary heights:

$$h_{j-1,j,m} = L_m^{2-D_{\mathcal{W}}} \mathcal{O}(1) ;$$

ii. for the elementary quotients:

$$\frac{h_{j-1,j,m}}{L_m} = L_m^{1-D_{\mathcal{W}}} \mathcal{O}(1) ,$$

as follows from Remark 2.4 above, and where

$$C_{inf} \leq \mathcal{O}(1) \leq C_{sup} .$$

Corollary 2.16 (Nonincreasing Sequence of Geometric Angles (Coming from Property 2.10)).

For the **geometric angles** $\theta_{j-1,j,m}$, $0 \leq j \leq (N_b - 1) N_b^m - 1$, $m \in \mathbb{N}$, we have the following result:

$$\tan \theta_{j-1,j,m} = \frac{L_m}{h_{j-1,j,m}} (N_b - 1) > \tan \theta_{j-1,j,m+1},$$

which yields

$$\theta_{j-1,j,m} > \theta_{j-1,j,m+1} \quad \text{and} \quad \theta_{j-1,j,m+1} \lesssim L_m^{D_{\mathcal{W}}-1}.$$

Proof.

i. One simply writes, successively:

$$\begin{aligned} \tan \theta_{j-1,j,m} &= \frac{L_m}{\left| \mathcal{W} \left(\frac{j}{(N_b - 1) N_b^m} \right) - \mathcal{W} \left(\frac{j-1}{(N_b - 1) N_b^m} \right) \right|} \\ &\geq \frac{\lambda L_m}{\left| \mathcal{W} \left(\frac{j}{(N_b - 1) N_b^{m+1}} \right) - \mathcal{W} \left(\frac{j-1}{(N_b - 1) N_b^{m+1}} \right) \right|} \\ &= \frac{\lambda (N_b - 1) N_b L_{m+1}}{\left| \mathcal{W} \left(\frac{j}{(N_b - 1) N_b^{m+1}} \right) - \mathcal{W} \left(\frac{j-1}{(N_b - 1) N_b^{m+1}} \right) \right|} \\ &= \lambda (N_b - 1) N_b \tan \theta_{j-1,j,m+1} \\ &> (N_b - 1) \tan \theta_{j-1,j,m+1} \end{aligned}$$

since $\lambda N_b > 1$. Then, i. holds.

ii. One also has

$$\theta_{j-1,j,m+1} < \arctan \frac{(N_b - 1) L_m}{h_{j-1,j,m}},$$

where

$$h_{j-1,j,m} = L_m^{2-D_{\mathcal{W}}} \mathcal{O}(1) \quad \text{and} \quad C_{inf} \leq \mathcal{O}(1) \leq C_{sup}.$$

This yields

$$\frac{(N_b - 1) L_m}{h_{j-1,j,m}} = L_m^{D_{\mathcal{W}}-1} \mathcal{O}(1) \quad \text{and} \quad (N_b - 1) C_{inf} \leq \mathcal{O}(1) \leq (N_b - 1) C_{sup}.$$

Consequently, $\theta_{j-1,j,m+1} \lesssim L_m^{D_{\mathcal{W}}-1}$, as claimed. □

Corollary 2.17 (Local Extrema of the Weierstrass Function (Coming from Property 2.10)).

i. The set of local maxima of the Weierstrass function on the interval $[0, 1]$ is given by

$$\left\{ \left(\frac{(N_b - 1)k}{N_b^m}, \mathcal{W} \left(\frac{(N_b - 1)k}{N_b^m} \right) \right) : 0 \leq k \leq N_b^m - 1, m \in \mathbb{N} \right\},$$

and corresponds to the extreme vertices of the polygons at a given step m (vertices connecting consecutive polygons).

ii. For odd values of N_b , the set of local minima of the Weierstrass function on the interval $[0, 1]$ is given by

$$\left\{ \left(\frac{(N_b - 1)k + \frac{N_b - 1}{2}}{(N_b - 1)N_b^m}, \mathcal{W} \left(\frac{(N_b - 1)k + \frac{N_b - 1}{2}}{(N_b - 1)N_b^m} \right) \right) : 0 \leq k \leq N_b^m - 1, m \in \mathbb{N} \right\},$$

and corresponds to the bottom vertices of the polygons at a given step m .

Property 2.18 (Existence of Reentrant Angles).

i. The initial polygon \mathcal{P}_0 , admits **reentrant interior angles**, at a vertex P_j , with $0 < j \leq N_b - 1$, in the sense that, with the right-hand rule, according to which angles are measured in a counter-clockwise direction $((P_j P_{j+1}), (P_j P_{j-1})) > \pi$, in the case when

$$0 < j \leq \frac{N_b - 3}{4} \quad \text{or} \quad \frac{3N_b - 1}{4} \leq j < N_b - 1$$

(see Figure 7), which does not occur for values of $N_b < 7$.

The number of reentrant angles is then equal to $2 \left\lceil \frac{N_b - 3}{4} \right\rceil$.

ii. At a given step $m \in \mathbb{N}^*$, with the above convention, a polygon $\mathcal{P}_{m,k}$ admits reentrant interior angles in the sole cases when $N_b \geq 7$, at vertices M_{k+j} , $1 \leq k \leq N_b^m$, $0 < j \leq N_b - 1$, as well as in the case when

$$0 < j \leq \frac{N_b - 3}{4} \quad \text{or} \quad \frac{3N_b - 1}{4} \leq j < N_b - 1.$$

The number of reentrant angles is then equal to $2 N_b^m \left\lceil \frac{N_b - 3}{4} \right\rceil$.

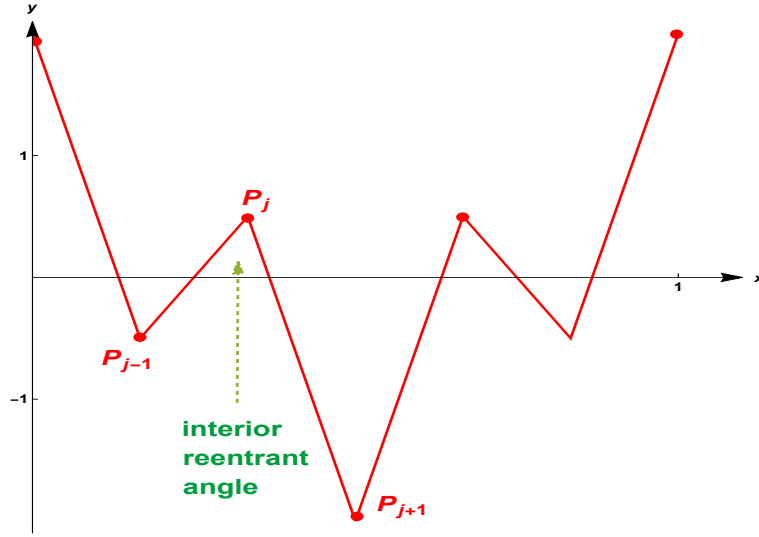


Figure 7: **An interior reentrant angle.** Here, $N_b = 7$ and $\lambda = \frac{1}{2}$.

Proof.

i. Due to the symmetry with respect to the vertical line $x = \frac{1}{2}$ (see Property 2.1), one can restrict oneself to the vertices P_j , with $0 < j < \frac{N_b - 1}{2}$.

The initial polygon \mathcal{P}_0 , admits reentrant interior angles at a vertex P_j , with $j + 1 < \frac{N_b - 1}{2}$, in the case when

$$((y'y), \widehat{(P_{j-1}P_j)}) > ((y'y), \widehat{(P_jP_{j+1})}) \quad (\spadesuit)$$

Since

$$P_j = (x_j, y_j) = \left(\frac{j}{N_b - 1}, \mathcal{W} \left(\frac{j}{N_b - 1} \right) \right) = \left(\frac{j}{N_b - 1}, \frac{1}{1 - \lambda} \cos \left(\frac{2\pi j}{N_b - 1} \right) \right),$$

one has

$$\tan((y'y), \widehat{(P_{j-1}P_j)}) = \frac{L_0}{\left| \mathcal{W} \left(\frac{j}{N_b - 1} \right) - \mathcal{W} \left(\frac{j-1}{N_b - 1} \right) \right|}$$

and

$$\tan((y'y), \widehat{(P_jP_{j+1})}) = \frac{L_0}{\left| \mathcal{W} \left(\frac{j+1}{N_b - 1} \right) - \mathcal{W} \left(\frac{j}{N_b - 1} \right) \right|},$$

where $L_0 = \frac{1}{N_b - 1}$.

Therefore, condition (\spadesuit) above corresponds to the case when

$$\left| \mathcal{W} \left(\frac{j+1}{N_b - 1} \right) - \mathcal{W} \left(\frac{j}{N_b - 1} \right) \right| > \left| \mathcal{W} \left(\frac{j}{N_b - 1} \right) - \mathcal{W} \left(\frac{j-1}{N_b - 1} \right) \right|,$$

i.e.,

$$\left| \cos\left(\frac{2\pi(j+1)}{N_b-1}\right) - \cos\left(\frac{2\pi j}{N_b-1}\right) \right| > \left| \cos\left(\frac{2\pi j}{N_b-1}\right) - \cos\left(\frac{2\pi(j-1)}{N_b-1}\right) \right|,$$

or, equivalently,

$$\left| 2 \sin \frac{\pi}{N_b-1} \sin\left(\frac{\pi(2j+1)}{N_b-1}\right) \right| > \left| 2 \sin \frac{\pi}{N_b-1} \sin\left(\frac{\pi(2j-1)}{N_b-1}\right) \right|,$$

and thus happens if

$$\left| \sin\left(\frac{\pi(2j+1)}{N_b-1}\right) \right| > \left| \sin\left(\frac{\pi(2j-1)}{N_b-1}\right) \right|.$$

Since

$$0 < \frac{\pi(2j-1)}{N_b-1} < \frac{\pi(2j+1)}{N_b-1} < \pi,$$

we conclude that condition (\spadesuit) occurs if

$$0 < \pi(2j-1)N_b-1 < \frac{\pi(2j+1)}{N_b-1} \leq \frac{\pi}{2},$$

i.e., if $0 < j \leq \frac{N_b-3}{4}$.

For vertices P_j , with $\frac{N_b+1}{2} < j < N_b-1$, the result is obtained thanks to the aforementioned symmetry. The initial polygon \mathcal{P}_0 , admits **reentrant interior angles** at a vertex P_j in the case when $\frac{3N_b-1}{4} \leq j < N_b-1$.

ii. The result is obtained by strong induction on the integer m . We restrict ourselves to the values $N_b \geq 7$, and consider j in $\left\{0, \dots, \left\lfloor \frac{N_b-3}{4} \right\rfloor\right\}$.

We claim that the result is satisfied at *the initial step* $m = 1$. Indeed, as was already encountered in the proof of Property 2.10, for any integer k in $\{0, \dots, N_b-1\}$, we have that

$$\left| \mathcal{W}\left(\frac{k(N_b-1)+j+1}{(N_b-1)N_b}\right) - \mathcal{W}\left(\frac{j}{(N_b-1)N_b}\right) \right| = \left| (1+\lambda) \left\{ \mathcal{W}\left(\frac{j+1}{N_b-1}\right) - \mathcal{W}\left(\frac{j}{N_b-1}\right) \right\} \right|$$

and

$$\left| \mathcal{W}\left(\frac{k(N_b-1)+j}{(N_b-1)N_b}\right) - \mathcal{W}\left(\frac{j-1}{(N_b-1)N_b}\right) \right| = \left| (1+\lambda) \left\{ \mathcal{W}\left(\frac{j}{N_b-1}\right) - \mathcal{W}\left(\frac{j-1}{N_b-1}\right) \right\} \right|.$$

Thus,

$$\begin{aligned} \frac{\tan \theta_{k(N_b-1)+j-1, k(N_b-1)+j, 1}}{\tan \theta_{k(N_b-1)+j, k(N_b-1)+j+1, 1}} &= \frac{\left| \mathcal{W} \left(\frac{k(N_b-1)+j+1}{(N_b-1)N_b} \right) - \mathcal{W} \left(\frac{k(N_b-1)+j}{(N_b-1)N_b} \right) \right|}{\left| \mathcal{W} \left(\frac{k(N_b-1)+j}{(N_b-1)N_b} \right) - \mathcal{W} \left(\frac{k(N_b-1)+j-1}{(N_b-1)N_b} \right) \right|}} \\ &= \frac{\left| \mathcal{W} \left(\frac{j+1}{N_b-1} \right) - \mathcal{W} \left(\frac{j}{N_b-1} \right) \right|}{\left| \mathcal{W} \left(\frac{j}{N_b-1} \right) - \mathcal{W} \left(\frac{j-1}{N_b-1} \right) \right|} > 1, \end{aligned}$$

which implies that

$$\theta_{k(N_b-1)+j-1, k(N_b-1)+j, 1} > \theta_{k(N_b-1)+j, k(N_b-1)+j+1, 1}$$

and yields the existence of an interior reentrant angle at the vertex

$$\left(\frac{k(N_b-1)+j}{(N_b-1)N_b}, \mathcal{W} \left(\frac{k(N_b-1)+j}{(N_b-1)N_b} \right) \right).$$

Let us now assume that, up to a given step $m \geq 1$, there is a reentrant interior angle at any vertex

$$\left(\frac{k(N_b-1)+j}{(N_b-1)N_b^{m-1}}, \mathcal{W} \left(\frac{k(N_b-1)+j}{(N_b-1)N_b^{m-1}} \right) \right), \quad \text{with } 0 \leq k \leq N_b^{m-1} - 1.$$

We then want to prove that there is a reentrant interior angle at any vertex

$$\left(\frac{k(N_b-1)+j}{(N_b-1)N_b^m}, \mathcal{W} \left(\frac{k(N_b-1)+j}{(N_b-1)N_b^m} \right) \right), \quad \text{with } 0 \leq k \leq N_b^m - 1.$$

As was the case in the proof of Property 2.10, in order to be able to use the induction hypothesis, we express any integer k in $\{0, \dots, N_b^m - 1\}$ in the following form:

$$k = \tilde{k} + i N_b^{m-1}, \quad 0 \leq \tilde{k} \leq N_b^{m-1} - 1, \quad 0 \leq i \leq N_b - 1.$$

Thus,

$$\begin{aligned} \mathcal{W} \left(\frac{k(N_b-1)+j+1}{(N_b-1)N_b^m} \right) - \mathcal{W} \left(\frac{j}{(N_b-1)N_b^m} \right) &= \lambda \left(\mathcal{W} \left(\frac{\tilde{k}(N_b-1)+j+1}{(N_b-1)N_b^{m-1}} \right) - \mathcal{W} \left(\frac{\tilde{k}(N_b-1)+j}{(N_b-1)N_b^{m-1}} \right) \right) \\ &\quad - 2 \sin \left(\frac{\pi}{(N_b-1)N_b^{m-1}} \right) \sin \left(\frac{(2(N_b-1)\tilde{k} + 2j + 1)\pi}{(N_b-1)N_b^{m-1}} \right), \end{aligned}$$

and

$$\begin{aligned} \mathcal{W} \left(\frac{k(N_b-1)+j}{(N_b-1)N_b^m} \right) - \mathcal{W} \left(\frac{j-1}{(N_b-1)N_b^m} \right) &= \lambda \left(\mathcal{W} \left(\frac{\tilde{k}(N_b-1)+j}{(N_b-1)N_b^{m-1}} \right) - \mathcal{W} \left(\frac{\tilde{k}(N_b-1)+j-1}{(N_b-1)N_b^{m-1}} \right) \right) \\ &\quad - 2 \sin \left(\frac{\pi}{(N_b-1)N_b^{m-1}} \right) \sin \left(\frac{(2(N_b-1)\tilde{k} + 2j - 1)\pi}{(N_b-1)N_b^{m-1}} \right). \end{aligned}$$

In light of Property 2.10, given such an integer k - and hence also, \tilde{k} and j - and since

$$0 \leq j \leq \left\lfloor \frac{N_b - 3}{4} \right\rfloor \leq \frac{N_b - 1}{2},$$

the only configuration to be considered corresponds to the case when

$$\theta_{\tilde{k}(N_b-1)+j-1, \tilde{k}(N_b-1)+j, m-1} > \theta_{\tilde{k}(N_b-1)+j, \tilde{k}(N_b-1)+j+1, m-1}$$

and

$$\mathcal{W}\left(\frac{\tilde{k}(N_b-1)+j-1}{(N_b-1)N_b^{m-1}}\right) - \mathcal{W}\left(\frac{j}{(N_b-1)N_b^{m-1}}\right) > 0 \quad , \quad \mathcal{W}\left(\frac{\tilde{k}(N_b-1)+j}{(N_b-1)N_b^{m-1}}\right) - \mathcal{W}\left(\frac{\tilde{k}(N_b-1)+j+1}{(N_b-1)N_b^{m-1}}\right) > 0.$$

Then,

$$\tan \theta_{\tilde{k}(N_b-1)+j-1, \tilde{k}(N_b-1)+j, m-1} > \tan \theta_{\tilde{k}(N_b-1)+j, \tilde{k}(N_b-1)+j+1, m-1};$$

i.e.,

$$\frac{L_{m-1}}{\left| \mathcal{W}\left(\frac{\tilde{k}(N_b-1)+j}{(N_b-1)N_b^{m-1}}\right) - \mathcal{W}\left(\frac{\tilde{k}(N_b-1)+j-1}{(N_b-1)N_b^{m-1}}\right) \right|} > \frac{L_{m-1}}{\left| \mathcal{W}\left(\frac{\tilde{k}(N_b-1)+j+1}{(N_b-1)N_b^{m-1}}\right) - \mathcal{W}\left(\frac{\tilde{k}(N_b-1)+j}{(N_b-1)N_b^{m-1}}\right) \right|},$$

which yields

$$\left| \mathcal{W}\left(\frac{\tilde{k}(N_b-1)+j+1}{(N_b-1)N_b^{m-1}}\right) - \mathcal{W}\left(\frac{\tilde{k}(N_b-1)+j}{(N_b-1)N_b^{m-1}}\right) \right| > \left| \mathcal{W}\left(\frac{\tilde{k}(N_b-1)+j}{(N_b-1)N_b^{m-1}}\right) - \mathcal{W}\left(\frac{\tilde{k}(N_b-1)+j-1}{(N_b-1)N_b^{m-1}}\right) \right|,$$

or, equivalently,

$$\mathcal{W}\left(\frac{\tilde{k}(N_b-1)+j}{(N_b-1)N_b^{m-1}}\right) - \mathcal{W}\left(\frac{\tilde{k}(N_b-1)+j+1}{(N_b-1)N_b^{m-1}}\right) > \mathcal{W}\left(\frac{\tilde{k}(N_b-1)+j-1}{(N_b-1)N_b^{m-1}}\right) - \mathcal{W}\left(\frac{\tilde{k}(N_b-1)+j}{(N_b-1)N_b^{m-1}}\right).$$

The *strong induction hypothesis*, which ensures the existence of a reentrant interior angle at the vertex

$$\left(\frac{(N_b-1)\tilde{k}+j}{(N_b-1)N_b^{m-2}}, \mathcal{W}\left(\frac{(N_b-1)\tilde{k}+j}{(N_b-1)N_b^{m-2}}\right) \right),$$

requires, in conjunction with

$$\mathcal{W}\left(\frac{\tilde{k}(N_b-1)+j}{(N_b-1)N_b^{m-2}}\right) - \mathcal{W}\left(\frac{\tilde{k}(N_b-1)+j+1}{(N_b-1)N_b^{m-2}}\right) > \mathcal{W}\left(\frac{\tilde{k}(N_b-1)+j-1}{(N_b-1)N_b^{m-2}}\right) - \mathcal{W}\left(\frac{\tilde{k}(N_b-1)+j}{(N_b-1)N_b^{m-2}}\right),$$

that

$$\sin\left(\frac{\pi(2\tilde{k}(N_b-1)+2j+1)}{(N_b-1)N_b^{m-2}}\right) > \sin\left(\frac{\pi(2\tilde{k}(N_b-1)+2j-1)}{(N_b-1)N_b^{m-2}}\right),$$

which corresponds to

$$0 < \frac{\pi (2 \tilde{k} (N_b - 1) + 2j + 1)}{(N_b - 1) N_b^{m-2}} < \frac{\pi (2 \tilde{k} (N_b - 1) + 2j - 1)}{(N_b - 1) N_b^{m-2}} \leq \frac{\pi}{2}$$

and, as a matter of fact, ensures that

$$0 < \frac{\pi (2 \tilde{k} (N_b - 1) + 2j + 1)}{(N_b - 1) N_b^{m-1}} < \frac{\pi (2 \tilde{k} (N_b - 1) + 2j - 1)}{(N_b - 1) N_b^{m-1}} \leq \frac{\pi}{2 N_b} < \frac{\pi}{2}.$$

One then has the following inequality:

$$\begin{aligned} & \lambda \left(\mathcal{W} \left(\frac{\tilde{k} (N_b - 1) + j}{(N_b - 1) N_b^{m-1}} \right) - \mathcal{W} \left(\frac{\tilde{k} (N_b - 1) + j + 1}{(N_b - 1) N_b^{m-1}} \right) \right) + 2 \sin \left(\frac{\pi}{(N_b - 1) N_b^{m-1}} \right) \sin \left(\frac{\pi (2 \tilde{k} (N_b - 1) + 2j + 1)}{(N_b - 1) N_b^{m-1}} \right) \\ & > \lambda \left(\mathcal{W} \left(\frac{\tilde{k} (N_b - 1) + j - 1}{(N_b - 1) N_b^{m-1}} \right) - \mathcal{W} \left(\frac{\tilde{k} (N_b - 1) + j}{(N_b - 1) N_b^{m-1}} \right) \right) + 2 \sin \left(\frac{\pi}{(N_b - 1) N_b^{m-1}} \right) \sin \left(\frac{\pi (2 \tilde{k} (N_b - 1) + 2j - 1)}{(N_b - 1) N_b^{m-1}} \right). \end{aligned}$$

Hence,

$$\begin{aligned} & \tan \theta_{\tilde{k} (N_b - 1) + j - 1, \tilde{k} (N_b - 1) + j, m} \\ & || \\ & \frac{L_m}{\left| \mathcal{W} \left(\frac{\tilde{k} (N_b - 1) + j}{(N_b - 1) N_b^m} \right) - \mathcal{W} \left(\frac{\tilde{k} (N_b - 1) + j - 1}{(N_b - 1) N_b^m} \right) \right|} \\ & = \frac{L_m}{\left| \lambda \left(\mathcal{W} \left(\frac{\tilde{k} (N_b - 1) + j}{(N_b - 1) N_b^m} \right) - \mathcal{W} \left(\frac{\tilde{k} (N_b - 1) + j - 1}{(N_b - 1) N_b^m} \right) \right) - 2 \sin \left(\frac{\pi}{(N_b - 1) N_b^{m-1}} \right) \sin \left(\frac{\pi (2 \tilde{k} (N_b - 1) + 2j - 1)}{(N_b - 1) N_b^{m-1}} \right) \right|} \\ & = \frac{L_m}{\lambda \left(\mathcal{W} \left(\frac{\tilde{k} (N_b - 1) + j - 1}{(N_b - 1) N_b^m} \right) - \mathcal{W} \left(\frac{j}{(N_b - 1) N_b^m} \right) \right) + 2 \sin \left(\frac{\pi}{(N_b - 1) N_b^{m-1}} \right) \sin \left(\frac{\pi (2 \tilde{k} (N_b - 1) + 2j - 1)}{(N_b - 1) N_b^{m-1}} \right)} \\ & > \frac{L_m}{\lambda \left(\mathcal{W} \left(\frac{\tilde{k} (N_b - 1) + j}{(N_b - 1) N_b^m} \right) - \mathcal{W} \left(\frac{\tilde{k} (N_b - 1) + j + 1}{(N_b - 1) N_b^m} \right) \right) + 2 \sin \left(\frac{\pi}{(N_b - 1) N_b^{m-1}} \right) \sin \left(\frac{\pi (2 \tilde{k} (N_b - 1) + 2j + 1)}{(N_b - 1) N_b^{m-1}} \right)} \\ & = \tan \theta_{\tilde{k} (N_b - 1) + j, \tilde{k} (N_b - 1) + j + 1, m}, \end{aligned}$$

which yields the expected result. Namely,

$$\theta_{\tilde{k} (N_b - 1) + j - 1, \tilde{k} (N_b - 1) + j, m} > \theta_{\tilde{k} (N_b - 1) + j, \tilde{k} (N_b - 1) + j + 1, m};$$

i.e., the presence of a reentrant angle at the j^{th} vertex of the polygon $\mathcal{P}_{m,k}$.

The result in the remaining case $\frac{3 N_b - 1}{4} \leq j < N_b - 1$ can be obtained in an entirely similar way. It corresponds to the cases when

$$\theta_{\tilde{k} (N_b - 1) + j - 1, \tilde{k} (N_b - 1) + j, m} < \theta_{\tilde{k} (N_b - 1) + j, \tilde{k} (N_b - 1) + j + 1, m}$$

and

$$\mathcal{W}\left(\frac{k(N_b - 1) + j - 1}{(N_b - 1)N_b^m}\right) - \mathcal{W}\left(\frac{k(N_b - 1) + j}{(N_b - 1)N_b^m}\right) < 0 \quad , \quad \mathcal{W}\left(\frac{k(N_b - 1) + j}{(N_b - 1)N_b^m}\right) - \mathcal{W}\left(\frac{k(N_b - 1) + j + 1}{(N_b - 1)N_b^m}\right) < 0 .$$

Therefore, the shape of the initial polygon \mathcal{P}_0 governs the shape of any polygon $\mathcal{P}_{m,k}$, $0 \leq k \leq N_b^m$, which, if $N_b \geq 7$, admits reentrant interior angles at vertices $M_{(N_b-1)k+j}$, $0 \leq k \leq N_b^m - 1$, $0 < j \leq N_b - 1$, in the case when

$$0 < j \leq \frac{N_b - 3}{4} \quad \text{or} \quad \frac{3N_b - 1}{4} \leq j < N_b - 1 .$$

This concludes the proof of Property 2.18. □

Definition 2.6 (Self-Shape Similarity of the Weierstrass Curve).

We will say that the Weierstrass Curve – as the two-dimensional Hausdorff and uniform limit curve of a sequence of polygonal prefractals, which satisfy Properties 2.10 and 2.18 – has *self-shape similarity*, in the sense that the shape of the initial polygon \mathcal{P}_0 governs the shape of all the polygons $\mathcal{P}_{m,k}$, with $0 \leq k \leq N_b^m$, at any step m of the prefractal approximation process. This self-shape similarity property is apparent in Figures 1, 2, 3. As for the existence of reentrant angles, it can be observed on the first two graphs of Figure 3, in the case when $N_b = 7$.

3 Tubular Neighborhood

Following [LRŽ17b], [LRŽ18] and [Lap19], we are presently interested in determining the *Complex Dimensions* of the Weierstrass Curve. For this purpose, one requires a fractal tube formula for the Curve; i.e., here, the area of a two-sided ε -neighborhood of the Curve, which is expected to be of the following form, in the case of simple Complex Dimensions:

$$\sum_{\omega \text{ Complex Dimension}} c_\omega \varepsilon^{2-\omega} \quad , \quad c_\omega \in \mathbb{C} , \quad (\star\star)$$

where, for any Complex Dimension ω , c_ω is directly expressed in terms of the residue at ω of the tube zeta function $\tilde{\zeta}_\omega$ (or of the distance zeta function ζ_ω).

More specifically, consistent with the corresponding results in [LRŽ17a], [LRŽ17b] and [LRŽ18],

$$c_\omega = \text{res} \left(\tilde{\zeta}_\omega, \omega \right) = \frac{1}{2 - \omega} \text{res} \left(\zeta_\omega, \omega \right) .$$

We shall proceed as in [LP06], by the second author and E. P. J. Pearse, as well as in the later paper [LPW11], by the same authors and S. Winter (see also [LvF00], §10.3, or [LvF13], §12.1). Note that these two papers were written prior to the development of the higher-dimensional theory of Complex Dimensions and fractal tube formulas, by the second author, G. Radunovic and D. Zubrinic, in the book [LRŽ17b] and in a series of accompanying papers by the same authors, including [LRŽ17a], [LRŽ18].

The proper fractal function to be used for this purpose, named the distance zeta function, was discovered by the second author in 2009, while the equivalent, but, equally convenient, tube zeta function, depending on the problem at hand, was later introduced by the aforementioned authors in the

above references. Both types of fractal zeta functions are connected via an explicit functional equation.

Consequently, once we have obtained the desired fractal tube formula for the Weierstrass Curve, we will be able to use the general results and methods of the higher-dimensional theory of Complex Dimensions in [LRŽ17a], [LRŽ17b] and [LRŽ18] in order to deduce the fractal zeta functions of the Weierstrass Curve: first, the tube zeta function and then, via the aforementioned functional equation connecting those two zeta functions, the distance zeta function. We will then conclude from the expression of either fractal zeta function (since $D_{\mathcal{W}} < 2$, they yield the same result here) the values of the possible Complex Dimensions of the Weierstrass Curve. For many of those Complex Dimensions, including the principal ones, in the terminology of [LRŽ17b] (i.e., those with real parts equal to the maximal real part $D_{\mathcal{W}} < 2$), we will also be able to determine that they are *actual* Complex Dimensions of the Weierstrass Curve, that is, poles of the tube zeta function, or, equivalently, of the distance zeta function.

We note that the only possible exceptions to the latter statement would be the potential Complex Dimensions with real part equal to 1 (except for 1 itself), some (or all) of which could have a vanishing residue; further theoretical or numerical work will be needed in order to deal with this last remaining issue.

Notation 8 (Euclidean Distance).

In the sequel, we denote by d the Euclidean distance.

Definition 3.1 ((m, ε) -Upper and Lower Neighborhoods).

Given a natural integer m , we denote by $d(M, \Gamma_{\mathcal{W}_m})$ the distance from M to $\Gamma_{\mathcal{W}_m}$. Then, for any sufficiently small positive number ε , we introduce:

i. The (m, ε) -Upper Neighborhood:

$$\mathcal{D}^+(\Gamma_{\mathcal{W}_m}, \varepsilon) = \left\{ M = (x, y) \in \mathbb{R}^2, y \geq \mathcal{W}(x) \text{ and } d(M, \Gamma_{\mathcal{W}_m}) \leq \varepsilon \right\};$$

ii. The (m, ε) -Lower Neighborhood:

$$\mathcal{D}^-(\Gamma_{\mathcal{W}_m}, \varepsilon) = \left\{ M = (x, y) \in \mathbb{R}^2, y \leq \mathcal{W}(x) \text{ and } d(M, \Gamma_{\mathcal{W}_m}) \leq \varepsilon \right\}.$$

Definition 3.2 ((m, ε) -Neighborhood).

Given a natural integer m , and $\varepsilon > 0$ as above in Definition 3.1, we define the (m, ε) -Neighborhood as the union of the upper and lower ones, as follows:

$$\mathcal{D}(\Gamma_{\mathcal{W}_m}, \varepsilon) = \mathcal{D}^-(\Gamma_{\mathcal{W}_m}, \varepsilon) \cup \mathcal{D}^+(\Gamma_{\mathcal{W}_m}, \varepsilon).$$

Definition 3.3 (Left-Side and Right-Side (m, ε) -Neighborhoods).

Given a natural integer m , and $\varepsilon > 0$ as above, we introduce:

i. the Left-Side (m, ε) -Neighborhood of the Curve as

$$\mathcal{D}_{\text{Left}}(\Gamma_{\mathcal{W}_m}, \varepsilon) = \left\{ M = (x, y) \in \left[0, \frac{1}{2}\right] \times \mathbb{R}, d(M, \Gamma_{\mathcal{W}_m}) \leq \varepsilon \right\};$$

ii. the Right-Side (m, ε) -Neighborhood of the Curve as

$$\mathcal{D}_{\text{Right}}(\Gamma_{\mathcal{W}_m}, \varepsilon) = \left\{ M = (x, y) \in \left[\frac{1}{2}, 1\right] \times \mathbb{R}, d(M, \Gamma_{\mathcal{W}_m}) \leq \varepsilon \right\}.$$

Those neighborhoods are symmetric with respect to the vertical line $x = \frac{1}{2}$; see Figures 5 and 13. They constitute, in a sense, a partition of the whole tubular neighborhood.

What stands out in our previous studies is the key role played by the *elementary lengths* L_m :

$$\forall m \in \mathbb{N} : \quad L_m = \frac{1}{(N_b - 1) N_b^m};$$

see Section 2 above above for a detailed discussion of the geometric framework.

For a given $m \in \mathbb{N}$, it is then natural to take ε in

$$\left(\frac{1}{(N_b - 1) N_b^{m+1}}, \frac{1}{(N_b - 1) N_b^m} \right],$$

and to introduce the map

$$\varepsilon \mapsto m(\varepsilon) = \lceil -\ln_{N_b}((N_b - 1)\varepsilon) \rceil = [m(\varepsilon)] + \{m(\varepsilon)\},$$

where $[\cdot]$ and $\{\cdot\}$ respectively denote the integer and fractional parts.

For notational simplicity, we temporarily set $x = m(\varepsilon) = -\ln_{N_b}((N_b - 1)\varepsilon)$.

Previous works give a very unfriendly expression for the absolute value of the *elementary heights*, $|h_{j,m}|$, as

$$|h_{j,m}| = \left| \lambda^m (y_{j+1} - y_j) - 2 \sum_{k=1}^m \lambda^{m-k} \sin\left(\frac{\pi}{N_b^{k+1}(N_b-1)}\right) \sin\left(\frac{\pi(2j+1)}{N_b^{k+1}(N_b-1)} + 2\pi \sum_{q=0}^k \frac{i_{m-q}}{N_b^{k-q}}\right) \right|,$$

for $(i_1, \dots, i_m) \in \{0, \dots, N_b - 1\}^m$. Although it is sufficient to compute the Minkowski dimension of the Curve, one also requires, in the present work, an explicit expression for the elementary lengths $L_m, m \in \mathbb{N}^*$.

Accordingly, one has

$$N_b^m = N_b^{[x]} = N_b^{x-\{x\}} \quad , \quad N_b^{-m} = N_b^{\{x\}-x} \quad ,$$

$$L_m = \frac{1}{(N_b - 1) N_b^m} = \frac{1}{N_b - 1} N_b^{x-\{x\}} \quad ,$$

$$-([x] + \{x\}) \ln N_b = \ln((N_b - 1) \varepsilon) \quad , \quad e^{-([x] + \{x\}) \ln N_b} = (N_b - 1) \varepsilon \quad , \quad \varepsilon = \frac{1}{N_b - 1} N_b^{-([x] + \{x\})} \quad .$$

The (m, ε) -Upper and Lower Neighborhoods introduced in Definition 3.1 are then obtained by means of rectangles and wedges, as depicted in Figures 8–14.

Proposition 3.1 ((m, ε) -Upper Neighborhood).

According to Property 2.4, given a strictly positive integer m , the (m, ε) -Upper Neighborhood is thus constituted of:

- i. $(N_b - 1) N_b^m$ **rectangles**, each of length $\ell_{j-1,j,m}$, for $1 \leq j \leq N_b^m - 1$, and height ε .

Those rectangles are also **overlapping ones**, at least at their bottom. If we denote by $M_{j,m}$ the common vertex between two consecutive overlapping rectangles (see Figure 10), the area that is thus counted twice corresponds to parallelograms, of height ε and basis $\varepsilon \cotan(\pi - \theta_{j-1,j,m} - \theta_{j,j+1,m})$; i.e., this area is equal to $\varepsilon^2 \cotan(\theta_{j-1,j,m} + \theta_{j,j+1,m})$.

Since one deals here with an upper neighborhood, one also has to subtract the areas of the **extra outer lower triangles**, i.e., $\frac{1}{2} \varepsilon (b_{j-1,j,m} + b_{j,j+1,m})$.

- ii. $N_b^m \left(1 + 2 \left\lceil \frac{N_b - 3}{4} \right\rceil \right) - 1$ **upper wedges** (to be understood in the strict sense, which means that the extreme ones are not taken into account here). If we denote by $M_{j,m}$ the vertex from which is issued the wedge (see Figure 14), the area of this latter wedge is given by

$$\frac{1}{2} (\pi - \theta_{j-1,j,m} - \theta_{j,j+1,m}) \varepsilon^2 \quad , \quad \text{for } 1 \leq j \leq N_b^m - 2 \quad .$$

The number of wedges is determined by the shape of the initial polygon \mathcal{P}_0 , as well by the existence of reentrant angles. This directly follows from Property 2.18. For the sake of simplicity, we set

$$r_b^+ = 1 + 2 \left\lceil \frac{N_b - 3}{4} \right\rceil \quad .$$

- iii. Two **extreme wedges** (see Figure 15), each of area equal to $\frac{1}{2} \pi \varepsilon^2$.

Proposition 3.2 ((m, ε) -Lower Neighborhood).

In the same way, given a strictly positive integer m , the (m, ε) -Lower Neighborhood is thus constituted of:

- i. $(N_b - 1) N_b^m$ **rectangles**, each of length $\ell_{j-1,j,m}$, for $1 \leq j \leq N_b^m - 1$, and height ε .

Those rectangles are also **overlapping ones**, this time at least at their top. If we denote by $M_{j,m}$ the common vertex between two consecutive overlapping rectangles, the area that is thus counted twice again corresponds to parallelograms, of height ε and basis $\varepsilon \cotan(\pi - \theta_{j-1,j,m} - \theta_{j,j+1,m})$; i.e., this area is equal to $\varepsilon^2 \cotan(\theta_{j-1,j,m} + \theta_{j,j+1,m})$.

Since one deals here with a lower neighborhood, one has this time to substract the areas of the **extra outer upper triangles**, namely, amounting to $\frac{1}{2} \varepsilon (b_{j-1,j,m} + b_{j,j+1,m})$.

- ii. $N_b^m \left(N_b - 2 \left\lfloor \frac{N_b - 3}{4} \right\rfloor \right) - 1$ **lower wedges**. If we denote by $M_{j,m}$ the vertex from which is issued the wedge, the area of this latter wedge is obtained as previously, and is given by

$$\frac{1}{2} (\pi - \theta_{j-1,j,m} - \theta_{j,j+1,m}) \varepsilon^2, \quad \text{for } 1 \leq j \leq N_b^m - 2.$$

The number of lower wedges is determined by the shape of the initial polygon \mathcal{P}_0 , as well as by the existence of reentrant angles. This directly comes from Property 2.18. For the sake of simplicity, we set $r_b^- = N_b - 2 \left\lfloor \frac{N_b - 3}{4} \right\rfloor$.

Remark 3.1.

- i. The number of upper overlapping rectangles is equal to the number of lower extra triangles, and also to the number of upper wedges.
- ii. The number of lower overlapping rectangles is equal to the number of upper extra triangles, and also to the number of lower wedges.
- iii. In light of i. and ii. just above, those numbers can be respectively calculated as being equal to

$$(r_b - 1) N_b^m \quad \text{and} \quad (N_b - r_b) N_b^m, \quad \text{for } 1 \leq r_b \leq N_b - 2.$$

- iv. Note that the small parameter ε has to be sufficiently small (say $0 < \varepsilon < \varepsilon_0$, for some $\varepsilon_0 > 0$ which exists, but appears difficult to specify explicitly) in order to avoid more unfriendly overlaps than the parallelograms; see Figure 16.

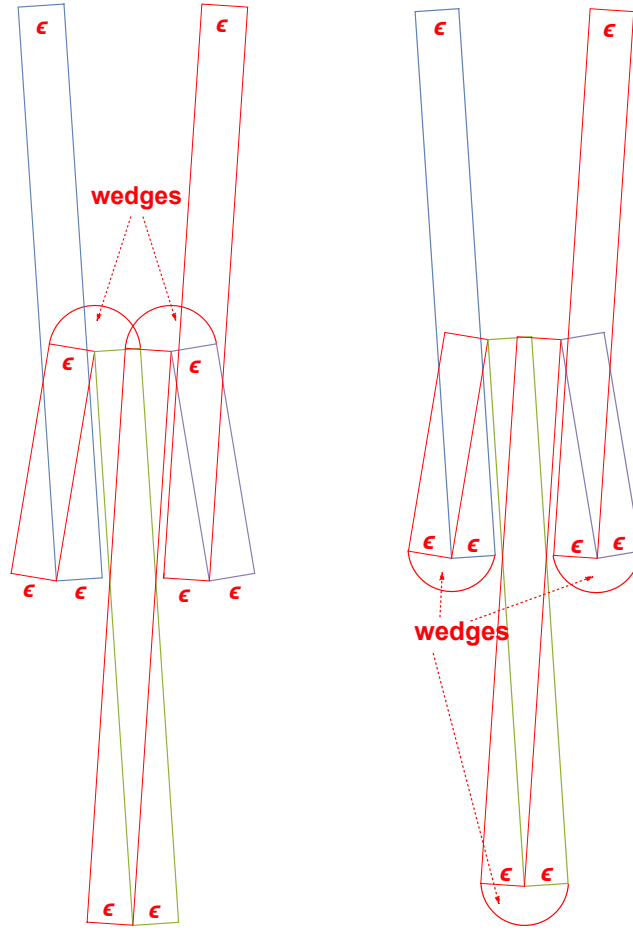


Figure 8: The $(1, \epsilon)$ -Upper and Lower Neighborhoods, in the case where $\lambda = \frac{1}{2}$ and $N_b = 3$.

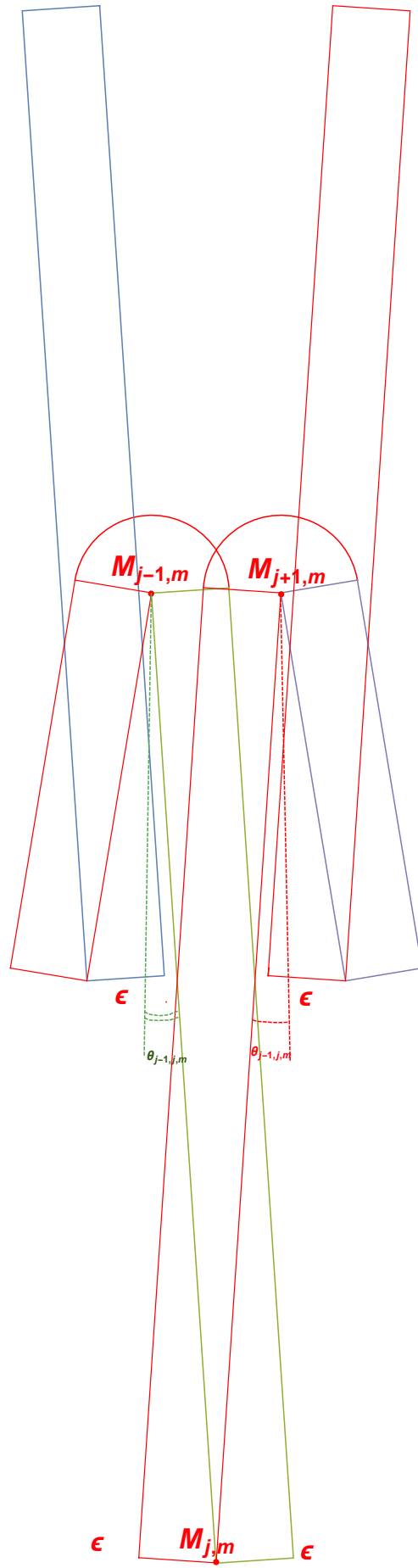


Figure 9: The $(1, \varepsilon)$ -Upper Neighborhood, in the case where $\lambda = \frac{1}{2}$ and $N_b = 3$.

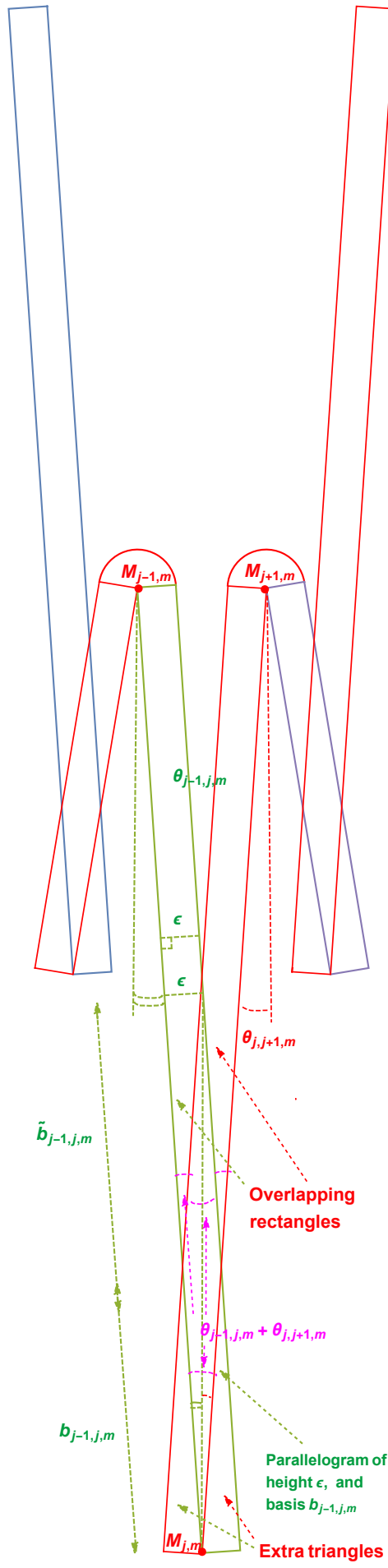


Figure 10: Two overlapping rectangles, in the case where $\lambda = \frac{1}{2}$ and $N_b = 3$.

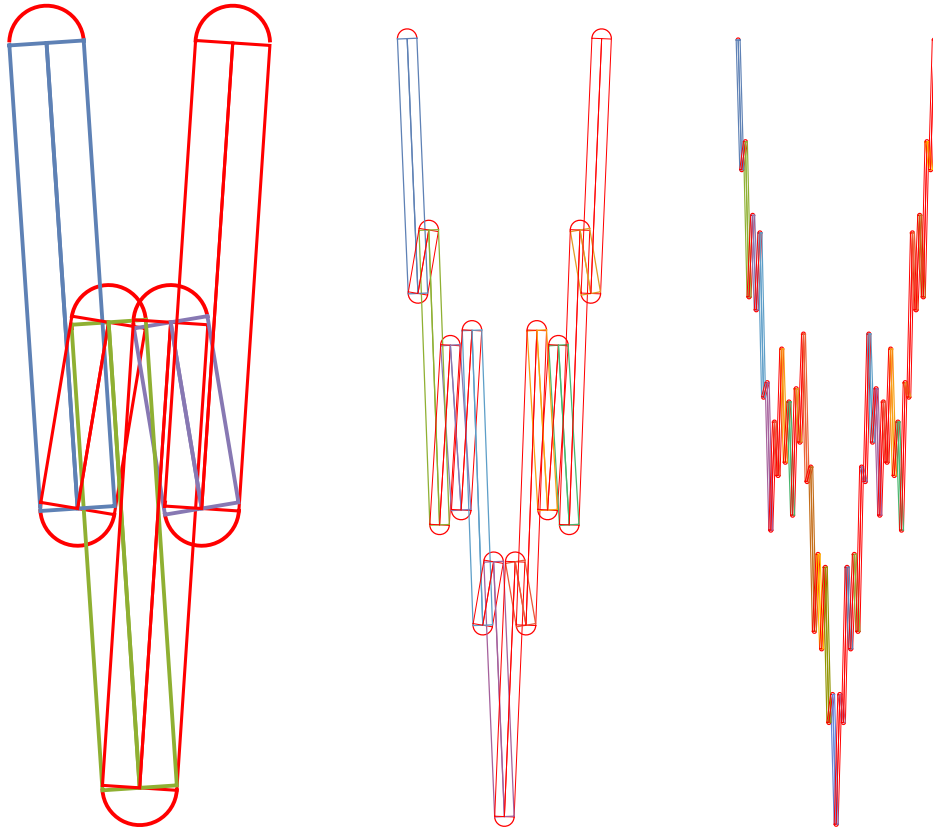


Figure 11: The $(1, \varepsilon)$, $(2, \varepsilon)$ and $(3, \varepsilon)$ -Neighborhoods, in the case where $\lambda = \frac{1}{2}$ and $N_b = 3$.

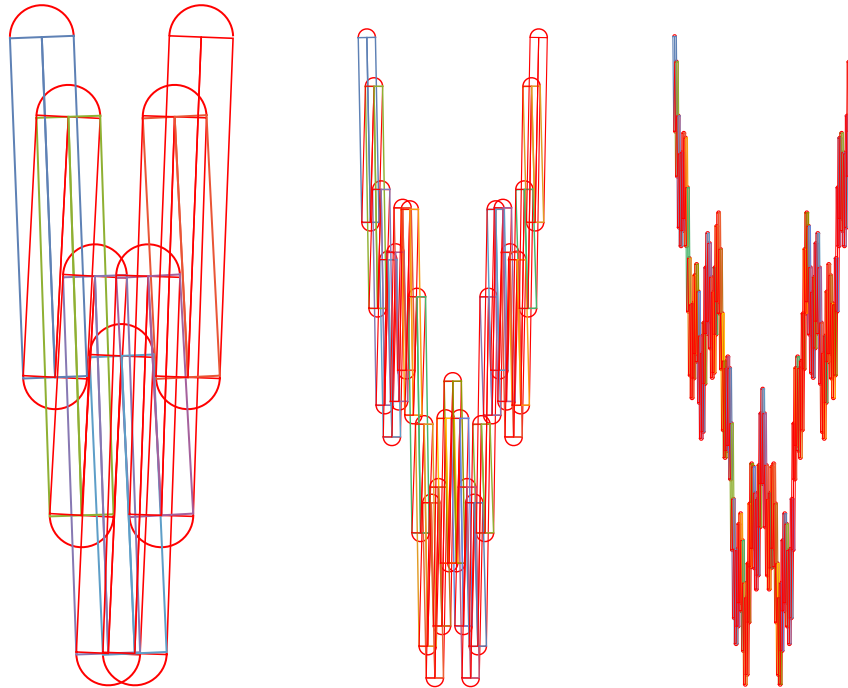


Figure 12: The $(1, \varepsilon)$, $(2, \varepsilon)$ and $(3, \varepsilon)$ -Upper Neighborhoods, in the case where $\lambda = \frac{1}{2}$ and $N_b = 4$.

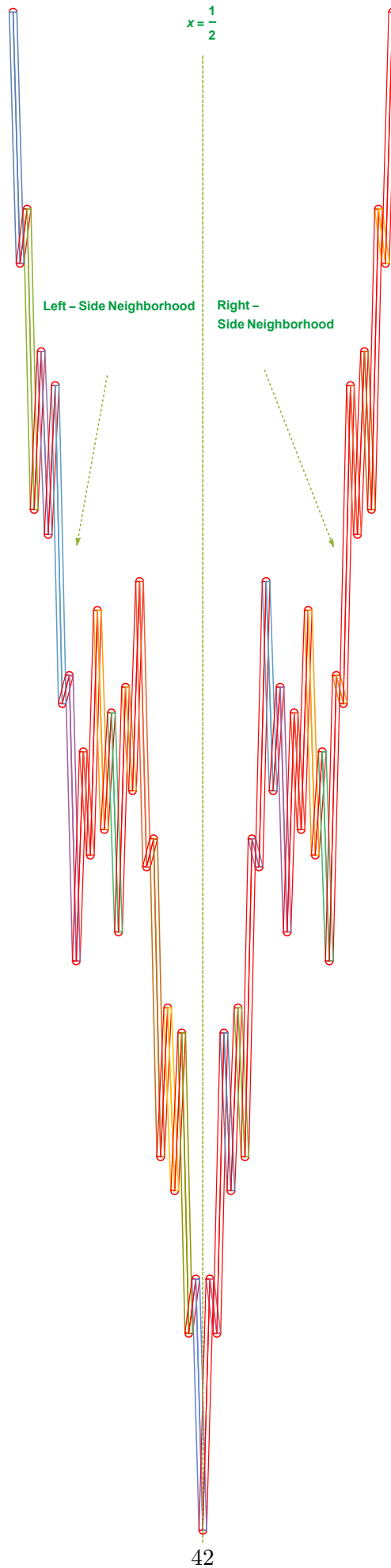


Figure 13: The $(3, \varepsilon)$ -Left and Right-Side Neighborhoods, in the case where $\lambda = \frac{1}{2}$ and $N_b = 3$.

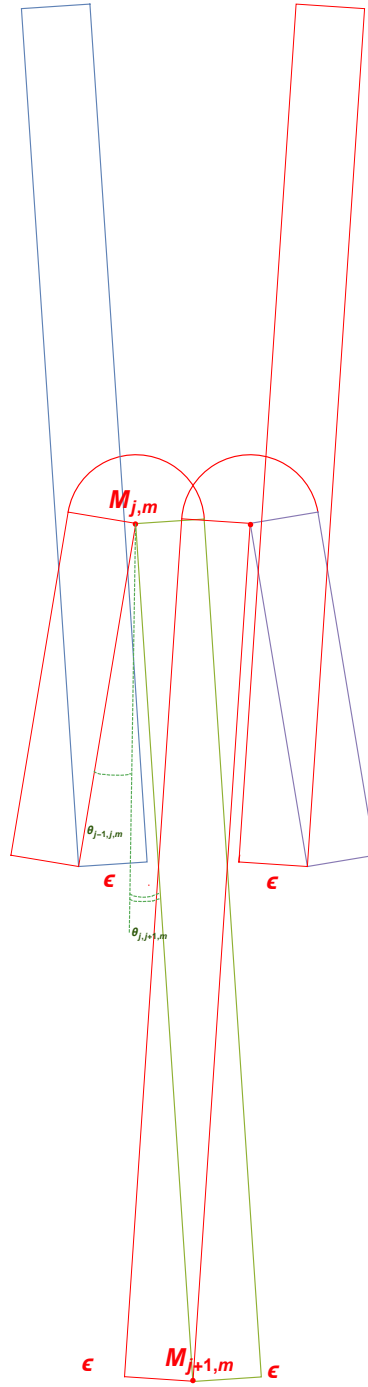


Figure 14: An upper wedge.



Figure 15: **The extreme wedges, in the case where $\lambda = \frac{1}{2}$ and $N_b = 3$.**

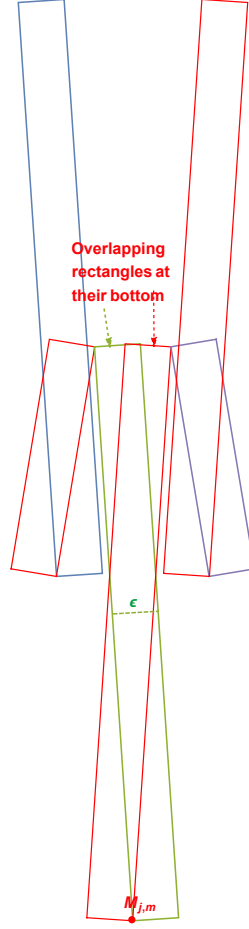


Figure 16: **Two overlapping rectangles, when the parameter ε is not sufficiently small: the overlap is a pentagon.**

In order to obtain a pleasant and understandable expression for the tubular volume at a given level $m \in \mathbb{N}^*$, we will make use of the following relations, coming from Corollary 2.15:

Proposition 3.3.

i. For the number of rectangles: $N_b^m = N_b^{x-\{x\}}$.

Due to the fact that

$$\varepsilon = \frac{1}{N_b - 1} N_b^{-([x]+\{x\})} = \frac{1}{N_b - 1} N_b^{-x} \quad , \quad N_b^{-x} = (N_b - 1) \varepsilon \quad , \quad N_b^x = \frac{1}{N_b - 1} \varepsilon^{-1} \quad ,$$

one thus also has

$$N_b^m \varepsilon = N_b^{x-\{x\}} \frac{1}{N_b - 1} N_b^{-x} = \frac{1}{N_b - 1} N_b^{-\{x\}} .$$

ii. For the elementary horizontal lengths:

$$L_m = \frac{1}{(N_b - 1) N_b^m} = \frac{1}{N_b - 1} N_b^{\{x\}-x} = N_b^{\{x\}} \varepsilon .$$

iii. For the elementary vertical heights:

$$h_{j-1,j,m} = \mathcal{O} \left(L_m^{2-D_{\mathcal{H}}} \right) = \mathcal{O} \left(N_b^{(2-D_{\mathcal{H}})(\{x\}-x)} \right) = N_b^{(2-D_{\mathcal{H}})(\{x\}-x)} \mathcal{O}(1) , \quad 1 \leq j \leq N_b^m - 1 .$$

iii. For the elementary ratios, $1 \leq j \leq N_b^m - 1$:

$$\frac{L_m}{h_{j-1,j,m}} = \mathcal{O} \left(L_m^{D_{\mathcal{H}}-1} \right) = \mathcal{O} \left(N_b^{(1-D_{\mathcal{H}})(\{x\}-x)} \right) = \mathcal{O} \left(N_b^{(1-D_{\mathcal{H}})\{x\}} \varepsilon \right) = N_b^{(1-D_{\mathcal{H}})\{x\}} \varepsilon \mathcal{O}(1) ,$$

and, similarly, for $1 \leq j \leq N_b^m - 2$:

$$\frac{L_m}{h_{j,j+1,m}} = \mathcal{O} \left(L_m^{D_{\mathcal{H}}-1} \right) = \mathcal{O} \left(N_b^{(1-D_{\mathcal{H}})(\{x\}-x)} \right) = \mathcal{O} \left(N_b^{(1-D_{\mathcal{H}})\{x\}} \varepsilon \right) = N_b^{(1-D_{\mathcal{H}})\{x\}} \varepsilon \mathcal{O}(1) .$$

Proposition 3.4 (Basis of the Parallelograms in Common to Overlapping Rectangles).

Given a natural integer m , and j in $\{1, \dots, (N_b - 1) N_b^m - 1\}$, the basis $b_{j-1,j,m}$ of the parallelogram in common to overlapping rectangles associated to the vertex $M_{j,m}$ is such that

$$b_{j-1,j,m} = N_b^{(3D_{\mathcal{H}}-2)\{x\}} \varepsilon^2 \mathcal{O}(1) .$$

Proof. One has

$$\tan \theta_{j-1,j,m} = \frac{\varepsilon}{b_{j-1,j,m} + \tilde{b}_{j-1,j,m}} ,$$

where

$$\tan (\theta_{j-1,j,m} + \theta_{j,j+1,m}) = \frac{\varepsilon}{\tilde{b}_{j-1,j,m}} .$$

Hence,

$$b_{j-1,j,m} + \tilde{b}_{j-1,j,m} = \varepsilon \left| \cotan \theta_{j-1,j,m} \right| ,$$

which yields

$$b_{j-1,j,m} = \varepsilon \left| \cotan \theta_{j-1,j,m} \right| - \tilde{b}_{j-1,j,m} = \varepsilon \left\{ \left| \cotan \theta_{j-1,j,m} \right| - \left| \cotan (\theta_{j-1,j,m} + \theta_{j,j+1,m}) \right| \right\} ;$$

i.e.,

$$\begin{aligned}
b_{j-1,j,m} &= \varepsilon \left(\frac{h_{j-1,j,m}}{L_m} - \left| \cotan \left(\arctan \frac{L_m}{h_{j-1,j,m}} + \arctan \frac{L_m}{h_{j,j+1,m}} \right) \right| \right) \\
&= \varepsilon \left(\frac{h_{j-1,j,m}}{L_m} - \left| \frac{\frac{L_m}{h_{j-1,j,m}} \frac{L_m}{h_{j,j+1,m}} - 1}{\frac{L_m}{h_{j-1,j,m}} + \frac{L_m}{h_{j,j+1,m}}} \right| \right) \\
&= \varepsilon \left(\frac{h_{j-1,j,m}}{L_m} - \frac{1 - \frac{L_m}{h_{j-1,j,m}} \frac{L_m}{h_{j,j+1,m}}}{\frac{L_m}{h_{j-1,j,m}} + \frac{L_m}{h_{j,j+1,m}}} \right).
\end{aligned}$$

Again, one needs to make an asymptotic expansion. A slight difficulty occurs, coming from the term

$$\frac{1}{\frac{L_m}{h_{j-1,j,m}} + \frac{L_m}{h_{j,j+1,m}}}.$$

The apparent problem is the following:

i. Either one uses, as previously, expressions of the form

$$\frac{1}{\frac{L_m}{h_{j-1,j,m}} + \frac{L_m}{h_{j,j+1,m}}} = N_b^{(D_{\mathcal{W}}-1)\{x\}} \mathcal{O}(1),$$

with nothing but a *black box* (which means, unknown terms) in factor of constants, that would yield Complex Dimensions with a real part equal to two, and would therefore lead to a contradiction because the Weierstrass Curve has box dimension $D_{\mathcal{W}} < 2$.

ii. Either, knowing that, which is not the more satisfactorily way of reasoning, from a mathematician's point of view, one copes with it and tries to find how to get rid of those terms.

Two configurations occur:

$$\leadsto \frac{L_m}{h_{j-1,j,m}} > \frac{L_m}{h_{j,j+1,m}}, \text{ in which case}$$

$$\frac{h_{j-1,j,m}}{L_m} - \frac{1}{\frac{L_m}{h_{j-1,j,m}} + \frac{L_m}{h_{j,j+1,m}}} = \frac{h_{j-1,j,m}}{L_m} - \frac{h_{j-1,j,m}}{L_m} + \text{smaller order and negligible terms}.$$

$$\leadsto \frac{L_m}{h_{j-1,j,m}} < \frac{L_m}{h_{j,j+1,m}}, \text{ in which case}$$

$$\frac{h_{j-1,j,m}}{L_m} - \frac{1}{\frac{L_m}{h_{j-1,j,m}} + \frac{L_m}{h_{j,j+1,m}}} = \frac{h_{j-1,j,m}}{L_m} - \frac{h_{j,j+1,m}}{L_m} + \text{smaller order and negligible terms}.$$

Fortunately, due to results obtained in the proof of Property 2.18, this situation occurs only in the case of reentrant angles, when $N_b \geq 7$, twice, for respectively $\left\lceil \frac{N_b - 3}{4} \right\rceil$ consecutive

vertices of polygons $\mathcal{P}_{m,k}$, $0 \leq k \leq N_b^m - 1$. Given a polygon $\mathcal{P}_{m,k}$, and as already encountered, one just has to reason on the associated first set of consecutive vertices. The annoying terms simplify two by two in a telescopic sum, from the first reentrant vertex, to the penultimate one. There remains the term coming from the first vertex with an interior reentrant angle, that will be denoted $M_{j,m}$, and the term coming from the ultimate one, $M_{j+p-1,m}$: due to the symmetry with respect to the vertical line $x = \frac{1}{2}$ (see Property 2.1), they are cancelled by those coming from the symmetric polygon, see Figure 17). To summarize, one gets a sum of the form

$$\frac{h_{j-1,j,m}}{L_m} - \underbrace{\frac{h_{j,j+1,m}}{L_m} + \frac{h_{j,j+1,m}}{L_m} - \frac{h_{j+1,j+2,m}}{L_m} + \frac{h_{j+1,j+2,m}}{L_m} \dots}_{\text{telescoping sum}} - \frac{h_{j+p,j+p+1,m}}{L_m}.$$

The remaining terms $\frac{h_{j-1,j,m}}{L_m}$ and $-\frac{h_{j+p,j+p+1,m}}{L_m}$ are the ones which will simplify with the exact opposites coming from the symmetric polygon with respect to the vertical line $x = \frac{1}{2}$ (see Figure 17), since

$$\begin{aligned} \frac{h_{j+p,j+p+1,m}}{L_m} &= \frac{1}{L_m} \left| \mathcal{W} \left(\frac{j+p+1}{(N_b-1)N_b^m} \right) - \mathcal{W} \left(\frac{j+p}{(N_b-1)N_b^m} \right) \right| \\ &= \frac{1}{L_m} \left| \mathcal{W} \left(\frac{(N_b-1)N_b^m - j - p - 1}{(N_b-1)N_b^m} \right) - \mathcal{W} \left(\frac{(N_b-1)N_b^m - j - p}{(N_b-1)N_b^m} \right) \right| \\ &= \frac{h_{(N_b-1)N_b^m - j - p - 1, (N_b-1)N_b^m - j - p, m}}{L_m}. \end{aligned}$$

Thus, in the end, there is no problem.

In the light of the above results, one may now rewrite $b_{j-1,j,m}$ as follows:

$$\begin{aligned} b_{j-1,j,m} &= N_b^{(D_{\mathcal{W}}-1)\{x\}} N_b^{2(D_{\mathcal{W}}-1)\{x\}} \varepsilon^2 \mathcal{O}(1) \\ &= N_b^{(3D_{\mathcal{W}}-2)\{x\}} \varepsilon^2 \mathcal{O}(1). \end{aligned}$$

This concludes the proof of Proposition 3.4. □

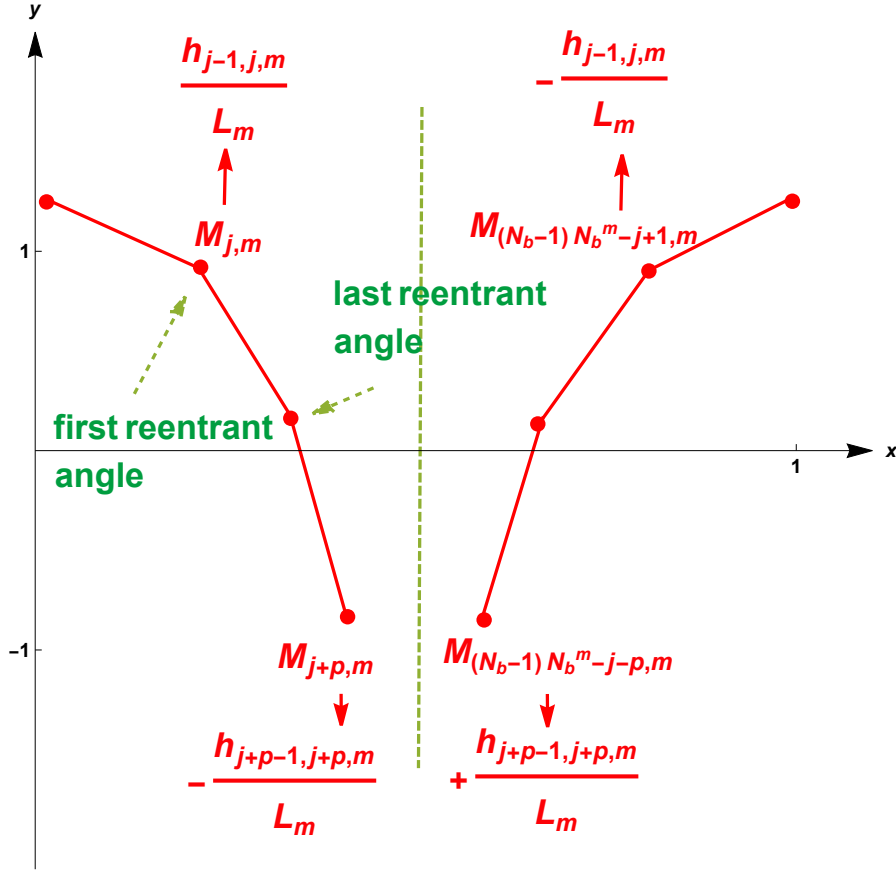


Figure 17: The symmetric points with respect to the vertical line $x = \frac{1}{2}$, leading to terms that cancel each other out in the proof of Proposition 3.4.

In the sequel, we will use the following two series expansions:

$$i. \quad \forall z \in [0, 1[: \quad \sqrt{1+z} = \sum_{k=0}^{\infty} \binom{\frac{1}{2}}{k} z^k,$$

where, for any pair of natural integer k , $\binom{\frac{1}{2}}{k}$ is the generalized binomial coefficient

$$\binom{\frac{1}{2}}{k} = \frac{\frac{1}{2} \times \left(\frac{1}{2} - 1\right) \times \left(\frac{1}{2} - 2\right) \times \cdots \times \left(\frac{1}{2} - k + 1\right)}{k!} = \frac{\left(\frac{1}{2}\right)_k}{k!}.$$

This expansion is thus valid for

$$z = \frac{L_m^2}{h_{j-1,j,m}^2} = \mathcal{O}\left(L_m^{2(D_{\mathcal{H}}-1)}\right) \ll 1.$$

$$ii. \quad \forall z \in [0, 1[: \quad \tan^{-1} z = \arctan z = \sum_{k=0}^{\infty} \frac{z^{2k+1}}{2k+1}, \text{ which is also valid for}$$

$$z = \frac{L_m^2}{h_{j-1,j,m}^2} = \mathcal{O}\left(L_m^{2(D_{\mathcal{H}}-1)}\right) \ll 1.$$

Notation 9. In the sequel, for the sake of simplicity, we will use the following notation:

- i. $\sum_{j \text{ rectangle}} \dots$, to denote the sum over the upper and lower rectangles.
- ii. $\sum_{j \text{ lower wedge}} \dots$, to denote the sum over the lower wedges.
- iii. $\sum_{j \text{ upper wedge}} \dots$, to denote the sum over the upper wedges.
- iv. $\sum_{j \text{ upper triangle}} \dots$, to denote the sum over the extra outer upper triangles.
- v. $\sum_{j \text{ lower triangle}} \dots$, to denote the sum over the extra outer upper triangles.
- vi. $\sum_{j \text{ lower parallelogram}} \dots$, to denote the sum over the upper overlapping rectangles.
- vii. $\sum_{j \text{ upper parallelogram}} \dots$, to denote the sum over the lower overlapping rectangles.

Proposition 3.5 (Contribution of the Rectangles to the Tubular Volume).

The contribution of the $(N_b - 1) N_b^m$ **rectangles** to the tubular volume is given by

$$\begin{aligned}
\mathcal{V}_{\text{Rectangles}}(\varepsilon) &= 2 \sum_{j \text{ rectangle}} \varepsilon \ell_{j-1,j,m} \\
&= 2 \sum_{j \text{ rectangle}} \varepsilon \sqrt{L_m^2 + h_{j-1,j,m}^2} \\
&= 2 \sum_{j \text{ rectangle}} \varepsilon h_{j-1,j,m} \sqrt{1 + \frac{L_m^2}{h_{j-1,j,m}^2}} \\
&= 2 \sum_{j \text{ rectangle}} \varepsilon h_{j-1,j,m} \sqrt{1 + \frac{L_m^2}{h_{j-1,j,m}^2}} \\
&= 2 \sum_{j \text{ rectangle}} \varepsilon h_{j-1,j,m} \sum_{k=0}^{\infty} \binom{\frac{1}{2}}{k} \frac{L_m^{2k}}{h_{j-1,j,m}^{2k}} \\
&= 2 \sum_{j \text{ rectangle}} \varepsilon h_{j-1,j,m} \sum_{k=0}^{\infty} \binom{\frac{1}{2}}{k} N_b^{k(2-D_{\mathcal{W}})\{x\}} \varepsilon^{k(2-D_{\mathcal{W}})} \mathcal{O}(1) \\
&= 2 \sum_{j \text{ rectangle}} \varepsilon \varepsilon^{2-D_{\mathcal{W}}} \mathcal{O}(1) \sum_{k=0}^{\infty} \binom{\frac{1}{2}}{k} N_b^{k(2-D_{\mathcal{W}})\{x\}} \varepsilon^{k(2-D_{\mathcal{W}})} \mathcal{O}(1) \\
&= 2 N_b^m \varepsilon^{2-D_{\mathcal{W}}} \mathcal{O}(1) \sum_{k=0}^{\infty} \binom{\frac{1}{2}}{k} N_b^{k(2-D_{\mathcal{W}})\{x\}} \varepsilon^{1+k(2-D_{\mathcal{W}})} \mathcal{O}(1) \\
&= 2 (N_b - 1) N_b^m \varepsilon \varepsilon^{2-D_{\mathcal{W}}} \sum_{k=0}^{\infty} \binom{\frac{1}{2}}{k} N_b^{k(2-D_{\mathcal{W}})\{x\}} \varepsilon^{k(2-D_{\mathcal{W}})} \mathcal{O}(1) \\
&= 2 N_b^{-\{x\}} \varepsilon^{2-D_{\mathcal{W}}} \sum_{k=0}^{\infty} \binom{\frac{1}{2}}{k} N_b^{k(2-D_{\mathcal{W}})\{x\}} \varepsilon^{k(2-D_{\mathcal{W}})} \mathcal{O}(1) \\
&= 2 \sum_{k=0}^{\infty} \binom{\frac{1}{2}}{k} N_b^{(k(2-D_{\mathcal{W}})-1)\{x\}} \varepsilon^{2-D_{\mathcal{W}}+k(2-D_{\mathcal{W}})} \mathcal{O}(1) .
\end{aligned}$$

Proposition 3.6 (Contribution of the Extreme, Upper and Lower Wedges to the Tubular Volume).

i. The contribution of the **extreme wedges** to the tubular volume is given by

$$\mathcal{V}_{\text{extreme wedges}}(\varepsilon) = \pi \varepsilon^2.$$

ii. The contribution of the $r_b^+ N_b^m - 1$ **upper wedges** to the tubular volume is given by

$$\begin{aligned} \mathcal{V}_{\text{upper wedges}}(\varepsilon) &= \frac{1}{2} \sum_{j \text{ upper wedge}} (\pi - \theta_{j-1,m} - \theta_{j,j+1,m}) \varepsilon^2 \\ &= \frac{1}{2} \sum_{j \text{ upper wedge}} \varepsilon^2 \left(\pi - \arctan \frac{L_m}{h_{j-1,j,m}} - \arctan \frac{L_m}{h_{j,j+1,m}} \right) \\ &= \frac{\varepsilon^2}{2} \sum_{j \text{ upper wedge}} \varepsilon^2 \left(\pi - \sum_{k=0}^{\infty} \frac{1}{2k+1} \frac{L_m^{2k+1}}{h_{j-1,j,m}^{2k+1}} - \sum_{k=0}^{\infty} \frac{1}{2k+1} \frac{L_m^{2k+1}}{h_{j,j+1,m}^{2k+1}} \right) \\ &= \frac{\varepsilon^2}{2} \sum_{j \text{ upper wedge}} \left(\pi - \sum_{k=0}^{\infty} \frac{1}{2k+1} N_b^{(2k+1)(1-D_{\mathcal{W}})\{x\}} \varepsilon^{2k+1} \mathcal{O}(1) \right) \\ &= \frac{\varepsilon^2}{2} (r_b^+ N_b^m - 1) \left(\pi - \sum_{k=0}^{\infty} \frac{1}{2k+1} N_b^{(2k+1)(1-D_{\mathcal{W}})\{x\}} \varepsilon^{2k+1} \mathcal{O}(1) \right) \\ &= \frac{\varepsilon^2}{2} \left(\frac{\varepsilon}{4} r_b^+ N_b^{-\{x\}} - \frac{\varepsilon^2}{2} \right) \left(\pi - \sum_{k=0}^{\infty} \frac{1}{2k+1} N_b^{(2k+1)(1-D_{\mathcal{W}})\{x\}} \varepsilon^{2k+1} \mathcal{O}(1) \right) \\ &= \frac{\pi}{2} \left(\frac{\varepsilon^3}{4} r_b^+ N_b^{-\{x\}} - \frac{\varepsilon^4}{2} \right) - \frac{\varepsilon^3}{4} r_b^+ \sum_{k=0}^{\infty} \frac{1}{2k+1} N_b^{-(2k+1)D_{\mathcal{W}}-2k\{x\}} \varepsilon^{2k+1} \mathcal{O}(1) \\ &\quad + \frac{\varepsilon^4}{4} \sum_{k=0}^{\infty} \frac{1}{2k+1} N_b^{-(2k+1)(D_{\mathcal{W}}-1)\{x\}} \varepsilon^{2k+1} \mathcal{O}(1). \end{aligned}$$

iii. In the same way, the contribution of the $r_b^- N_b^m - 1$ **lower wedges** to the tubular volume is given by

$$\begin{aligned} \mathcal{V}_{\text{lower wedges}}(\varepsilon) &= \frac{\pi}{2} \left(\frac{\varepsilon^3}{4} r_b^- N_b^{-\{x\}} - \frac{\varepsilon^4}{2} \right) - \frac{\varepsilon^3}{4} r_b^- \sum_{k=0}^{\infty} \frac{1}{2k+1} N_b^{-(2k+1)D_{\mathcal{W}}-2k\{x\}} \varepsilon^{2k+1} \mathcal{O}(1) \\ &\quad + \frac{\varepsilon^4}{4} \sum_{k=0}^{\infty} \frac{1}{2k+1} N_b^{-(2k+1)(D_{\mathcal{W}}-1)\{x\}} \varepsilon^{2k+1} \mathcal{O}(1). \end{aligned}$$

Proposition 3.7 (Negative Contribution of the Extra Outer Triangles to the Tubular Volume).

i. The negative contribution of the $(N_b - r_b^+ - 1) N_b^m$ **extra outer lower triangles** to the tubular volume is given by

$$\begin{aligned}
\mathcal{V}_{\text{extra outer lower triangles}}(\varepsilon) &= -\frac{\varepsilon}{2} \sum_{j \text{ triangle}} \{b_{j-1,j,m} + b_{j,j+1,m}\} \\
&= -\frac{\varepsilon}{2} \sum_{j \text{ lower triangle}} N_b^{(3D_{\mathcal{W}}-2)\{x\}} \varepsilon^2 \mathcal{O}(1) \\
&= -\frac{\varepsilon}{2} (N_b - r_b^+ - 1) N_b^m N_b^{(3D_{\mathcal{W}}-2)\{x\}} \varepsilon^2 \mathcal{O}(1) \\
&= -\frac{\varepsilon^2}{2} (N_b - r_b^+ - 1) N_b^{-\{x\}} N_b^{(3D_{\mathcal{W}}-2)\{x\}} \mathcal{O}(1) .
\end{aligned}$$

ii. In the same way, the negative contribution of the $(N_b - r_b^- - 1) N_b^m$ **extra outer upper triangles** to the tubular volume is given by

$$\mathcal{V}_{\text{extra outer upper triangles}}(\varepsilon) = -\frac{\varepsilon^2}{2} (N_b - r_b^- - 1) N_b^{-\{x\}} N_b^{(3D_{\mathcal{W}}-2)\{x\}} \mathcal{O}(1) .$$

Proposition 3.8 (Negative Contribution of the Overlapping Rectangles to the Tubular Volume).

The negative contribution of the **upper and lower overlapping rectangles** to the tubular volume is given by

$$\mathcal{V}_{\text{upper and lower parallelograms}}(\varepsilon) = -\varepsilon \sum_{j \text{ upper and lower parallelogram}} b_{j-1,j,m} - \varepsilon^2 N_b^{(3D_{\mathcal{W}}-2)\{x\}} \mathcal{O}(1) .$$

4 Fractal Tube Formulas, Complex Dimensions and Average Minkowski Content

4.1 Preliminaries

Property 4.1 (Fourier Series Expansion of the One-Periodic Map $x \mapsto N_b^{-\{x\}}$ [LvF13]).

The fractional part map $\{\cdot\}$ is one-periodic. Hence, it is also the case of the map $x \mapsto N_b^{-\{x\}}$, which admits, with respect to the real variable x , the following Fourier Series expansion:

$$N_b^{-\{x\}} = \frac{N_b - 1}{N_b} \sum_{m \in \mathbb{Z}} \frac{e^{2i\pi m x}}{\ln N_b + 2i m \pi} = \frac{N_b - 1}{N_b} \sum_{m \in \mathbb{Z}} \frac{(N_b - 1)^{-i m p} \varepsilon^{-i m p}}{\ln N_b + 2i m \pi} ,$$

where the exponential Fourier coefficients c_m have been obtained through

$$\begin{aligned} c_m &= \int_0^1 N_b^{-t} e^{-2i\pi m t} dt = \int_0^1 e^{-t \ln N_b} e^{-2i\pi m t} dt = -\frac{1}{\ln N_b + 2i m \pi} \left[e^{-t \ln N_b} e^{-2i\pi m t} \right]_0^1 \\ &= \frac{1}{\ln N_b + 2i m \pi} \left[1 - \frac{1}{N_b} \right] = \frac{N_b - 1}{N_b} \frac{1}{\ln N_b + 2i m \pi}. \end{aligned}$$

Thus, for any $x \in \mathbb{R}$ and any $\varepsilon > 0$,

$$N_b^{-\{x\}} = \frac{N_b - 1}{N_b} \sum_{m \in \mathbb{Z}} \frac{e^{2i\pi m x}}{\ln N_b + 2i m \pi}.$$

Note that since

$$x = -\ln_{N_b}((N_b - 1)\varepsilon),$$

one has, for every $m \in \mathbb{Z}$,

$$e^{2i\pi m x} = e^{-2i\pi m \ln_{N_b}((N_b - 1)\varepsilon)} = e^{-2i\pi m \frac{\ln((N_b - 1)\varepsilon)}{\ln N_b}}.$$

Definition 4.1 (Oscillatory Period).

Following [LvF00], [LvF13], [LRŽ17b], we introduce the *oscillatory period* of the Weierstrass Curve:

$$p = \frac{2\pi}{\ln N_b}.$$

Definition 4.2 (m^{th} -Order Vibration Mode).

Given a relative integer m (i.e., $m \in \mathbb{Z}$), we define the m^{th} -order vibration mode as the one associated to mp .

Property 4.2. For any relative integer m , as given in Property 4.1,

$$e^{2i\pi m x} = e^{-i m p \ln((N_b - 1)\varepsilon)} = ((N_b - 1)\varepsilon)^{-i m p} = (N_b - 1)^{-i m p} \varepsilon^{-i m p}.$$

Thus, for any $x \in \mathbb{R}$ and any $\varepsilon > 0$,

$$N_b^{-\{x\}} = \frac{N_b - 1}{N_b} \sum_{m \in \mathbb{Z}} \frac{(N_b - 1)^{-i m p} \varepsilon^{-i m p}}{\ln N_b + 2i m \pi}, \quad N_b^{-D_{\mathcal{W}}\{x\}} = \frac{N_b^{D_{\mathcal{W}}} - 1}{N_b^{D_{\mathcal{W}}}} \sum_{m \in \mathbb{Z}} \frac{(N_b^{D_{\mathcal{W}}} - 1)^{-i m p} \varepsilon^{-i m p}}{D_{\mathcal{W}} \ln N_b + 2i m \pi},$$

and, for any natural integer k , we have that

$$\begin{aligned} N_b^{(k(2-D_{\mathcal{W}})-1)\{x\}} &= \frac{N_b^{-(1-k(2-D_{\mathcal{W}})-1)}}{N_b^{1-k(2-D_{\mathcal{W}})}} \sum_{m \in \mathbb{Z}} \frac{\left(N_b^{1-k(2-D_{\mathcal{W}})}\right)^{-im\pi} \varepsilon^{-im\pi}}{\ln N_b^{1-k(2-D_{\mathcal{W}})} + 2im\pi} \\ &= \frac{N_b^{1-k(2-D_{\mathcal{W}})} - 1}{N_b^{1-k(2-D_{\mathcal{W}})}} \sum_{m \in \mathbb{Z}} \frac{\left(N_b^{1-k(2-D_{\mathcal{W}})} - 1\right)^{-im\pi} \varepsilon^{-im\pi}}{(1-k(2-D_{\mathcal{W}})) \ln N_b + 2im\pi}. \end{aligned}$$

Definition 4.3 (Distance and Tube Zeta Functions Associated to an Arbitrary Bounded Set of \mathbb{R}^2).

Let A be an arbitrary (nonempty) bounded subset of \mathbb{R}^2 , with upper Minkowski dimension denoted by D_A ; see Definition 4.5 below.

Then, given a fixed number $\varepsilon > 0$, and an arbitrary ε -neighborhood (or tubular neighborhood) of A ,

$$\mathcal{D}_A(\varepsilon) = \{M \in \mathbb{R}^2, d(M, A) \leq \varepsilon\},$$

of tubular volume $\mathcal{V}_A(\varepsilon)$, the *distance zeta function* ζ_A of A is defined (as in [LRŽ17b], Definition 2.1.1, page 45), for all s in \mathbb{C} with sufficiently large real part (in fact, for $\Re(s) > D_A$), by

$$\zeta_A(s) = \int_{M \in \mathcal{D}_A(\varepsilon)} d(M, A)^{s-2} dM.$$

As for the *tube zeta function* $\tilde{\zeta}_A$ of A , it is defined (as in [LRŽ17b], Definition 2.2.8, page 118), for all s in \mathbb{C} with sufficiently large real part (in fact, also for $\Re(s) > D_A$), by

$$\tilde{\zeta}_A(s) = \int_0^\varepsilon t^{s-3} \mathcal{V}_A(t) dt = \int_0^\varepsilon t^{s-2} \mathcal{V}_A(t) \frac{dt}{t}.$$

Remark 4.1. We note that it is shown in [LRŽ17b] that different choices of $\varepsilon > 0$ in Definition 4.3 lead to distance (respectively, tube) zeta functions differing by an entire function, and that ζ_A and $\tilde{\zeta}_A$ are connected by the following *functional equation* (in the present case, when $A \subset \mathbb{R}^2$), for the same value of $\varepsilon > 0$,

$$\zeta_A(s) = \varepsilon^{s-2} \mathcal{V}_A(\varepsilon) + (2-s) \tilde{\zeta}_A(s). \quad (\diamond)$$

Furthermore, assume that the upper Minkowski dimension of A , D_A (which, by [LRŽ17b], Theorem 2.1.11, page 57 and (\diamond)) coincides with the abscissa of convergence of ζ_A and $\tilde{\zeta}_A$, is such that $D_A < 2$. It then follows from the above results (see [LRŽ17b], Corollary 2.2.20, page 127) that ζ_A and $\tilde{\zeta}_A$ have the same poles (denoted by ω) with residues connected by the relation

$$\operatorname{res}(\tilde{\zeta}_A, \omega) = \frac{1}{2-\omega} \operatorname{res}(\zeta_A, \omega), \quad (\diamond\diamond)$$

in case ω is a simple pole; and, similarly for the principal parts of ζ_A and $\tilde{\zeta}_A$ at ω , in case ω is a multiple pole. It follows, in particular, that the Complex Dimensions of A can be indifferently defined as the (visible) poles of ζ_A or of $\tilde{\zeta}_A$.

4.2 Fractal Tube Formulas and Fractal Zeta Functions

In order to obtain the main results of this section – namely, Theorems 4.7, 4.8 and 4.11, along with Corollary 4.9 below, we consider the contribution to the fractal tube formulas brought by the various types of geometric elements in the ε -neighborhood of $\Gamma_{\mathcal{W}}$, here, the rectangles and the wedges (in Properties 4.3 and 4.4 respectively), thereby supplementing the study of the positive or negative contributions of the rectangles, triangles and extreme wedges carried out earlier in Section 3, and synthetized in Propositions 3.5–3.8 above.

Property 4.3 (Tube Formula and Tube Zeta Function Associated to the Contribution of the Rectangles to the Tubular Volume).

The contribution of the $2(N_b - 1)N_b^m$ rectangles to the tubular volume is

$$\begin{aligned}\mathcal{V}_{\text{Rectangles}}(\varepsilon) &= 2 \sum_{k=0}^{\infty} \binom{\frac{1}{2}}{k} N_b^{-(1-k(2-D_{\mathcal{W}}))} \{x\} \varepsilon^{2-D_{\mathcal{W}}+k(2-D_{\mathcal{W}})} \mathcal{O}(1) \\ &= 2 \sum_{k=0}^{\infty} \binom{\frac{1}{2}}{k} \frac{N_b^{1-k(2-D_{\mathcal{W}})} - 1}{N_b^{1-k(2-D_{\mathcal{W}})}} \sum_{m \in \mathbb{Z}} \frac{(N_b - 1)^{-im p} \varepsilon^{2-D_{\mathcal{W}}+k(2-D_{\mathcal{W}})-im p}}{(1 - k(2 - D_{\mathcal{W}})) \ln N_b + 2im\pi} \mathcal{O}(1) .\end{aligned}$$

For the sake of clarity, and in order to avoid confusion between various occurrences of $\mathcal{O}(1)$, we will write it under the form

$$\mathcal{V}_{\text{Rectangles}}(\varepsilon) = C_{\text{Rectangles}} \sum_{k=0}^{\infty} \binom{\frac{1}{2}}{k} \frac{N_b^{1-k(2-D_{\mathcal{W}})} - 1}{N_b^{1-k(2-D_{\mathcal{W}})}} \sum_{m \in \mathbb{Z}} \frac{(N_b - 1)^{-im p} \varepsilon^{2-D_{\mathcal{W}}+k(2-D_{\mathcal{W}})-im p}}{(1 - k(2 - D_{\mathcal{W}})) \ln N_b + 2im\pi} ,$$

where $C_{\text{Rectangles}}$ denotes a strictly positive and finite constant.

The associated tube zeta function [LRŽ17b] is first obtained, for any complex number s such that $\Re(s) > D_{\mathcal{W}}$, through

$$\begin{aligned}\tilde{\zeta}_{\text{Rectangles}}(s) &= \int_0^\varepsilon t^{s-3} \mathcal{V}_{\text{Rectangles}}(t) dt \\ &= C_{\text{Rectangles}} \sum_{k=0}^{\infty} \binom{\frac{1}{2}}{k} \frac{N_b^{1-k(2-D_{\mathcal{W}})} - 1}{N_b^{1-k(2-D_{\mathcal{W}})}} \sum_{m \in \mathbb{Z}} \frac{(N_b - 1)^{-im p}}{(1 - k(2 - D_{\mathcal{W}})) \ln N_b + 2im\pi} \int_0^\varepsilon t^{s-3} t^{2-D_{\mathcal{W}}+k(2-D_{\mathcal{W}})-im p} dt \\ &= C_{\text{Rectangles}} \sum_{k=0}^{\infty} \binom{\frac{1}{2}}{k} \frac{N_b^{1-k(2-D_{\mathcal{W}})} - 1}{N_b^{1-k(2-D_{\mathcal{W}})}} \sum_{m \in \mathbb{Z}} \frac{(N_b - 1)^{-im p}}{(1 - k(2 - D_{\mathcal{W}})) \ln N_b + 2im\pi} \frac{\varepsilon^{s-D_{\mathcal{W}}+k(2-D_{\mathcal{W}})-im p}}{s - D_{\mathcal{W}} + k(2 - D_{\mathcal{W}}) - im p} .\end{aligned}$$

By meromorphic continuation to all of \mathbb{C} , one then obtains the tube zeta function $\tilde{\zeta}_{\text{Rectangles}}$ for all $s \in \mathbb{C}$, as given by the last two equalities just above.

The associated Complex Dimensions arise as

$$D_{\mathcal{W}} - k(2 - D_{\mathcal{W}}) + im p , \quad \text{with } k \in \mathbb{N}, m \in \mathbb{Z} .$$

Note that, thanks to the results of Corollary 2.15, the one-periodic function (with respect to the variable $\ln_{N_b} \varepsilon^{-1}$, see Property 4.1), associated to $D_{\mathcal{W}}$, is bounded between two strictly positive and finite constants.

Property 4.4 (Tube Formula and Tube Zeta Function Associated to the Contribution of the Wedges to the Tubular Volume).

The contribution of the *wedges* to the tubular volume is

$$\begin{aligned}
\mathcal{V}_{\text{wedges}}(\varepsilon) &= \mathcal{V}_{\text{upper wedges}}(\varepsilon) + \mathcal{V}_{\text{lower wedges}}(\varepsilon) + \mathcal{V}_{\text{extreme wedges}}(\varepsilon) \\
&= \frac{r_b \pi \varepsilon^3}{8} N_b^{-\{x\}} - \frac{\pi \varepsilon^4}{2} + \pi \varepsilon^2 \\
&\quad - \frac{\varepsilon^3}{4} r_b \sum_{k=0}^{\infty} \frac{1}{2k+1} N_b^{-((2k+1)D_{\mathcal{W}}-2k)\{x\}} \varepsilon^{2k+1} \mathcal{O}(1) \\
&\quad + \frac{\varepsilon^4}{2} \sum_{k=0}^{\infty} \frac{1}{2k+1} N_b^{-(2k+1)(D_{\mathcal{W}}-1)\{x\}} \varepsilon^{2k+1} \mathcal{O}(1) \\
&= \frac{r_b \pi}{8} \frac{N_b - 1}{N_b} \sum_{m \in \mathbb{Z}} \frac{(N_b - 1)^{-im} \varepsilon^{3-im}}{\ln N_b + 2im\pi} - \frac{\pi \varepsilon^4}{2} + \pi \varepsilon^2 \\
&\quad - \frac{1}{4} r_b \sum_{k=0}^{\infty} \frac{1}{2k+1} \frac{N_b^{((2k+1)D_{\mathcal{W}}-2k)} - 1}{N_b^{((2k+1)D_{\mathcal{W}}-2k)}} \sum_{m \in \mathbb{Z}} \frac{(N_b^{((2k+1)D_{\mathcal{W}}-2k)} - 1)^{-im} \varepsilon^{2k+1-im}}{((2k+1)D_{\mathcal{W}} - 2k) \ln N_b + 2im\pi} \mathcal{O}(1) \\
&\quad + \frac{1}{2} \sum_{k=0}^{\infty} \frac{1}{2k+1} \frac{N_b^{(2k+1)(D_{\mathcal{W}}-1)} - 1}{N_b^{(2k+1)(D_{\mathcal{W}}-1)}} \sum_{m \in \mathbb{Z}} \frac{(N_b^{(2k+1)(D_{\mathcal{W}}-1)} - 1)^{-im} \varepsilon^{5+2k-im}}{(2k+1)(D_{\mathcal{W}} - 1) \ln N_b + 2im\pi} \mathcal{O}(1).
\end{aligned}$$

As before, for the sake of clarity, we will rewrite it in the form

$$\begin{aligned}
\mathcal{V}_{\text{wedges}}(\varepsilon) &= C_{\text{wedges}}^1 \sum_{m \in \mathbb{Z}} \frac{(N_b - 1)^{-im} \varepsilon^{3-im}}{\ln N_b + 2im\pi} - \frac{\pi \varepsilon^4}{2} + \pi \varepsilon^2 \\
&\quad - C_{\text{wedges}}^2 \sum_{k=0}^{\infty} \frac{1}{2k+1} \frac{N_b^{((2k+1)D_{\mathcal{W}}-2k)} - 1}{N_b^{((2k+1)D_{\mathcal{W}}-2k)}} \sum_{m \in \mathbb{Z}} \frac{(N_b^{((2k+1)D_{\mathcal{W}}-2k)} - 1)^{-im} \varepsilon^{2k+1-im}}{((2k+1)D_{\mathcal{W}} - 2k) \ln N_b + 2im\pi} \\
&\quad + C_{\text{wedges}}^3 \sum_{k=0}^{\infty} \frac{1}{2k+1} \frac{N_b^{(2k+1)(D_{\mathcal{W}}-1)} - 1}{N_b^{(2k+1)(D_{\mathcal{W}}-1)}} \sum_{m \in \mathbb{Z}} \frac{(N_b^{(2k+1)(D_{\mathcal{W}}-1)} - 1)^{-im} \varepsilon^{5+2k-im}}{(2k+1)(D_{\mathcal{W}} - 1) \ln N_b + 2im\pi},
\end{aligned}$$

where C_{wedges}^1 , C_{wedges}^2 , and C_{wedges}^3 denote strictly positive and finite constants.

The associated tube zeta function [LRŽ17b] is first obtained, for any complex number s such that $\Re(s) > D_{\mathcal{W}}$, through

$$\begin{aligned}
\tilde{\zeta}_{wedges}(s) &= \int_0^\varepsilon t^{s-3} \mathcal{V}_{wedges}(t) dt \\
&= C_{wedges}^1 \sum_{m \in \mathbb{Z}} \frac{(N_b - 1)^{-i m p}}{\ln N_b + 2 i m \pi} \int_0^\varepsilon t^{s-i m p} dt + \pi \int_0^\varepsilon t^{s-1} dt - \frac{\pi}{2} \int_0^\varepsilon t^{s+1} dt \\
&\quad - C_{wedges}^2 \sum_{k=0}^\infty \frac{1}{2k+1} \frac{N_b^{((2k+1)D_{\mathcal{W}}-2k)} - 1}{N_b^{((2k+1)D_{\mathcal{W}}-2k)}} \sum_{m \in \mathbb{Z}} \frac{(N_b^{((2k+1)D_{\mathcal{W}}-2k)} - 1)^{-i m p}}{((2k+1)D_{\mathcal{W}}-2k) \ln N_b + 2 i m \pi} \int_0^\varepsilon t^{s+2k+1-i m p} dt \\
&\quad + C_{wedges}^3 \sum_{k=0}^\infty \frac{1}{2k+1} \frac{N_b^{(2k+1)(D_{\mathcal{W}}-1)} - 1}{N_b^{(2k+1)(D_{\mathcal{W}}-1)}} \sum_{m \in \mathbb{Z}} \frac{(N_b^{(2k+1)(D_{\mathcal{W}}-1)} - 1)^{-i m p}}{(2k+1)(D_{\mathcal{W}}-1) \ln N_b + 2 i m \pi} \int_0^\varepsilon t^{s-2+2k-i m p} dt \\
&= C_{wedges}^1 \sum_{m \in \mathbb{Z}} \frac{(N_b - 1)^{-i m p}}{\ln N_b + 2 i m \pi} \frac{\varepsilon^{s+1-i m p}}{s+1-i m p} + \frac{\pi \varepsilon^s}{s} - \frac{\pi \varepsilon^{s+2}}{2(s+2)} \\
&\quad - C_{wedges}^2 \sum_{k=0}^\infty \frac{1}{2k+1} \frac{N_b^{((2k+1)D_{\mathcal{W}}-2k)} - 1}{N_b^{((2k+1)D_{\mathcal{W}}-2k)}} \sum_{m \in \mathbb{Z}} \frac{(N_b^{((2k+1)D_{\mathcal{W}}-2k)} - 1)^{-i m p}}{((2k+1)D_{\mathcal{W}}-2k) \ln N_b + 2 i m \pi} \frac{\varepsilon^{s+2k+1-i m p}}{s+2k+1-i m p} \\
&\quad + C_{wedges}^3 \sum_{k=0}^\infty \frac{1}{2k+1} \frac{N_b^{(2k+1)(D_{\mathcal{W}}-1)} - 1}{N_b^{(2k+1)(D_{\mathcal{W}}-1)}} \sum_{m \in \mathbb{Z}} \frac{(N_b^{(2k+1)(D_{\mathcal{W}}-1)} - 1)^{-i m p}}{(2k+1)(D_{\mathcal{W}}-1) \ln N_b + 2 i m \pi} \frac{\varepsilon^{s+3+2k-i m p}}{s+3+2k-i m p}.
\end{aligned}$$

By meromorphic continuation to all of \mathbb{C} , one then obtains the tube zeta function $\tilde{\zeta}_{wedges}$ for all $s \in \mathbb{C}$, as given by the last two equalities just above.

The associated Complex Dimensions arise as

$$-1 + i m p, \quad 1 - 2k + i m p, \quad -3 - 2k + i m p, \quad \text{with } k \in \mathbb{N}, m \in \mathbb{Z}, \text{ along with } 0 \text{ and } -2.$$

Note that for $k \geq 2$ (and any $m \in \mathbb{Z}$), the last two families of (possible) Complex Dimensions fully overlap. We will take this fact into account in Theorems 4.10 and 4.11 below.

Property 4.5 (Tube Formula and Tube Zeta Function Associated to the Contribution of the Extra Outer Triangles to the Tubular Volume).

As for the negative contribution of the $(N_b - r_b - 1) N_b^m$ *extra outer triangles* to the tubular volume, one obtains

$$\begin{aligned}
\mathcal{V}_{\text{extra outer triangles}}(\varepsilon) &= \mathcal{V}_{\text{extra outer lower triangles}}(\varepsilon) + \mathcal{V}_{\text{extra outer upper triangles}}(\varepsilon) \\
&= -\frac{\varepsilon^2}{2} N_b^{(3D_{\mathcal{W}}-2)\{x\}} \mathcal{O}(1) \\
&= -\frac{N_b^{2-3D_{\mathcal{W}}} - 1}{N_b^{2-3D_{\mathcal{W}}}} \sum_{m \in \mathbb{Z}} \frac{(N_b^{2-3D_{\mathcal{W}}} - 1)^{-i m p}}{(2-3D_{\mathcal{W}}) \ln N_b + 2 i m \pi} \varepsilon^{2-i m p} \mathcal{O}(1).
\end{aligned}$$

As previously, for the sake of clarity, we will write it in the following form:

$$\mathcal{V}_{\text{extra outer triangles}}(\varepsilon) = -C_{\text{triangles}} \sum_{m \in \mathbb{Z}} \frac{(N_b^{2-3D_{\mathcal{W}}} - 1)^{-im p} \varepsilon^{2-im p}}{(2-3D_{\mathcal{W}}) \ln N_b + 2im\pi},$$

where $C_{\text{triangles}}$ denotes a strictly positive and finite constant.

The associated tube zeta function [LRŽ17b] is first obtained, for any complex number s such that $\Re(s) > D_{\mathcal{W}}$, through

$$\begin{aligned} \tilde{\zeta}_{\text{extra triangles}}(s) &= \int_0^\varepsilon t^{s-3} \mathcal{V}_{\text{extra outer triangles}}(t) dt \\ &= -C_{\text{triangles}} \sum_{m \in \mathbb{Z}} \frac{(N_b^{2-3D_{\mathcal{W}}} - 1)^{-im p}}{(2-3D_{\mathcal{W}}) \ln N_b + 2im\pi} \int_0^\varepsilon t^{s-2-im p} dt \\ &= -C_{\text{triangles}} \sum_{m \in \mathbb{Z}} \frac{(N_b^{2-3D_{\mathcal{W}}} - 1)^{-im p}}{(2-3D_{\mathcal{W}}) \ln N_b + 2im\pi} \frac{\varepsilon^{s-1-im p}}{s-1-im p}. \end{aligned}$$

By meromorphic continuation to all of \mathbb{C} , one then obtains the tube zeta function $\tilde{\zeta}_{\text{extra triangles}}$ for all $s \in \mathbb{C}$, as given by the last two equalities just above.

The associated Complex Dimensions arise as

$$1 + im p, \text{ with } m \in \mathbb{Z}.$$

Property 4.6 (Tube Formula and Tube Zeta Function Associated to the Contribution of the Parallelograms to the Tubular Volume).

The last contribution, coming from the parallelograms, is given by

$$\begin{aligned} \mathcal{V}_{\text{parallelograms}}(\varepsilon) &= \mathcal{V}_{\text{lower parallelograms}}(\varepsilon) + \mathcal{V}_{\text{upper parallelograms}}(\varepsilon) \\ &= -\frac{(N_b - 2)}{2(N_b - 1)} \left\{ \frac{N_b^{D_{\mathcal{W}}} - 1}{N_b^{D_{\mathcal{W}}}} \sum_{m \in \mathbb{Z}} \frac{(N_b^{D_{\mathcal{W}}} - 1)^{-im p} \varepsilon^{2-im p}}{D_{\mathcal{W}} \ln N_b + 2im\pi} \mathcal{O}(1) \right. \\ &\quad \left. - \frac{N_b^{2-D_{\mathcal{W}}} - 1}{N_b^{2-D_{\mathcal{W}}}} \sum_{m \in \mathbb{Z}} \frac{(N_b^{2-D_{\mathcal{W}}} - 1)^{-im p} \varepsilon^{-im p}}{(2-D_{\mathcal{W}}) \ln N_b + 2im\pi} \mathcal{O}(1) \right\}. \end{aligned}$$

Again, we write it in the following form:

$$\mathcal{V}_{\text{parallelograms}}(\varepsilon) = -C_{\text{parallelograms}} \sum_{m \in \mathbb{Z}} \frac{(N_b^{2-3D_{\mathcal{W}}} - 1)^{-im p} \varepsilon^{2-im p}}{(2-3D_{\mathcal{W}}) \ln N_b + 2im\pi},$$

where $C_{\text{parallelograms}}$ denotes a strictly positive and finite constant.

The associated tube zeta function [LRŽ17b] is first obtained, for any complex number s such that $\Re(s) > D_{\mathcal{W}}$, through

$$\begin{aligned}\tilde{\zeta}_{\text{parallelograms}}(s) &= \int_0^\varepsilon t^{s-3} \mathcal{V}_{\text{parallelograms}}(t) dt \\ &= -C_{\text{parallelograms}} \sum_{m \in \mathbb{Z}} \frac{(N_b^{2-3D_{\mathcal{W}}} - 1)^{-im p}}{(2-3D_{\mathcal{W}}) \ln N_b + 2im\pi} \int_0^\varepsilon t^{s-2-im p} dt \\ &= -C_{\text{parallelograms}} \sum_{m \in \mathbb{Z}} \frac{(N_b^{2-3D_{\mathcal{W}}} - 1)^{-im p}}{(2-3D_{\mathcal{W}}) \ln N_b + 2im\pi} \frac{\varepsilon^{s-1-im p}}{s-1-im p}.\end{aligned}$$

By meromorphic continuation to all of \mathbb{C} , one then obtains the tube zeta function $\tilde{\zeta}_{\text{extra triangles}}$ for all $s \in \mathbb{C}$, as given by the last two equalities just above.

The associated Complex Dimensions arise as

$$1 + im p, \text{ with } m \in \mathbb{Z}.$$

The above results stated in Properties 4.3 – 4.6 can now be combined in order to yield the following key theorems:

Theorem 4.7 (Fractal Tube Formula for The Weierstrass Curve).

Given $\varepsilon > 0$ sufficiently small, the tubular volume $\mathcal{V}_{\mathcal{W}}(\varepsilon)$, or two-dimensional Lebesgue measure of the ε -neighborhood of the Curve,

$$\mathcal{D}(\varepsilon) = \left\{ M = (x, y) \in \mathbb{R}^2, d(M, \Gamma_{\mathcal{W}_{m(\varepsilon)}}) \leq \varepsilon \right\},$$

is given by

$$\begin{aligned}\mathcal{V}_{\mathcal{W}}(\varepsilon) &= \mathcal{V}_{\text{Rectangles}}(\varepsilon) + \mathcal{V}_{\text{wedged}}(\varepsilon) + \mathcal{V}_{\text{extra outer triangles}}(\varepsilon) + \mathcal{V}_{\text{parallelograms}}(\varepsilon) \\ &= C_{\text{Rectangles}} \sum_{k=0}^{\infty} \binom{\frac{1}{2}}{k} \frac{N_b^{1-k(2-D_{\mathcal{W}})} - 1}{N_b^{1-k(2-D_{\mathcal{W}})}} \sum_{m \in \mathbb{Z}} \frac{(N_b - 1)^{-im p}}{(1-k(2-D_{\mathcal{W}})) \ln N_b + 2im\pi} \varepsilon^{2-D_{\mathcal{W}}+k(2-D_{\mathcal{W}})-im p} \\ &\quad + C_{\text{wedged}}^1 \sum_{m \in \mathbb{Z}} \frac{(N_b - 1)^{-im p} \varepsilon^{3-im p}}{\ln N_b + 2im\pi} + \pi \varepsilon^2 - \frac{\pi \varepsilon^4}{2} \\ &\quad - C_{\text{wedged}}^2 \sum_{k=0}^{\infty} \frac{1}{2k+1} \frac{N_b^{((2k+1)D_{\mathcal{W}}-2k)} - 1}{N_b^{((2k+1)D_{\mathcal{W}}-2k)}} \sum_{m \in \mathbb{Z}} \frac{(N_b^{((2k+1)D_{\mathcal{W}}-2k)} - 1)^{-im p} \varepsilon^{2k+1-im p}}{((2k+1)D_{\mathcal{W}}-2k) \ln N_b + 2im\pi} \\ &\quad + C_{\text{wedged}}^3 \sum_{k=0}^{\infty} \frac{1}{2k+1} \frac{N_b^{(2k+1)(D_{\mathcal{W}}-1)} - 1}{N_b^{(2k+1)(D_{\mathcal{W}}-1)}} \sum_{m \in \mathbb{Z}} \frac{(N_b^{(2k+1)(D_{\mathcal{W}}-1)} - 1)^{-im p} \varepsilon^{5+2k-im p}}{(2k+1)(D_{\mathcal{W}}-1) \ln N_b + 2im\pi} \\ &\quad - (C_{\text{triangles}} + C_{\text{parallelograms}}) \sum_{m \in \mathbb{Z}} \frac{(N_b^{2-3D_{\mathcal{W}}} - 1)^{-im p}}{(2-3D_{\mathcal{W}}) \ln N_b + 2im\pi} \varepsilon^{2-im p},\end{aligned}$$

where $C_{\text{rectangles}}$, C_{wedged}^ℓ , $\ell = 1, 2, 3$, $C_{\text{triangles}}$, and $C_{\text{parallelograms}}$ denote the strictly positive and finite constants respectively introduced in Properties 4.3 – 4.6 above.

For the sake of clarity, and in order to highlight the role played by the one-periodic functions (with respect to the variable $\ln_{N_b} \varepsilon^{-1}$, see Property 4.1), one can exchange the sums over k and m , which enables one to obtain an expression of the following form:

$$\begin{aligned} \mathcal{V}_{\mathcal{W}}(\varepsilon) &= \sum_{m \in \mathbb{Z}, k \in \mathbb{N}} f_{m,k, \text{Rectangles}} \varepsilon^{2-D_{\mathcal{W}}+k(2-D_{\mathcal{W}})-i m p} \\ &+ \sum_{m \in \mathbb{Z}, k \in \mathbb{N}} \left(f_{m,k, \text{wedges},1} \varepsilon^{3-i m p} + f_{m,k, \text{wedges},2} \varepsilon^{1+2k-i m p} + f_{m,k, \text{wedges},3} \varepsilon^{5+2k-i m p} \right) \\ &+ \sum_{m \in \mathbb{Z}, k \in \mathbb{N}} f_{m,k, \text{triangles, parallelograms}} \varepsilon^{2-i m p} + \pi \varepsilon^2 - \frac{\pi \varepsilon^4}{2}, \end{aligned}$$

where the notation $f_{m,k, \text{Rectangles}}$, $f_{m,k, \text{wedges}, \ell}$, $1 \leq \ell \leq 3$, and $f_{m,k, \text{triangles, parallelograms}}$, respectively account for the coefficients associated to the sums corresponding to the contribution of the rectangles, wedges, triangles and parallelograms.

Theorem 4.8 (Tube Zeta Function for the Weierstrass Curve).

Given $\varepsilon > 0$ sufficiently small, the tube zeta function associated to the Weierstrass Curve, $\tilde{\zeta}_{\mathcal{W}}(s)$, defined as in [LRŽ17b] (see Definition 4.3 above), admits a meromorphic continuation to all of \mathbb{C} , and is given, for any complex number s , by the following expression:

$$\begin{aligned} \tilde{\zeta}_{\mathcal{W}}(s) &= \tilde{\zeta}_{\text{Rectangles}}(s) + \tilde{\zeta}_{\text{wedges}}(s) + \tilde{\zeta}_{\text{extra outer triangles}}(s) + \tilde{\zeta}_{\text{parallelograms}}(s) \\ &= C_{\text{Rectangles}} \sum_{k=0}^{\infty} \left(\frac{1}{2} \right) \frac{N_b^{1-k(2-D_{\mathcal{W}})} - 1}{N_b^{1-k(2-D_{\mathcal{W}})}} \sum_{m \in \mathbb{Z}} \frac{(N_b - 1)^{-i m p}}{(1 - k(2 - D_{\mathcal{W}})) \ln N_b + 2 i m \pi} \frac{\varepsilon^{s-D_{\mathcal{W}}+k(2-D_{\mathcal{W}})-i m p}}{s - D_{\mathcal{W}} + k(2 - D_{\mathcal{W}}) - i m p} \\ &+ C_{\text{wedges}}^1 \sum_{m \in \mathbb{Z}} \frac{(N_b - 1)^{-i m p}}{\ln N_b + 2 i m \pi} \frac{\varepsilon^{s+1-i m p}}{s + 1 - i m p} + \frac{\pi \varepsilon^s}{s} - \frac{\pi \varepsilon^{s+2}}{4(s+2)} \\ &- C_{\text{wedges}}^2 \sum_{k=0}^{\infty} \frac{1}{2k+1} \frac{N_b^{((2k+1)D_{\mathcal{W}}-2k)} - 1}{N_b^{((2k+1)D_{\mathcal{W}}-2k)}} \sum_{m \in \mathbb{Z}} \frac{(N_b^{((2k+1)D_{\mathcal{W}}-2k)} - 1)^{-i m p}}{((2k+1)D_{\mathcal{W}} - 2k) \ln N_b + 2 i m \pi} \frac{\varepsilon^{s+2k-1-i m p}}{s + 2k - 1 - i m p} \\ &+ C_{\text{wedges}}^3 \sum_{k=0}^{\infty} \frac{1}{2k+1} \frac{N_b^{(2k+1)(D_{\mathcal{W}}-1)} - 1}{N_b^{(2k+1)(D_{\mathcal{W}}-1)}} \sum_{m \in \mathbb{Z}} \frac{(N_b^{(2k+1)(D_{\mathcal{W}}-1)} - 1)^{-i m p}}{(2k+1)(D_{\mathcal{W}} - 1) \ln N_b + 2 i m \pi} \frac{\varepsilon^{s+3+2k-i m p}}{s + 3 + 2k - i m p} \\ &- (C_{\text{triangles}} + C_{\text{parallelograms}}) \sum_{m \in \mathbb{Z}} \frac{(N_b^{2-3D_{\mathcal{W}}} - 1)^{-i m p}}{(2 - 3D_{\mathcal{W}}) \ln N_b + 2 i m \pi} \frac{\varepsilon^{s-1-i m p}}{s - 1 - i m p}. \end{aligned}$$

For the sake of clarity, and in order to highlight the role played by the one-periodic functions (with respect to the variable $\ln_{N_b} \varepsilon^{-1}$, see Property 4.1), one can exchange the sums over k and m , which enables one to obtain an expression of the following form:

$$\begin{aligned} \tilde{\zeta}_{\mathcal{W}}(s) &= \sum_{m \in \mathbb{Z}, k \in \mathbb{N}} f_{m,k, \text{Rectangles}} \frac{\varepsilon^{s-D_{\mathcal{W}}+k(2-D_{\mathcal{W}})-i m p}}{s - D_{\mathcal{W}} + k(2 - D_{\mathcal{W}}) - i m p} \\ &+ \sum_{m \in \mathbb{Z}, k \in \mathbb{N}} \left(f_{m,k, \text{wedges},1} \frac{\varepsilon^{s+1-i m p}}{s + 1 - i m p} + f_{m,k, \text{wedges},2} \frac{\varepsilon^{s+2k-1-i m p}}{s + 2k - 1 - i m p} + f_{m,k, \text{wedges},3} \frac{\varepsilon^{s+3+2k-i m p}}{s + 3 + 2k - i m p} \right) \\ &+ \sum_{m \in \mathbb{Z}, k \in \mathbb{N}} f_{m,k, \text{triangles, parallelograms}} \frac{\varepsilon^{s-1-i m p}}{s - 1 - i m p} + \frac{\pi \varepsilon^s}{s} - \frac{\pi \varepsilon^{s+2}}{4(s+2)}, \end{aligned}$$

where, as already introduced in Theorem 4.7, the notation $f_{m,k,\text{Rectangles}}$, $f_{m,k,\text{wedges},\ell}$, $1 \leq \ell \leq 3$, and $f_{m,k,\text{triangles, parallelograms}}$, respectively account for the coefficients associated to the sums corresponding to the contribution of the rectangles, wedges, triangles and parallelograms.

Corollary 4.9 ((of Theorem 4.8) Distance Zeta Function for the Weierstrass Curve).

According to the functional equation given in [LRŽ17b] (Theorem 2.2.1., page 112), and recalled in equation (♦) of Remark 4.1 above, the distance zeta function, $\zeta_{\mathcal{W}}$, associated to the Weierstrass Curve is obtained, for any complex number s , through

$$\begin{aligned}\zeta_{\mathcal{W}}(s) &= \int_{M \in \mathcal{D}(\varepsilon)} d(M, \Gamma_{\mathcal{W}})^{s-2} dM \\ &= \varepsilon^{s-2} \mathcal{V}_{\mathcal{W}}(\varepsilon) + (2-s) \int_0^\varepsilon t^{s-3} \mathcal{V}_{\mathcal{W}}(t) dt \\ &= \varepsilon^{s-2} \mathcal{V}_{\mathcal{W}}(\varepsilon) + (2-s) \tilde{\zeta}_{\mathcal{W}}(s),\end{aligned}$$

where $\mathcal{V}_{\mathcal{W}}$ denotes the tubular volume obtained in Theorem 4.7 above or in Theorem 4.11 below, and where $\tilde{\zeta}_{\mathcal{W}}(s)$ is given in Theorem 4.8. The first two equalities are valid for $\Re(s) > D_{\mathcal{W}}$, while the last one is valid for all s in \mathbb{C} . Furthermore, the distance zeta function $\zeta_{\mathcal{W}}$ admits a meromorphic continuation to all of \mathbb{C} , given by the last equality just above.

Remark 4.2. Since $D_{\mathcal{W}} < 2$, it follows from the above expressions, as well from the general theory developed in [LRŽ17b], that $\zeta_{\mathcal{W}}$ and $\tilde{\zeta}_{\mathcal{W}}$ have exactly the same poles, with precisely related residues, for simple poles, which is the case here. Hence, they define the same Complex Dimensions. This is true because, with the obvious following notation, and for $0 < \varepsilon_1 < \varepsilon_2$, the difference of $\zeta_{\mathcal{W},\varepsilon_1}$ and $\zeta_{\mathcal{W},\varepsilon_2}$ is an entire function; and, similarly, for $\tilde{\zeta}_{\mathcal{W},\varepsilon_1} - \tilde{\zeta}_{\mathcal{W},\varepsilon_2}$; see [LRŽ17b], Proposition 2.1.76 on page 100, and Proposition 2.2.13 on page 123. Furthermore, the Complex Dimensions – i.e., the poles of $\zeta_{\mathcal{W}}$, or, equivalently, of $\tilde{\zeta}_{\mathcal{W}}$, are independent of the choice of the parameter ε . The same is true for the residues of $\zeta_{\mathcal{W}}$ (as well as of $\tilde{\zeta}_{\mathcal{W}}$) at any pole, i.e., at any Complex Dimension. See Remark 4.1 above, including equation (♦♦).

Remark 4.3 (Periodic Functions Associated to the Poles of the Zeta Functions).

The one-periodic functions (with respect to the variable $\ln_{N_b} \varepsilon^{-1}$, see Property 4.1), respectively associated to the following values,

- i. $D_{\mathcal{W}} - k(2 - D_{\mathcal{W}})$, with $k \in \mathbb{N}$,
- ii. 1,

are nonconstant, since their m^{th} Fourier coefficients, with $m \in \mathbb{Z}$, $m \neq 0$, which are respectively proportional to the strictly positive and finite constants $C_{\text{Rectangles}}^\ell$, C_{wedges}^ℓ , for $1 \leq \ell \leq 3$, and $C_{\text{triangles}} + C_{\text{parallelograms}}$, are thus nonzero. We refer to Theorem 4.11 below for the specific manner in which these periodic functions arise. (See also Subsection 4.3.2.)

4.3 Complex Dimensions

We deduce at once the Complex Dimensions of the Weierstrass Curve from the fractal tube formula and the expression for the tube zeta function obtained in Theorems 4.7 and 4.8, respectively.

4.3.1 Main Results

Theorem 4.10 (Complex Dimensions of the Weierstrass Curve).

The possible Complex Dimensions of the Weierstrass Curve are all simple, and given as follows:

$$D_{\mathcal{W}} - k(2 - D_{\mathcal{W}}) + i m p, \quad \text{with } k \in \mathbb{N}, m \in \mathbb{Z},$$

$$1 - 2k + i m p, \quad \text{with } k \in \mathbb{N}, m \in \mathbb{Z}, \text{ along with } -2 \text{ and } 0,$$

where $p = \frac{2\pi}{\ln N_b}$ is the oscillatory period of the Weierstrass Curve.

Furthermore, the one-periodic functions (with respect to the variable $\ln_{N_b} \varepsilon^{-1}$, see Property 4.1), respectively associated to the values $D_{\mathcal{W}} - k(2 - D_{\mathcal{W}})$, $k \in \mathbb{N}$, are nonconstant. (See also Subsection 4.3.2 below for the exceptional cases.)

In addition, all of the Fourier coefficients of those periodic functions are nonzero, which implies that there are infinitely many Complex Dimensions that are nonreal, including all of those with maximal real part $D_{\mathcal{W}}$, which are the principal Complex Dimensions, in the terminology of [LRŽ17b], and therefore give rise to geometric oscillations (or vibrations) with the largest amplitude, in the fractal tube formula obtained in Theorem 4.7 above and reformulated in Theorem 4.11 below.

Finally, for each $k \in \mathbb{N}$ and $m \in \mathbb{Z}$, $D_{\mathcal{W}} - k(2 - D_{\mathcal{W}}) + i m p$, $1 + i m p$, -2 and 0 are all simple Complex Dimensions of the Weierstrass Curve; i.e., they are simple poles of the tube (or, equivalently, of the distance) zeta function.

Consequently, the Weierstrass Curve is fractal, in the sense of the theory of Complex Dimensions developed in [LvF00] [LvF13], [LRŽ17b] and [Lap19].

We refer to Subsection 4.3.2 for a discussion of the exceptional cases, and to Subsection 4.3.3 for a possible interpretation of our results.

Theorem 4.11 (Condensed Fractal Tube Formula for The Weierstrass Curve (Corollary of Theorem 4.7)).

Given $\varepsilon > 0$ sufficiently small, the tubular volume $\mathcal{V}_{\mathcal{W}}(\varepsilon)$ of the ε -neighborhood $\mathcal{D}(\varepsilon)$ of the Weierstrass Curve, can be expressed in the following manner:

$$\begin{aligned} \mathcal{V}_{\mathcal{W}}(\varepsilon) = & \sum_{k=0}^{\infty} \varepsilon^{2-(D_{\mathcal{W}}-k(2-D_{\mathcal{W}}))} G_{k,D_{\mathcal{W}}} \left(\ln_{N_b} \left(\frac{1}{\varepsilon} \right) \right) \\ & + \sum_{k=0}^{\infty} \varepsilon^{2-(1-2k)} G_{k,1} \left(\ln_{N_b} \left(\frac{1}{\varepsilon} \right) \right) + \pi \varepsilon^2 - \frac{\pi \varepsilon^4}{2}, \end{aligned}$$

where, for any natural integer k , $G_{k,D_{\mathcal{W}}}$ and $G_{k,1}$ denote, respectively, continuous one-periodic functions (with respect to the variable $\ln_{N_b} \varepsilon^{-1}$, see Property 4.1) associated to all of the Complex Dimensions of real parts $D_{\mathcal{W}} - k(2 - D_{\mathcal{W}})$ and $1 - 2k$, where $k \in \mathbb{N}$ is arbitrary. Furthermore, all of the

Fourier coefficients of the periodic functions $G_{k,D_{\mathcal{W}}}$ (for any $k \in \mathbb{N}$) and $G_{0,1}$ are nonzero. In particular, these periodic functions are not constant. Moreover, the functions $G_{0,D_{\mathcal{W}}}$ and $G_{0,1}$ are bounded away from zero and infinity.

This amounts to an expression of the form

$$\mathcal{V}_{\mathcal{W}}(\varepsilon) = \sum_{\substack{\alpha \text{ real part of a Complex Dimension} \\ \alpha \notin \{-2, 0\}}} \varepsilon^{2-\alpha} G_{\alpha} \left(\ln_{N_b} \left(\frac{1}{\varepsilon} \right) \right) + \pi \varepsilon^2 - \frac{\pi \varepsilon^4}{2},$$

where, for any real part α of a Complex Dimension, with $\alpha \notin \{-2, 0\}$, G_{α} denotes a continuous and one-periodic function.

4.3.2 Exceptional Cases

One might naturally question the following exceptional cases:

i. $D_{\mathcal{W}} - k_0 (2 - D_{\mathcal{W}}) = 0$, for some $k_0 \in \mathbb{N}$, which occurs when

$$D_{\mathcal{W}} = \frac{2k_0}{1+k_0}, \text{ i.e., } 2 + \frac{\ln \lambda}{\ln N_b} = \frac{2k_0}{1+k_0}, \text{ or } \lambda = N_b^{-\frac{2}{1+k_0}}.$$

According to the terminology of [LRŽ17b], Chapter 4, or [LvF13], Chapter 12, this first case corresponds to the situation when the Weierstrass Curve is *fractal in dimension 0*. We then happen to have a discrete line of Complex Dimensions with real part 0,

$$\mathcal{L}_0 = \{0 + i m p, m \in \mathbb{Z}\} = \{i m p, m \in \mathbb{Z}\},$$

which is obtained by merger with the discrete line of *actual* Complex Dimensions,

$$\mathcal{L}_{D_{\mathcal{W}}, k_0} = \left\{ \underbrace{D_{\mathcal{W}} - k_0 (2 - D_{\mathcal{W}})}_{0 \text{ here}} + i m p, m \in \mathbb{Z} \right\}.$$

Note that the *actual* Complex Dimensions are *not double* (i.e., of multiplicity two). This directly comes from the expression obtained in Theorem 4.8 for the fractal tube zeta function $\tilde{\zeta}_{\mathcal{W}}$, which becomes here, for any complex number s ,

$$\begin{aligned} \tilde{\zeta}_{\mathcal{W}}(s) &= \sum_{m \in \mathbb{Z}} f_{m, k_0, \text{Rectangles}} \frac{\varepsilon^{s-i m p}}{s - i m p} \\ &= \sum_{m \in \mathbb{Z}, k \in \mathbb{N}, k \neq k_0} f_{m, k, \text{Rectangles}} \frac{\varepsilon^{s-D_{\mathcal{W}}+k(2-D_{\mathcal{W}})-i m p}}{s - D_{\mathcal{W}} + k(2-D_{\mathcal{W}}) - i m p} \\ &\quad + \sum_{m \in \mathbb{Z}, k \in \mathbb{N}} \left(f_{m, k, \text{wedges}, 1} \frac{\varepsilon^{s+1-i m p}}{s + 1 - i m p} + f_{m, k, \text{wedges}, 2} \frac{\varepsilon^{s+2k-1-i m p}}{s + 2k - 1 - i m p} + f_{m, k, \text{wedges}, 3} \frac{\varepsilon^{s+3+2k-i m p}}{s + 3 + 2k - i m p} \right) \\ &\quad + \sum_{m \in \mathbb{Z}, k \in \mathbb{N}} f_{m, k, \text{triangles, parallelograms}} \frac{\varepsilon^{s-1-i m p}}{s - 1 - i m p} + \frac{\pi \varepsilon^s}{s} - \frac{\pi \varepsilon^{s+2}}{4(s+2)}, \end{aligned}$$

where, as was already seen in Theorem 4.7, the notation $f_{m,k,\text{Rectangles}}, f_{m,k,\text{wedges},\ell}$, with $1 \leq \ell \leq 3$, and $f_{m,k,\text{triangles, parallelograms}}$, respectively account for the coefficients associated to the sums corresponding to the contribution of the rectangles, wedges, triangles and parallelograms.

This could also be deduced from the fact if the pole $s = 0$ were double, we would have terms involving $\ln \varepsilon$ in the expression of $\tilde{\zeta}_{\mathcal{W}}$, because, for any integer $m \in \mathbb{Z}$ and any complex number s ,

$$\varepsilon^{s-imp} = e^{(s-imp) \ln \varepsilon};$$

see [LvF13], Subsection 6.1.1, pages 180–182.

The novelty of this case is that we have Complex Dimensions above 0.

ii. $D_{\mathcal{W}} - k_1 (2 - D_{\mathcal{W}}) = 1$, for some $k_1 \in \mathbb{N}$, which occurs when

$$D_{\mathcal{W}} = \frac{1 + 2k_1}{1 + k_1}; \text{ i.e., } 2 + \frac{\ln \lambda}{\ln N_b} = \frac{1 + 2k_1}{1 + k_1} \text{ or, equivalently, } \lambda = N_b^{-\frac{1}{1+k_1}}.$$

Since, here, $\lambda N_b \neq 1$, it follows that $k_1 \neq 0$.

According to the terminology mentioned in *i.*, this second case corresponds to the situation when the Weierstrass Curve is *fractal in dimension 1*. We then happen to have a discrete line of Complex Dimensions with real part 1,

$$\mathcal{L}_1 = \{1 + imp, m \in \mathbb{Z}\},$$

which is obtained by merger with the discrete line of *actual* Complex Dimensions,

$$\mathcal{L}_{D_{\mathcal{W}}, k_1} = \left\{ \underbrace{D_{\mathcal{W}} - k_1 (2 - D_{\mathcal{W}})}_{1 \text{ here}} + imp, m \in \mathbb{Z} \right\}.$$

Note again that the *actual* Complex Dimensions are *not double*. As above, this directly comes from the expression obtained in Theorem 4.8 for the fractal tube zeta function, which becomes here, for any complex number s ,

$$\begin{aligned} \tilde{\zeta}_{\mathcal{W}}(s) &= \sum_{m \in \mathbb{Z}} (f_{m,k_1,\text{Rectangles}} + f_{m,0,\text{wedges},2}) \frac{\varepsilon^{s-1-imp}}{s-1-imp} \\ &= \sum_{m \in \mathbb{Z}, k \in \mathbb{N}, k \neq k_1} f_{m,k,\text{Rectangles}} \frac{\varepsilon^{s-D_{\mathcal{W}}+k(2-D_{\mathcal{W}})-imp}}{s-D_{\mathcal{W}}+k(2-D_{\mathcal{W}})-imp} \\ &\quad + \sum_{m \in \mathbb{Z}, k \in \mathbb{N}^*} f_{m,k,\text{wedges},2} \frac{\varepsilon^{s+2k-1-imp}}{s+2k-1-imp} \\ &\quad + \sum_{m \in \mathbb{Z}, k \in \mathbb{N}} \left(f_{m,k,\text{wedges},1} \frac{\varepsilon^{s+1-imp}}{s+1-imp} + f_{m,k,\text{wedges},3} \frac{\varepsilon^{s+3+2k-imp}}{s+3+2k-imp} \right) \\ &\quad + \sum_{m \in \mathbb{Z}, k \in \mathbb{N}} f_{m,k,\text{triangles, parallelograms}} \frac{\varepsilon^{s-1-imp}}{s-1-imp} + \frac{\pi \varepsilon^s}{s} - \frac{\pi \varepsilon^{s+2}}{4(s+2)}. \end{aligned}$$

What is new in this case is that we are sure that every possible Complex Dimension on \mathcal{L}_1 , i.e., every complex number $1 + i m p$, with $m \in \mathbb{Z}$, is an *actual* Complex Dimension of the Weierstrass Curve, because the same is true for each point of $\mathcal{L}_{D_{\mathcal{W}}, k_1}$.

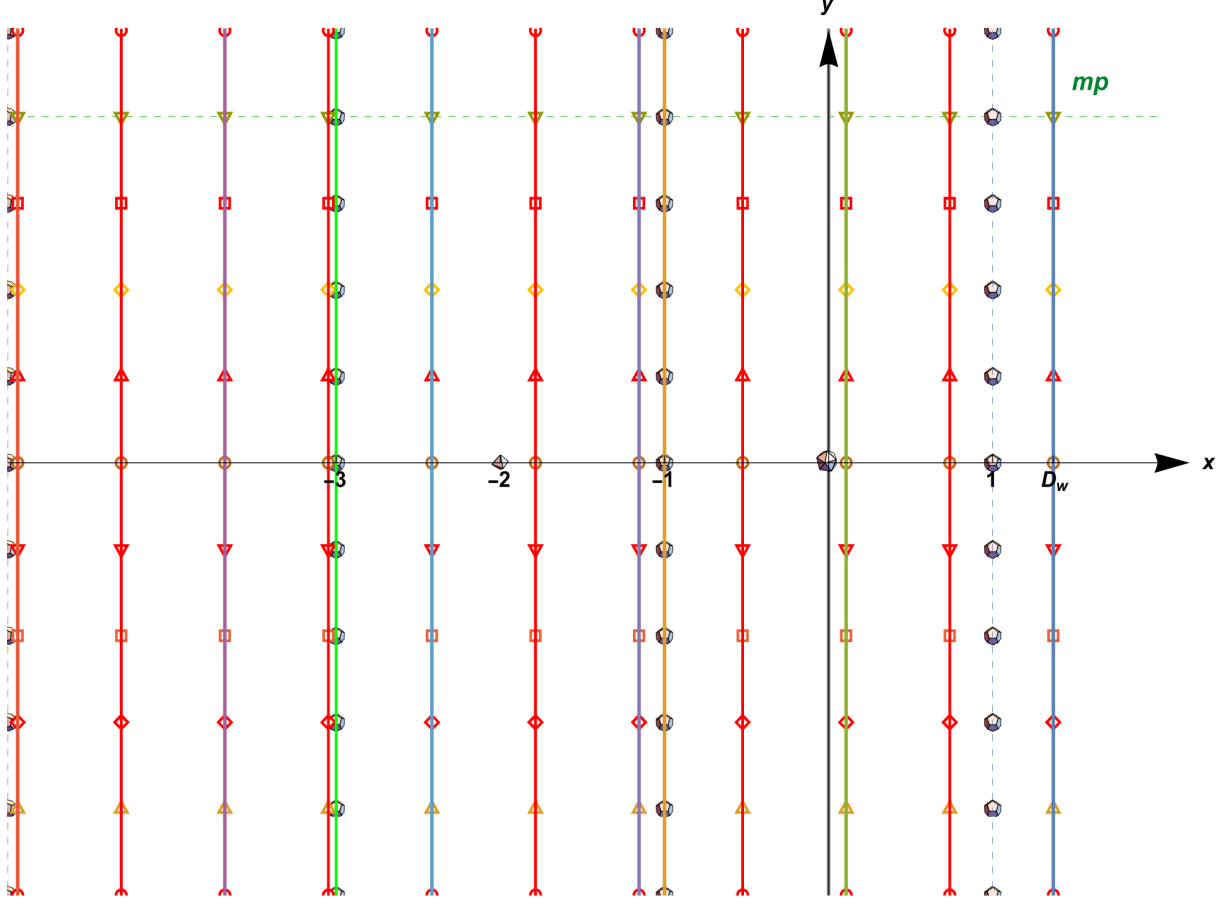


Figure 18: **The Complex Dimensions of the Weierstrass Curve.** The nonzero Complex Dimensions are periodically distributed (with the same period $p = \frac{2\pi}{\ln N_b}$, the oscillatory period of $\Gamma_{\mathcal{W}}$) along countably many vertical lines, with abscissae $D_{\mathcal{W}} - k(2 - D_{\mathcal{W}})$ and $1 - 2k$, where $k \in \mathbb{N}$ is arbitrary. In addition, 0 and -2 are Complex Dimensions of $\Gamma_{\mathcal{W}}$. (See also Subsection 4.3.2 for the exceptional cases.)

4.3.3 Possible Interpretation

Figure 18 gives *the distribution of Complex Dimensions*. To understand their deep meaning, one may place on an horizontal mp line, of equation $y = mp$. Such a line corresponds to the m^{th} -order vibration mode, the one associated to the m^{th} prefactal graph, but which can also be interpreted as coming from:

- i. The vertical line $x = 0$, or, in other words, oscillations coming from *points*: indeed, the prefactal graph $\Gamma_{\mathcal{W}_m}$ is, at first, constituted of points.

- ii. The vertical line $x = 1$, which this time correspond to oscillations coming from *lines* (or, rather, line segments): prefractal as it is, $\Gamma_{\mathcal{W}_m}$ is constituted of lines, in an Euclidean space of dimension two.
- iii. The vertical line $x = D_{\mathcal{W}}$, which, this time, corresponds to oscillations coming from the whole prefractal $\Gamma_{\mathcal{W}_m}$ itself.
- iv. The vertical lines $x = D_{\mathcal{W}} - k (2 - D_{\mathcal{W}})$, with k in $\mathbb{N}^* = \mathbb{N} \setminus \{0\}$.

For $k \leq m$, it corresponds to oscillations coming from the prefractal graphs $\Gamma_{\mathcal{W}_{m-k}}$, a phenomenon which can be understood via the following consideration:

Switching from the $(m - k)^{th}$ prefractal graph, to the m^{th} one, $0 < k \leq m$, is done by applying k iterates of the T_j maps,

$$T_{j_1 \dots j_k} = T_{j_1} \circ \dots \circ T_{j_k}.$$

In terms of the vertical distance between consecutive vertices, this amounts to a multiplication of the amplitudes by $\lambda^k = N_b^{-k(2-D_{\mathcal{W}})}$, associated to a sum of cosine expressions.

It thus provides an interesting interpretation of the real parts

$$D_{\mathcal{W}} - k (2 - D_{\mathcal{W}}) \quad , \quad \text{for } 0 < k \leq m,$$

in so far as the m^{th} prefractal graph bears, in a sense, the oscillations of its predecessors.

There remains the lines $x = D_{\mathcal{W}} - k (2 - D_{\mathcal{W}})$, with $k > m$.

In order to interpret them, one could think in the same way, but, without associated graphs, how? Except if they could exist, in some way. This will be the purpose of our next extension of the prefractal sequence $(\Gamma_{\mathcal{W}_m})_{m \in \mathbb{N}}$, a priori indexed by nonnegative integers, to negative ones, via the new concept of *antefractals*.

4.3.4 Compatibility with the General Theory of Complex Dimensions

Our results in Theorem 4.7 and Theorem 4.11 above on the fractal tube formula for the Weierstrass Curve $\Gamma_{\mathcal{W}}$ are compatible with the general (exact, pointwise) fractal tube formulas (via either tube or distance zeta functions) obtained in the higher-dimensional theory of Complex Dimensions in [LRŽ17b] (Chapter 5), or in [LRŽ18], and extending the fractal tube formulas for fractal strings obtained in [LvF00] and [LvF13] (Chapter 8). Compare, e.g., in the case of simple poles and under the hypothesis of strong languidity (a strong form of polynomial growth condition) of either $\tilde{\zeta}_{\mathcal{W}}$ or $\zeta_{\mathcal{W}}$ [LRŽ17b], Theorem 5.1.16, page 427, or Theorem 5.3.17, page 449, respectively. Indeed, according to the aforementioned results, we would have that the tubular volume is given as follows:

$$\mathcal{V}_{\mathcal{W}}(\varepsilon) = \sum_{\omega} \text{res}(\tilde{\zeta}_{\mathcal{W}}, \omega) \varepsilon^{2-\omega} = \sum_{\omega} \frac{\text{res}(\zeta_{\mathcal{W}}, \omega)}{2-\omega} \varepsilon^{2-\omega},$$

where, in each of these two sums, ω ranges through all of the Complex Dimensions of $\Gamma_{\mathcal{W}}$ (i.e., the poles of either $\tilde{\zeta}_{\mathcal{W}}$ or, equivalently, $\zeta_{\mathcal{W}}$).

Recall from equation ($\blacklozenge\blacklozenge$) in Remark 4.1 above that

$$\text{res}(\zeta_{\mathcal{W}}, \omega) = (2 - \omega) \text{res}(\tilde{\zeta}_{\mathcal{W}}, \omega).$$

In order to obtain the fractal tube formula in Theorem 4.7 (and hence also, in Theorem 4.11), however, we did not need to appeal to the aforementioned results of the general theory, by first calculating $\tilde{\zeta}_{\mathcal{W}}$ or $\zeta_{\mathcal{W}}$ (using their basic scaling and symmetry properties described in [LRŽ17b], along with the geometric properties of $\Gamma_{\mathcal{W}}$ described in Section 2 above) and then, verifying that the appropriate notion of strong languidity is satisfied. This could have been done, but was unnecessary in our present situation.

Instead, as was explained earlier, we first directly calculated the tubular volume $\mathcal{V}_{\mathcal{W}}(\varepsilon)$ in Theorem 4.7, and then deduced from the resulting fractal tube formula, via Mellin transformation, an explicit expression for $\tilde{\zeta}_{\mathcal{W}}$ – and further, for the distance zeta function $\zeta_{\mathcal{W}}$, via the functional equation recalled in relation (\blacklozenge) of Remark 4.1. Finally, as would have been the case if we had adopted the first method outlined above, we deduced (in Theorem 4.10) the values of the (possible) Complex Dimensions of $\Gamma_{\mathcal{W}}$, as the poles of $\tilde{\zeta}_{\mathcal{W}}$ (or, equivalently, of $\zeta_{\mathcal{W}}$, since $D_{\mathcal{W}} < 2$).

4.4 Minkowski Dimension, Minkowski Nondegeneracy, and Average Minkowski Content

We next obtain new and refined results concerning the geometry – and, in particular, the Minkowski nondegeneracy, non Minkowski measurability, as well as the average Minkowski content of the Weierstrass Curve. For this purpose, and for the benefit of the reader who may not be familiar with these notions, we first recall several definitions.

Definition 4.4 (Lower and Upper r -Dimensional Minkowski Contents).

Given a bounded set A of \mathbb{R}^2 , and $\varepsilon > 0$, let us denote by $\mathcal{V}_A(\varepsilon)$ the Lebesgue measure of the ε -neighborhood of A , $\mathcal{D}_A(\varepsilon)$, defined as

$$\mathcal{D}_A(\varepsilon) = \left\{ M = (x, y) \in \mathbb{R}^2, d(M, A) \leq \varepsilon \right\}.$$

For any nonnegative real number r , we define, as in [LRŽ17b], the *lower r -dimensional Minkowski content* (resp., the *upper r -dimensional Minkowski content*) of the set A as

$$\mathcal{M}_{\star}^r(A) = \liminf_{\varepsilon \rightarrow 0^+} \frac{\mathcal{V}_A(\varepsilon)}{\varepsilon^{2-r}} \quad \left(\text{resp., } \mathcal{M}^{\star, r}(A) = \limsup_{\varepsilon \rightarrow 0^+} \frac{\mathcal{V}_A(\varepsilon)}{\varepsilon^{2-r}} \right).$$

Definition 4.5 (Minkowski Dimension).

If the *lower Minkowski* (or box) *dimension* of a bounded set A of \mathbb{R}^2 ,

$$\inf \{ r \in \mathbb{R} : \mathcal{M}_{\star}^r(A) = 0 \},$$

and its *upper Minkowski* (or box) *dimension*,

$$\inf \{ r \in \mathbb{R} : \mathcal{M}^{\star, r}(A) = 0 \},$$

coincide, then their common value, denoted by D_A , is the *Minkowski* (or box) *dimension* of the set A .

Definition 4.6 (Minkowski Nondegeneracy and Minkowski Measurability).

Let A be a bounded subset of \mathbb{R}^2 , and $\varepsilon > 0$ sufficiently small. Then, as defined in [LRŽ17b], the set $A \subset \mathbb{R}^2$ is said to be *Minkowski nondegenerate* if its lower and upper Minkowski contents, $\mathcal{M}_\star^d(A) = \liminf_{\varepsilon \rightarrow 0^+} \frac{\mathcal{V}_A(\varepsilon)}{\varepsilon^{2-d}}$ and $\mathcal{M}^{\star,d}(A) = \limsup_{\varepsilon \rightarrow 0^+} \frac{\mathcal{V}_A(\varepsilon)}{\varepsilon^{2-d}}$, for some $d > 0$, are respectively positive and finite. Note that it then follows from the assumption of Minkowski nondegeneracy of A that the Minkowski dimension of A , D_A in Definition 4.5, exists, and that $d = D_A$.

Finally, the set $A \subset \mathbb{R}^2$ is said to be *Minkowski measurable* if it is Minkowski nondegenerate and

$$\mathcal{M}_\star^{D_A}(A) = \mathcal{M}^{\star,D_A}(A) ;$$

i.e., if the following limit exists in $]0, +\infty[$ (and necessarily equals this common value):

$$\mathcal{M}^{D_A}(A) = \lim_{\varepsilon \rightarrow 0^+} \frac{\mathcal{V}_A(\varepsilon)}{\varepsilon^{2-D_A}} .$$

Then, $\mathcal{M}^{D_A}(A)$ is called the *Minkowski content* of A .

Definition 4.7 (Average Lower and Upper Minkowski Contents).

We hereafter use the same notation as in Definitions 4.4 and 4.6 just above, where A denotes a bounded set \mathbb{R}^2 , and $\varepsilon > 0$ a fixed number. Then, as can be found in [LRŽ17b], Definition 2.4.1., page 178, we define the *average lower-dimensional Minkowski content* (resp., *average upper-dimensional Minkowski content*) of A as

$$\widetilde{\mathcal{M}}_\star^{D_A}(A) = \liminf_{r \rightarrow +\infty} \frac{1}{\ln r} \int_{\frac{1}{r}}^\varepsilon t^{D_A-3} \mathcal{V}_A(t) dt \quad \left(\text{resp., } \widetilde{\mathcal{M}}^{\star,D_A}(A) = \limsup_{r \rightarrow +\infty} \frac{1}{\ln r} \int_{\frac{1}{r}}^\varepsilon t^{D_A-3} \mathcal{V}_A(t) dt \right) .$$

In the case when both of these values coincide, their common value, denoted by $\widetilde{\mathcal{M}}^{D_A}(A)$, is called the *average Minkowski content* of A , which is then said to *exist*. Accordingly,

$$\widetilde{\mathcal{M}}^{D_A}(A) = \lim_{r \rightarrow +\infty} \frac{1}{\ln r} \int_{\frac{1}{r}}^\varepsilon t^{D_A-3} \mathcal{V}_A(t) dt .$$

Without loss of generality, we may choose $\varepsilon = 1$ in the present definition. Indeed, the value of $\widetilde{\mathcal{M}}^{D_A}(A)$ is independent of the choice of $\varepsilon > 0$.

We can now state several new geometric consequences of our above results, especially, Theorems 4.7 and 4.11.

Theorem 4.12 (Lower, Upper and Average $D_{\mathcal{W}}$ -Dimensional Minkowski Contents).

The lower and upper $D_{\mathcal{W}}$ -dimensional Minkowski contents, $\mathcal{M}_{\star}^{D_{\mathcal{W}}}(\Gamma_{\mathcal{W}})$ and $\mathcal{M}^{\star, D_{\mathcal{W}}}(\Gamma_{\mathcal{W}})$, of the Weierstrass Curve $\Gamma_{\mathcal{W}}$ take strictly positive and finite values, and are such that

$$\frac{C_{\text{Rectangles}}}{N_b} < \mathcal{M}_{\star}^{D_{\mathcal{W}}}(\Gamma_{\mathcal{W}}) < \mathcal{M}^{\star, D_{\mathcal{W}}}(\Gamma_{\mathcal{W}}) \leq C_{\text{Rectangles}},$$

where $C_{\text{Rectangles}}$ denotes the strictly positive and finite constant introduced in Property 4.3.

Moreover, the values of $\mathcal{M}_{\star}^{D_{\mathcal{W}}}(\Gamma_{\mathcal{W}})$ and $\mathcal{M}^{\star, D_{\mathcal{W}}}(\Gamma_{\mathcal{W}})$ are respectively equal to the minimum and maximum value of the one-periodic function $G_{D_{\mathcal{W}}} = G_{0, D_{\mathcal{W}}}$ introduced in Theorem 4.11, associated to $D_{\mathcal{W}}$ in the expression of the fractal tube formula given in the same theorem (recall that the periodicity is with respect to the variable $\ln_{N_b} \varepsilon^{-1}$, see Property 4.1).

Finally, the average Minkowski content (which is independent of the choice of $\varepsilon > 0$) exists and is given by the mean value of the one-periodic function $G_{D_{\mathcal{W}}}$, as well as by the residues of $\zeta_{\mathcal{W}}$ at $s = D_{\mathcal{W}}$:

$$\widetilde{\mathcal{M}}^{D_{\mathcal{W}}}(\Gamma_{\mathcal{W}}) = \int_0^1 G_{D_{\mathcal{W}}}(x) dx = \text{res}(\zeta_{\mathcal{W}}, D_{\mathcal{W}}) = \frac{\text{res}(\zeta_{\mathcal{W}}, D_{\mathcal{W}})}{2 - D_{\mathcal{W}}}. \quad (\spadesuit\spadesuit)$$

Hence, $\widetilde{\mathcal{M}}^{D_{\mathcal{W}}}$ is nontrivial; in fact, $0 < \mathcal{M}_{\star}^{D_{\mathcal{W}}}(\Gamma_{\mathcal{W}}) < \widetilde{\mathcal{M}}^{D_{\mathcal{W}}}(\Gamma_{\mathcal{W}}) < \mathcal{M}^{\star, D_{\mathcal{W}}}(\Gamma_{\mathcal{W}}) < \infty$.

Proof. One has

$$\begin{aligned} \mathcal{M}^{\star, D_{\mathcal{W}}}(\Gamma_{\mathcal{W}}) &= \limsup_{\varepsilon \rightarrow 0^+} \left\{ \sum_{m \in \mathbb{Z}, k \in \mathbb{N}} f_{m,k, \text{Rectangles}} \varepsilon^{k(2-D_{\mathcal{W}})-im p} \right. \\ &\quad + \varepsilon^{D_{\mathcal{W}}} \sum_{m \in \mathbb{Z}, k \in \mathbb{N}} \left\{ f_{m,k, \text{wedges}, 1} \varepsilon^{1-im p} + f_{m,k, \text{wedges}, 2} \varepsilon^{-1+2k-im p} + f_{m,k, \text{wedges}, 3} \varepsilon^{3+2k-im p} \right\} \\ &\quad \left. + \varepsilon^{D_{\mathcal{W}}} \sum_{m \in \mathbb{Z}, k \in \mathbb{N}} f_{m,k, \text{triangles, parallelograms}} \varepsilon^{-im p} + \varepsilon^{D_{\mathcal{W}}} \pi - \varepsilon^{D_{\mathcal{W}}} \frac{\pi \varepsilon^2}{2} \right\} \\ &= \limsup_{\varepsilon \rightarrow 0^+} \sum_{m \in \mathbb{Z}} f_{m,0, \text{Rectangles}} \varepsilon^{-im p} \\ &= \limsup_{\varepsilon \rightarrow 0^+} C_{\text{Rectangles}} \frac{N_b - 1}{N_b} \sum_{m \in \mathbb{Z}} \frac{(N_b - 1)^{-im p}}{\ln N_b + 2im \pi} \varepsilon^{-im p} = \limsup_{x \rightarrow +\infty} C_{\text{Rectangles}} N_b^{-\{x\}}. \end{aligned}$$

In the same way,

$$\mathcal{M}_{\star}^{D_{\mathcal{W}}}(\Gamma_{\mathcal{W}}) = \liminf_{x \rightarrow +\infty} C_{\text{Rectangles}} N_b^{-\{x\}}.$$

Thanks to Property 4.2, and with $0 \leq \{x\} < 1$, we have that

$$N_b^{-\{x\}} = \frac{N_b - 1}{N_b} \sum_{m \in \mathbb{Z}} \frac{(N_b - 1)^{-im p} \varepsilon^{-im p}}{\ln N_b + 2im \pi}, \quad \text{with } x = -\ln_{N_b}((N_b - 1)\varepsilon),$$

This yields $\frac{1}{N_b} < N_b^{-\{x\}} \leq 1$, and thus,

$$\frac{C_{\text{Rectangles}}}{N_b} < \mathcal{M}_\star^{D_{\mathcal{W}}}(\Gamma_{\mathcal{W}}) < \mathcal{M}^{\star, D_{\mathcal{W}}}(\Gamma_{\mathcal{W}}) \leq C_{\text{Rectangles}}.$$

The constant $C_{\text{Rectangles}}$ being strictly positive and finite (see Property 4.3), this accounts for a strictly positive (resp., finite) value of the lower (resp., upper) Minkowski content $\mathcal{M}_\star^{D_{\mathcal{W}}}(\Gamma_{\mathcal{W}})$ (resp., $\mathcal{M}^{\star, D_{\mathcal{W}}}(\Gamma_{\mathcal{W}})$).

Also, the one-periodic function (with respect to the variable $\ln_{N_b} \varepsilon^{-1}$, see Property 4.1),

$$G_{D_{\mathcal{W}}} = G_{0, D_{\mathcal{W}}} : \quad x \mapsto \frac{N_b - 1}{N_b} C_{\text{Rectangles}} \sum_{m \in \mathbb{Z}} \frac{(N_b - 1)^{-i m p} \varepsilon^{-i m p}}{\ln N_b + 2 i m \pi} = N_b^{-\{x\}},$$

associated to the value $D_{\mathcal{W}}$ is nonconstant, because it has nonzero m^{th} Fourier coefficients, with $m \neq 0$, as can be seen from the fractal tube formula, and as stated in Theorem 4.11.

The last part of the theorem, regarding the average Minkowski content of $\Gamma_{\mathcal{W}}$, follows at once from [LRŽ17b], Theorem 2.3.25, page 157.

□

Corollary 4.13 ((of Theorem 4.12) Minkowski Dimension – Minkowski Nondegeneracy).

The Weierstrass Curve $\Gamma_{\mathcal{W}}$ is Minkowski nondegenerate. Furthermore, the number $D_{\mathcal{W}} = 2 - \ln_{N_b} \frac{1}{\lambda}$ is a simple Complex Dimension of $\Gamma_{\mathcal{W}}$, and it coincides with the Minkowski Dimension of $\Gamma_{\mathcal{W}}$, which must also exist. Moreover, $\Gamma_{\mathcal{W}}$ is not Minkowski measurable.

Proof. In light of Theorem 4.12, the nondegeneracy directly follows from the definition. The statement concerning $D_{\mathcal{W}}$ then follows from Definition 4.6, in particular.

Furthermore, $\Gamma_{\mathcal{W}}$ is not Minkowski measurable; i.e., here, $\mathcal{M}_\star^{D_{\mathcal{W}}}(\Gamma_{\mathcal{W}}) < \mathcal{M}^{\star, D_{\mathcal{W}}}(\Gamma_{\mathcal{W}})$. This last statement also follows from Theorem 4.12, because the one-periodic function $G_{D_{\mathcal{W}}}$ is nonconstant, and so (by the aforementioned results in [LRŽ17b], Theorem 2.3.25 page 157),

$$\mathcal{M}_\star^{D_{\mathcal{W}}}(\Gamma_{\mathcal{W}}) = \min_{[0,1]} G_{D_{\mathcal{W}}} < \max_{[0,1]} G_{D_{\mathcal{W}}} = \mathcal{M}^{\star, D_{\mathcal{W}}}(\Gamma_{\mathcal{W}}).$$

Then, since the lower $D_{\mathcal{W}}$ -dimensional Minkowski contents of the Weierstrass Curve is strictly positive, by applying the result given in [LRŽ17b] (see Theorem 2.2.3, page 114), we can recover, in a different way, the fact that the number $D_{\mathcal{W}}$ is the Minkowski (or box-counting) dimension of the Weierstrass Curve.

This fact can also be directly deduced from our fractal tube formula, Theorem 4.7 (or Theorem 4.11), combined with the definition of the Minkowski dimension (Definition 4.5).

Moreover, since the distance zeta function $\zeta_{\mathcal{W}}$ associated to the Curve can clearly be meromorphically extended to a connected neighborhood of $s = D_{\mathcal{W}}$ in the Complex Plane, $D_{\mathcal{W}}$ is a simple pole of $\zeta_{\mathcal{W}}$. As was pointed out at the end of Theorem 4.12, in agreement with the general theory

in [LRŽ17b] (see Theorem 2.3.25, page 157), the connection with the associated residue of the tube zeta function $\tilde{\zeta}_{\mathcal{W}}$ and distance zeta function $\zeta_{\mathcal{W}}$ is then given by (✱✱) in Theorem 4.12. Note that these residues do not depend on ε , in agreement with the general theory in [LRŽ17b]. \square

4.5 The Non-Integer Case

An interesting question is the generalization of our previous results to *the non-integer case*; i.e., to the case when the Weierstrass function \mathcal{W} is defined, for any real number x , by

$$\mathcal{W}(x) = \sum_{n=0}^{\infty} \lambda^n \cos(2\pi b^n x),$$

where the real number b does not belong to the set of natural integers.

We plan to provide the details in a later work, but for now limit ourselves to a few comments.

From the geometric point of view, one cannot handle things in the same way. For instance, one cannot resort to a finite IFS, and the function, apart from its parity, has no periodicity property.

Yet, the associated graph being the attractor of the infinite set of maps, $\mathcal{T}_{\mathcal{W}} = \{T_i\}_{i \in \mathbb{Z}}$, such that, for any integer i and (x, y) in \mathbb{R}^2 ,

$$T_i(x, y) = \left(\frac{x+i}{b}, \lambda y + \cos\left(2\pi \left(\frac{x+i}{b}\right)\right) \right),$$

it is natural to consider the associated *infinite IFS* (IIFS), $\mathcal{T}_{\mathcal{W}}$. As a consequence, the resulting prefractal graphs are infinite ones.

The local Hölder and reverse-Hölder continuity properties of the Weierstrass function then enable us to resort to estimates that are equivalent to the ones obtained in Corollaries 2.11 and 2.12, and, consequently, to the resulting ones about the elementary heights obtained in Corollary 2.15.

As for the tubular neighborhood, due to the polygonal approximation induced by the prefractals, it is still obtained by means of rectangles and wedges.

In the integer case, extra terms coming from overlapping rectangles vanished, thanks to the symmetry with respect to the vertical line $x = \frac{1}{2}$, as described in Proposition 3.4. In the non-integer case, one simply replaces this symmetry with the one with respect to the vertical axis $x = 0$.

In this light, it is expected that a similar method, suitably adapted, would lead to a fractal tube formula of the same type as the one obtained in Theorem 4.7, where the powers of the small parameter ε would be, respectively, and as previously,

$$\varepsilon^{2-D_{\mathcal{W}}+k(2-D_{\mathcal{W}})-im p}, \quad \varepsilon^{3-im p}, \quad \varepsilon^{1+2k-im p}, \quad \varepsilon^{5+2k-im p}, \quad \varepsilon^{2-im p}, \quad \varepsilon^2, \quad \varepsilon^4,$$

which would yield the same results concerning the possible Complex Dimensions, along with the upper and lower, as well as the average, Minkowski contents of the Weierstrass Curve.

As in the integer case, the terms involving $\varepsilon^{2-D_{\mathcal{W}}+k(2-D_{\mathcal{W}})-im p}$ come from the contribution of the rectangles. The one-periodic functions (with respect to the variable $\ln_b \varepsilon^{-1}$ this time), respectively associated to the values $D_{\mathcal{W}} - k(2 - D_{\mathcal{W}})$, $k \in \mathbb{N}$, are thus nonconstant, with all of their Fourier coefficients being nonzero. Hence, as in Theorem 4.10, for each $k \in \mathbb{N}$ and $m \in \mathbb{Z}$, $D_{\mathcal{W}} - k(2 - D_{\mathcal{W}}) + im p$, are all simple Complex Dimensions of the Weierstrass Curve; i.e., they are simple poles of the tube (or, equivalently, of the distance) zeta function.

We also mention that we could deal with the case $\lambda b < 1$, exactly in the same manner, and with the same conclusions. Actually, it is noteworthy that, in the present paper, all of our results remain valid when $\lambda N_b < 1$, where $b = N_b$ is an integer greater than or equal to two. Observe that in the latter case, the Weierstrass Curve $\Gamma_{\mathcal{W}}$ is of class C^1 , but is still fractal, because it has nonreal Complex Dimensions (in fact, infinitely many of them).

5 Concluding Comments

In the light of our results, the box dimension $D_{\mathcal{W}}$ stands as a simple pole of the tube and distance zeta functions associated to the \mathcal{W} -Curve. It is also the abscissa of holomorphic continuation of those functions, which therefore cannot be extended holomorphically to the left of $D_{\mathcal{W}}$. According to [LRŽ17b], part c. of Theorem 2.1.11, page 57, and the last statement of Theorem 2.2.11, page 121, this additional result follows from the fact that $D_{\mathcal{W}}$ exists, $\mathcal{M}_{\star}^{D_{\mathcal{W}}}(\Gamma_{\mathcal{W}}) > 0$ and $D_{\mathcal{W}} < 2$. It can also be deduced from Theorem 4.7, or else from Theorem 4.10.

Now, as was alluded to in the Introduction, the determination of the possible Complex Dimensions of a fractal object, being deeply connected with its intrinsic vibrational properties, is thus directly associated to its cohomological properties: what are the topological invariants of the Weierstrass Curve? This is the question we will try to answer in the forthcoming second part of our study, [DL22b].

Behind the fractal series expansion of the Weierstrass function, another expansion, indexed by the Complex Dimensions obtained in our fractal tube formulas (see Theorems 4.7 and 4.11 above), naturally arises. Intuitively, one understands that the terms of the expansion come from the cohomological groups associated to the prefractal sequence of finite graphs that converges towards the Curve. This is all the more interesting, as those groups possess the same symmetries as the Curve, which means that a specific differentiation could be achieved on this, however, everywhere singular object; see [DL22a] and [DL22b].

As was evoked in Subsection 4.5, we also intend, in a future work, to extend our results to the general case, i.e., when the Weierstrass function \mathcal{W} is defined, for any real number x , by

$$\mathcal{W}(x) = \sum_{n=0}^{\infty} \lambda^n \cos(2\pi b^n x)$$

where the real number b does not belong to the set of natural integers. This goes along with a generalization of the results of the present paper to a large class of Weierstrass-like functions (see the paper [Dav19]), including the Takagi function, the Knopp functions and the Koch parametrized Curve; see [DL23].

References

- [BBR14] Krzysztof Barański, Balázs Bárány, and Julia Romanowska. On the dimension of the graph of the classical Weierstrass function. *Advances in Mathematics*, 265:791–800, 2014.
- [BD85] Michael F. Barnsley and Stephen G. Demko. Iterated function systems and the global construction of fractals. *The Proceedings of the Royal Society of London*, A(399):243–275, 1985.
- [Bou04] Nicolas Bourbaki. *Theory of Sets*. Elements of Mathematics (Berlin). Springer-Verlag, Berlin, 2004. Reprint of the 1968 English translation [Hermann, Paris; MR0237342].
- [BU37] Abram S. Besicovitch and Harold Douglas Ursell. Sets of Fractional dimensions (v): On Dimensional Numbers of Some Continuous Curves. *J. London Math. Soc.*, 12(1):18–25, 1937.
- [Dav18] Claire David. Bypassing dynamical systems: A simple way to get the box-counting dimension of the graph of the Weierstrass function. *Proceedings of the International Geometry Center*, 11(2):1–16, 2018.
- [Dav19] Claire David. On fractal properties of Weierstrass-type functions. *Proceedings of the International Geometry Center*, 12(2):43–61, 2019.
- [Dav21] Claire David. Wandering across the Weierstrass function, while revisiting its properties. *Analysis of PDE-Morningside Lecture Notes (edited by Jean-Yves Chemin, Ping Zhang and Fang-Hua Lin)*, 6, 2021.
- [Dev03] Robert L. Devaney. *An Introduction to Chaotic Dynamical Systems*. Westview Press, 2003.
- [DL22a] Claire David and Michel L. Lapidus. Fractal Complex Dimensions and cohomology of the Weierstrass curve, 2022.
- [DL22b] Claire David and Michel L. Lapidus. Weierstrass fractal drums - II - Towards a fractal cohomology, 2022.
- [DL23] Claire David and Michel L. Lapidus. Complex Dimensions of nowhere differentiable Weierstrass-type functions (tentative title), in preparation, 2023.
- [ELMR15] Kate E. Ellis, Michel L. Lapidus, Michael C. Mackenzie, and John A. Rock. Partition zeta functions, multifractal spectra, and tapestries of complex dimensions. In M. Frame and N. Cohen, editors, *Benoît Mandelbrot: A Life in Many Dimensions*. The Mandelbrot Memorial, pages 267–322. World Scientific Publishers, Singapore and London, 2015.
- [Fal86] Kenneth Falconer. *The Geometry of Fractal Sets*. Cambridge University Press, 1986.
- [Har16] Godfrey Harold Hardy. Weierstrass’s Non-Differentiable Function. *Transactions of the American Mathematical Society*, 17(3):301–325, 1916.
- [HL93] Tian-You Hu and Ka-Sing Lau. Fractal dimensions and singularities of the Weierstrass type functions. *Transactions of the American Mathematical Society*, 335(2):649–665, 1993.
- [HL21] Hamed Herichi and Michel L. Lapidus. *Quantized Number Theory, Fractal Strings and the Riemann Hypothesis: From Spectral Operators to Phase Transitions and Universality*. World Scientific Publishing, Singapore and London, 2021.
- [Hun98] Brian Hunt. The Hausdorff dimension of graphs of Weierstrass functions. *Proceedings of the American Mathematical Society*, 12(1):791–800, 1998.

- [Hut81] John E. Hutchinson. Fractals and self similarity. *Indiana University Mathematics Journal*, 30:713–747, 1981.
- [Kel17] Gerhard Keller. A simpler proof for the dimension of the graph of the classical Weierstrass function. *Annales de l'Institut Henri Poincaré – Probabilités et Statistiques*, 53(1):169–181, 2017.
- [KMPY84] James L. Kaplan, John Mallet-Paret, and James A. Yorke. The Lyapunov dimension of a nowhere differentiable attracting torus. *Ergodic Theory and Dynamical Systems*, 4:261–281, 1984.
- [Lap91] Michel L. Lapidus. Fractal drum, inverse spectral problems for elliptic operators and a partial resolution of the Weyl-Berry conjecture. *Transactions of the American Mathematical Society*, 325:465–529, 1991.
- [Lap92] Michel L. Lapidus. Spectral and fractal geometry: From the Weyl-Berry conjecture for the vibrations of fractal drums to the Riemann zeta-function. In *Differential Equations and Mathematical Physics (Birmingham, AL, 1990)*, volume 186 of *Math. Sci. Engrg.*, pages 151–181. Academic Press, Boston, MA, 1992.
- [Lap93] Michel L. Lapidus. Vibrations of fractal drums, the Riemann hypothesis, waves in fractal media and the Weyl-Berry conjecture. In *Ordinary and Partial Differential Equations, Vol. IV (Dundee, 1992)*, volume 289 of *Pitman Research Notes Mathematical Series*, pages 126–209. Longman Sci. Tech., Harlow, 1993.
- [Lap08] Michel L. Lapidus. *In Search of the Riemann Zeros: Strings, Fractal Membranes and Noncommutative Spacetimes*. American Mathematical Society, Providence, RI, 2008.
- [Lap19] Michel L. Lapidus. An overview of complex fractal dimensions: From fractal strings to fractal drums, and back. In *Horizons of Fractal Geometry and Complex Dimensions*, volume 731 of *Contemporary Mathematics*, pages 143–265. Amer. Math. Soc., Providence, RI, 2019.
- [Lap22] Michel L. Lapidus. *From Complex Fractal Dimensions and Quantized Number Theory To Fractal Cohomology: A Tale of Oscillations, Unreality and Fractality*, book in preparation. World Scientific Publishing, Singapore and London, 2022.
- [Led92] François Ledrappier. On the dimension of some graphs. in symbolic dynamics and its applications (New Haven, CT, 1991). *Contemp. Math.*, 135:285–293, 1992.
- [LLVR09] Michel L. Lapidus, Jacques Lévy Véhel, and John A. Rock. Fractal strings and multifractal zeta functions (special issue dedicated to the memory of Moshe Flato). *Letters in Mathematical Physics*, 88(1):101–129, 2009.
- [LM95] Michel L. Lapidus and Helmut Maier. The Riemann hypothesis and inverse spectral problems for fractal strings. *Journal of the London Mathematical Society. Second Series*, 52(1):15–34, 1995.
- [LP93] Michel L. Lapidus and Carl Pomerance. The Riemann zeta-function and the one-dimensional Weyl-Berry conjecture for fractal drums. *Proceedings of the London Mathematical Society. Third Series*, 66(1):41–69, 1993.
- [LP06] Michel L. Lapidus and Erin P. J. Pearse. A tube formula for the Koch snowflake curve, with applications to complex dimensions. *Journal of the London Mathematical Society. Second Series*, 74(2):397–414, 2006.

- [LPW11] Michel L. Lapidus, Erin P. J. Pearse, and Steffen Winter. Pointwise tube formulas for fractal sprays and self-similar tilings with arbitrary generators. *Advances in Mathematics*, 227(4):1349–1398, 2011.
- [LR09] Michel L. Lapidus and John A. Rock. Towards zeta functions and complex dimensions of multifractals. *Complex Var. Elliptic Equ.*, 54(6):545–559, 2009.
- [LRŽ17a] Michel L. Lapidus, Goran Radunović, and Darko Žubrinić. Distance and tube zeta functions of fractals and arbitrary compact sets. *Advances in Mathematics*, 307:1215–1267, 2017.
- [LRŽ17b] Michel L. Lapidus, Goran Radunović, and Darko Žubrinić. *Fractal Zeta Functions and Fractal Drums: Higher-Dimensional Theory of Complex Dimensions*. Springer Monographs in Mathematics. Springer, New York, 2017.
- [LRŽ18] Michel L. Lapidus, Goran Radunović, and Darko Žubrinić. Fractal tube formulas for compact sets and relative fractal drums: Oscillations, complex dimensions and fractality. *Journal of Fractal Geometry. Mathematics of Fractals and Related Topics*, 5(1):1–119, 2018.
- [LvF00] Michel L. Lapidus and Machiel van Frankenhuysen. *Fractal Geometry and Number Theory: Complex Dimensions of Fractal Strings and Zeros of Zeta Functions*. Birkhäuser Boston, Inc., Boston, MA, 2000.
- [LvF13] Michel L. Lapidus and Machiel van Frankenhuysen. *Fractal Geometry, Complex Dimensions and Zeta Functions: Geometry and Spectra of Fractal Strings*. Springer Monographs in Mathematics. Springer, New York, second revised and enlarged edition (of the 2006 edition), 2013.
- [LY85] François Ledrappier and Lai-Sang Young. The metric entropy of diffeomorphisms. ii. Relations between entropy, exponents and dimension. *Ann. of Math.*, 2(122):540–574, 1985.
- [Man77] Benoît B. Mandelbrot. *Fractals: Form, Chance, and Dimension*. W. H. Freeman & Co Ltd, San Francisco, 1977.
- [Man83] Benoît B. Mandelbrot. *The Fractal Geometry of Nature*. English translation, revised and enlarged edition (of the 1977 edition). W. H. Freeman & Co, New York, 1983.
- [Ols01] Lars Ole Ronnow Olsen. Review: Fractal Geometry and Number Theory. Complex Dimensions of Fractal Strings and Zeros of Zeta Functions by M. L. Lapidus and M. van Frankenhuysen, Birkhäuser. *Bulletin of the London Mathematical Society*, 33:254–255, 2001.
- [Ols13a] Lars Ole Ronnow Olsen. Multifractal tubes. In *Further Developments in Fractals and Related Fields*, Trends Math., pages 161–191. Birkhäuser/Springer, New York, 2013.
- [Ols13b] Lars Ole Ronnow Olsen. Multifractal tubes: Multifractal zeta-functions, multifractal Steiner formulas and explicit formulas. In *Fractal Geometry and Dynamical Systems in Pure and Applied Mathematics. I. Fractals in Pure Mathematics*, volume 600 of *Contemp. Math.*, pages 291–326. Amer. Math. Soc., Providence, RI, 2013.
- [PU89] Feliks Przytycki and Mariusz Urbański. On the Hausdorff dimension of some fractal sets. *Studia Mathematica*, 93(2):155–186, 1989.
- [She18] Weixiao Shen. Hausdorff dimension of the graphs of the classical Weierstrass functions. *Mathematische Zeitschrift*, 289:223–266, 2018.

- [Tit39] Edward Charles Titchmarsh. *The Theory of Functions*. Oxford University Press, second edition, 1939.
- [Wei75] Karl Weierstrass. Über continuirliche Funktionen eines reellen Arguments, die für keinen Werth des letzteren einen bestimmten Differential quotienten besitzen. *Journal für die reine und angewandte Mathematik*, 79:29–31, 1875.
- [Zyg02] Antoni Zygmund. *Trigonometric Series. Vols. I, II*. Cambridge Mathematical Library. Cambridge University Press, Cambridge, third edition, 2002. With a foreword by Robert A. Fefferman.